Baseline chemical properties and biodiversity monitoring using environmental DNA in the Eastern Shore Islands Area of Interest

Nicholas W. Jeffery, Carrie-Ellen Gabriel, Mandi Newhook, Darlene Childs, Harri Pettitt-Wade, Meghan C. McBride, Evan Cronmiller, Vicky Yaroshewski, Susan G. Heaslip, Heidi Gavel, Kumiko Azetsu-Scott, Ryan R.E. Stanley

Science Branch

Fisheries and Oceans Canada

Bedford Institute of Oceanography

1 Challenger Drive

Dartmouth, Nova Scotia

B2Y 4A2

2026

Canadian Technical Report of Fisheries and Aquatic Sciences 3828

Fisheries and Oceans Canada | Pêches et Océans Canada

Canada

Canadian Technical Report of Fisheries and Aquatic Sciences

Technical reports contain scientific and technical information that contributes to existing knowledge but which is not normally appropriate for primary literature. Technical reports are directed primarily toward a worldwide audience and have an international distribution. No restriction is placed on subject matter and the series reflects the broad interests and policies of Fisheries and Oceans Canada, namely, fisheries and aquatic sciences.

Technical reports may be cited as full publications. The correct citation appears above the abstract of each report. Each report is abstracted in the data base *Aquatic Sciences and Fisheries Abstracts*.

Technical reports are produced regionally but are numbered nationally. Requests for individual reports will be filled by the issuing establishment listed on the front cover and title page.

Numbers 1-456 in this series were issued as Technical Reports of the Fisheries Research Board of Canada. Numbers 457-714 were issued as Department of the Environment, Fisheries and Marine Service, Research and Development Directorate Technical Reports. Numbers 715-924 were issued as Department of Fisheries and Environment, Fisheries and Marine Service Technical Reports. The current series name was changed with report number 925.

Rapport technique canadien des sciences halieutiques et aquatiques

Les rapports techniques contiennent des renseignements scientifiques et techniques qui constituent une contribution aux connaissances actuelles, mais qui ne sont pas normalement appropriés pour la publication dans un journal scientifique. Les rapports techniques sont destinés essentiellement à un public international et ils sont distribués à cet échelon. II n'y a aucune restriction quant au sujet; de fait, la série reflète la vaste gamme des intérêts et des politiques de Pêches et Océans Canada, c'est-à-dire les sciences halieutiques et aquatiques.

Les rapports techniques peuvent être cités comme des publications à part entière. Le titre exact figure au-dessus du résumé de chaque rapport. Les rapports techniques sont résumés dans la base de données *Résumés des sciences aquatiques et halieutiques.*

Les rapports techniques sont produits à l'échelon régional, mais numérotés à l'échelon national. Les demandes de rapports seront satisfaites par l'établissement auteur dont le nom figure sur la couverture et la page du titre.

Les numéros 1 à 456 de cette série ont été publiés à titre de Rapports techniques de l'Office des recherches sur les pêcheries du Canada. Les numéros 457 à 714 sont parus à titre de Rapports techniques de la Direction générale de la recherche et du développement, Service des pêches et de la mer, ministère de l'Environnement. Les numéros 715 à 924 ont été publiés à titre de Rapports techniques du Service des pêches et de la mer, ministère des Pêches et de l'Environnement. Le nom actuel de la série a été établi lors de la parution du numéro 925.

Canadian Technical Report
of Fisheries and Aquatic Sciences 3828

2026

Baseline chemical properties and biodiversity monitoring using environmental DNA in the Eastern Shore Islands Area of Interest

by

Nicholas W. Jeffery, Carrie-Ellen Gabriel, Mandi Newhook, Darlene Childs, Harri Pettitt-Wade, Meghan C. McBride, Evan Cronmiller, Vicky Yaroshewski, Susan G. Heaslip, Heidi Gavel, Kumiko Azetsu-Scott, Ryan R.E. Stanley

Science Branch
Fisheries and Oceans Canada
Bedford Institute of Oceanography
1 Challenger Drive
Dartmouth, Nova Scotia
B2Y 4A2

© His Majesty the King in Right of Canada, as represented by the Minister of the Department of Fisheries and Oceans, 2026

This work is licensed under the Open Government Licence

Cat. No. Fs 97-6/3828E-PDF ISBN: 978-1-100-01204-9 ISSN 1488-5379

https://doi.org/10.60825/ntyk-c735

Correct citation for this publication:

Jeffery, N.W., Gabriel, C-E., Newhook, M., Childs, D., Pettitt-Wade, H., McBride, M., Cronmiller E., Yaroshewski, V., Heaslip, S.G., Gavel, H., Azetsu-Scott, K., Stanley, R.R.E. 2026. Baseline chemical properties and biodiversity monitoring using environmental DNA in the Eastern Shore Islands Area of Interest. Can. Tech. Rep. Fish. Aquat. Sci. 3828: x + 83 p. https://doi.org/10.60825/ntyk-c735

TABLE OF CONTENTS

LIST OF TABLES V
LIST OF FIGURES VI
ABSTRACT IX
RÉSUMÉ X
INTRODUCTION 1
OCEANOGRAPHIC BASELINES AND THE MARINE CARBONATE SYSTEM 2
ATLANTIC SALMON AND FRESHWATER CONNECTIVITY 3
METABARCODING AND EDNA: NON-INVASIVE TOOLS FOR BIODIVERSITY MONITORING 4
MATERIALS AND METHODS 5
DATA AVAILABILITY 5
WATER SAMPLING 5
OCEAN CHEMISTRY ANALYSES 6
ENVIRONMENTAL DNA SAMPLING 8
Offshore eDNA Transects 8
eDNA Sequencing 8
Bioinformatic Processing and Analyses 9
RESULTS 9
BASELINE PHYSICAL AND CHEMICAL CHARACTERIZATION – CARBONATE SYSTEM, NUTRIENTS, AND TRACERS 9
RIVER SAMPLES 11
ENVIRONMENTAL DNA – EUKARYOTIC DIVERSITY 12
Summary of eDNA Detections 12
2021-2022 Results 12
2023 Results 13
DISCUSSION 14
COASTAL PHYSICAL ENVIRONMENT 14
NUTRIENT DYNAMICS 15
COASTAL AND FRESHWATER CARBONATE DYNAMICS AND OCEAN ACIDIFICATION 16
EDNA METABARCODING AND BIODIVERSITY 19
LINKAGES BETWEEN THE ENVIRONMENT AND BIOLOGICAL COMMUNITIES 21
RECOMMENDATIONS FOR FUTURE SAMPLING AND MONITORING 22
ACKNOWLEDGEMENTS 24
TABLES 25
FIGURES 27

REFERENCES 59
APPENDICES 68

LIST OF TABLES

Table 1. Physical and chemical data for 3 rivers (**Napu'saqnuk** St. Mary's River, Sherbrooke; West River, **Weijuik** Sheet Harbour; and **Nukumkiaq** Moser River) located within the Eastern Shore Islands Area of Interest on August 13, 2021. Sampling locations are shown in Figure 1. DIC = total inorganic carbon, TA = total alkalinity, AOU = apparent oxygen utilization. 25

Table 2. The eDNA primer sets, their target taxa, and references for each year of eDNA analyses. 26

LIST OF FIGURES

Figure 1. Location of seawater sampling sites taken between August 9 and 14, 2021 following a 4x4 transect design spaced 65km alongshore and 20km from the nearshore to the outer boundary of the AOI (white circles). The same four transects were sampled in 2022 and 2023 for environmental DNA only. Additional samples were taken from three third-order river sites (**Napu'saqnuk** St. Mary's River (not shown –45.1742° N, -61.9797° W); **Nukumkiaq** Moser River; and West River,**Weijuik** Sheet Harbour and ESI-00; blue circles) in the Eastern Shore Islands Area of Interest (AOI). Locations overlaid on a 10 m resolution bathymetry raster masked to the extent of the AOI. Draft network sites denoted by polygons with black borders. 27

Figure 2. Map of the Atlantic Zone of Eastern Canada, showing ocean currents in blue. A yellow star indicates the location of the Eastern Shore Islands Area of Interest (AOI), and a red star at HL_2, fixed station monitoring site off **Kjipuktuk** Halifax, Nova Scotia. Figure modified from Lemay et al. (2018)..... 28

Figure 3. An example CTD profile from August 11, 2021, at station ESI_16. The top left panel shows the temperature and salinity profiles with depth, while the top right panel shows the potential density anomaly of water and the square of buoyancy frequency (N^2) profiles with pressure. The bottom left panel shows conservative temperature (θ) plotted against salinity, and the bottom right panel shows the CTD profile location offshore of Nova Scotia. All plots are derived from the oce R package (Kelley and Richards 2024). 29

Figure 4. T-S diagram with isopycnals for data from all stations sampled between August 9 to 14, 2021 from the along the Eastern Shore Islands AOI transects in Figure 1. Each point's colour represents the depth the sample was collected (legend at right). 30

Figure 5. Section plots of salinity (Sal00, left) and temperature (Tv268C, right) data, including bathymetry, for 4 transects sampled between August 9 and 14, 2021. The discrete sample locations through depth are indicated with black dots. The x-axis denotes the section distance along the transect, extending from inshore to offshore. Salinity is lowest at the surface and highest in the deepest areas of the transects, while temperature is highest at the surface. Evidence of a cold intermediate layer is shown in the temperature plots as purple colouring. 31

Figure 6. Section plots of total alkalinity (TA, left) and total dissolved inorganic carbon (TIC, right) data, including bathymetry, for 4 transects sampled between August 9 and 14, 2021. The discrete sample locations through depth are indicated with black dots. The x-axis denotes the section distance along the transect, extending from inshore to offshore. A general increase in both TA and TIC as depth increases is shown..... 32

Figure 7. Section plots of data, including bathymetry, for 4 transects sampled between August 9 and 14, 2021 showing pCO_2 (left) and CH_4 (right) along the 4 study transects, enumerated on each plot. The discrete sample locations through depth are indicated with black dots..... 33

Figure 8. Section plots of data, including bathymetry, for 4 transects sampled between August 9 and 14, 2021 showing pH (left) and Ω aragonite saturation (right) along the 4 study transects, enumerated on each plot. The discrete sample locations through depth are indicated with black dots..... 34

Figure 9. Section plots of data, including bathymetry, for 4 transects sampled between August 9 and 14, 2021 showing Dissolved oxygen and AOU along the 4 study transects, enumerated on each plot. The discrete sample locations through depth are indicated with black dots..... 35

Figure 10. Alongshore section plots with bathymetry for salinity, temperature, saturation state of aragonite (W_{arag}) and dissolved oxygen data from sites sampled August 9 to 14, 2021, for the most

nearshore sites of each of the 4 study transects: **Nukumkiaq** Moser River (ESI-1 to ESI-4), **Weijuik** Sheet Harbour (ESI-00 and ESI-5 to ESI-8), **Ketmenipukwek** Ship Harbour (ESI-9 to ESI-12), and **Winipukwejk** Jeddore (ESI-13 to ESI-16). The discrete sample locations through depth are indicated with black dots. 37

Figure 11. Alongshore section plots with bathymetry for salinity, temperature, saturation state of aragonite (Ω_{arag}) and dissolved oxygen data from sites sampled August 9 to 14, 2021, for the farthest offshore sites of each of the 4 study transects: **Nukumkiaq** Moser River (ESI-1 to ESI-4), **Weijuik** Sheet Harbour (ESI-00 and ESI-5 to ESI-8), **Ketmenipukwek** Ship Harbour (ESI-9 to ESI-12), and **Winipukwejk** Jeddore (ESI-13 to ESI-16). The discrete sample locations through depth are indicated with black dots. 39

Figure 12. A) Scatterplot of $\delta^{18}O$ plotted against salinity for the marine samples along the **Weijuik** Sheet Harbour transect. The river samples range from -6.06 to -7.30 ‰ and are not shown here. The relationship between these variables is linear, with high correlation ($r^2 = 0.933$), which improves ($r^2 = 0.996$) when the shallow nearshore samples (ESI-0, ESI-5 and ESI-6) are treated separately. B) Section plot of $\delta^{18}O$ for the **Weijuik** Sheet Harbour transect. Note the influence of river samples, located near the coast, and the higher salinity slope water influence offshore. 40

Figure 13. Box plot of total inorganic nitrogen (nitrate + nitrite + ammonium) along sections through depth for the **Nukumkiaq** Moser River (ESI-1 to ESI-4), **Weijuik** Sheet Harbour (ESI-00 and ESI-5 to ESI-8), **Ketmenipukwek** Ship Harbour (ESI-9 to ESI-12), and **Winipukwejk** Jeddore (ESI-13 to ESI-16) transects in order of sampling between August 9 and 14, 2021. The colour corresponds to the transect name (legend) and within each transect, the sites (left to right) are ordered inshore to offshore. 41

Figure 14. Ternary plot of the % nutrient contribution (% silicate versus % total nitrogen vs. % phosphate) for all sites sampled for all depths. The black dot represents reference point of the idealized Redfield Ratio (16:16:1 Si:N:P). The marine sites are nitrogen limited, whereas the river sites (in green) are silicate and/or phosphate limited. 42

Figure 15. Fish species detected in eDNA using the 12S (top) and 16S (bottom) mitochondrial markers across 16 sites (4 offshore transects with 4 sites each) sampled from the CCGS M. Perley in summer 2021. 43

Figure 16. Non-metric multidimensional scaling plot of 2021 Perley eDNA fish data (12S = left, 16S = right). Surface samples generally clustered close together regardless of station, while benthic samples were more dispersed. 44

Figure 17. Fish species detected from the offshore in 2022 using the 12S (top) and 16s (bottom) eDNA markers. The log-transformed read count is shown on the y-axis for each species. While there is substantial overlap in fish species detected between the two marker types, more species of elasmobranchs (sharks and skates) were identified using the 16S marker. 45

Figure 18. Non-metric multidimensional scaling plot of fish eDNA samples collected in 2022 using Jaccard distances (12S = left, 16S = right). For both markers there was substantial overlap between surface and benthic eDNA samples suggesting similarity in the communities recovered by eDNA metabarcoding. 46

Figure 19. Invertebrate and algal species detected from the offshore in 2022 using the COI eDNA marker. The log-transformed read count is shown on the y-axis for each species. The most abundant species is the picophytoplankton Micromonas pusilla, followed by several species of copepods (Oithona similis and Tortanus discaudatus). 47

Figure 20. Krona plot of animal diversity at the genus level detected by the 2022 COI eDNA marker. The percentages beside each genus name refer to the diversity of amplicon sequence variants (ASV) that

make up the total proportion of the total ASVs found in the samples (i.e., higher percentages mean more ASVs are found in that species). The phytoplankton Micromonas pusilla was removed from the plot because it made up the majority of eDNA reads. 48

Figure 21. NMDS of 2022 COI data with points coloured by water depth. For the COI data, the bottom and surface samples largely separate along NMDS1, with the exception of four samples. There is significant clustering of samples by water depth, with deeper samples separating from shallower samples along NMDS2. 49

Figure 22. Fish (top panel) and invertebrate species (bottom) detected from the offshore in 2023 using the 12S (top) and COI (bottom) eDNA markers. The log-transformed read count is shown on the y-axis for each species. 50

Figure 23. Krona plot of chordate diversity at the genus level detected by the 2023 12S eDNA marker. The percentages beside each genus refer to the diversity of amplicon sequence variants (ASV) that make up the total proportion of the total ASVs found in the samples (i.e., higher percentages mean more ASVs are found in that species). Bony fishes (Teleostei) make up the majority of detections, while elasmobranchs (blue) and cetaceans (green) make up smaller proportions of detected genera. 51

Figure 24. Bubble plot of all fish species detected in surface eDNA samples collected along the **Weijuik** Sheet Harbour transect in spring and fall 2023. The size of the bubble is proportional to the number of eDNA reads for that species, while the colour corresponds to the water depth of the station. 53

Figure 25. Bubble plot of all fish species detected in bottom eDNA samples collected along the **Weijuik** Sheet Harbour transect in spring, summer, and fall 2023. Only station ESI-06 was sampled in the summer. The size of the bubble is proportional to the number of eDNA reads for that species, while the colour corresponds to the water depth of the station. 54

Figure 26. Alluvial plot showing the most commonly detected (>8000 DNA reads) fish species using eDNA metabarcoding (12S marker) along a single transect south of **Weijuik** Sheet Harbour aboard the CCGS M. Perley in 2023. The plot shows the seasons and water sample location (surface vs. benthic samples) each species of fish was found in, and the colours represent the sampling station in the transect – ESI-05 is closest to the mouth of **Weijuik** Sheet Harbour, while ESI_08 is farthest offshore. Atlantic Herring (Clupea harengus) are the most abundant fish detected, and they are found in all sample stations, seasons, and in both surface and bottom samples. 55

Figure 27. Krona plot of animal diversity at the genus level detected by the 2023 COI eDNA marker. The percentages beside each genus refer to the diversity of amplicon sequence variants (ASV) that make up the total proportion of the total ASVs found in the samples (i.e., higher percentages mean more ASVs are found in that species). 56

Figure 28. Alluvial plot showing the most commonly detected (>4000 DNA reads) invertebrates using eDNA metabarcoding (12S marker) along a single transect south of **Weijuik** Sheet Harbour aboard the CCGS M. Perley in 2023. The plot shows the seasons and water sample location (surface vs. benthic samples) each invertebrate was found in, and the colours represent the sampling station in the transect – ESI_05 is closest to the mouth of **Weijuik** Sheet Harbour, while ESI_08 is farthest offshore. 57

Figure 29. NMDS of Perley 2023 seasonal data (12S=left, COI=right). Only one station was sampled in summer (ESI-6). The polygons represent the season the samples were collected (spring, summer, and fall), while the point colours correspond to the sampling sites. Both markers show a clear separation of spring and fall fish and invertebrate communities, with summer being intermediate to both seasons. .. 58

ABSTRACT

Jeffery, N.W., Gabriel, C-E., Newhook, M., Childs, D., Pettitt-Wade, H., McBride, M., Cronmiller E., Yaroshewski, V., Heaslip, S.G., Gavel, H., Azetsu-Scott, K., Stanley, R.R.E. 2026. Baseline chemical properties and biodiversity monitoring using environmental DNA in the Eastern Shore Islands Area of Interest. Can. Tech. Rep. Fish. Aquat. Sci. 3828: x + 83 p.
https://doi.org/10.60825/ntyk-c735

The Eastern Shore Islands (ESI) form a uniquely dense archipelago of islands, coastal features, and diverse subtidal habitats on the Eastern Shore of Nova Scotia (NS). This physical and ecological diversity led to the identification of the area as an Area of Interest (AOI) for potential designation as a Marine Protected Area under Canada's *Oceans Act*. To support a holistic understanding of the AOI and to inform future management, we collected baseline physical and chemical oceanographic data and environmental DNA (eDNA) samples along four transects extending from nearshore environments to the outer bounds of the AOI, characterizing habitat conditions and the biodiversity they support. Follow-up eDNA sampling in 2022 and 2023 established a time series to track changes in fish, invertebrate, and algal communities. Temperature and salinity profiles in the AOI were typical of the Atlantic coastal zone of Nova Scotia, with temperatures around 20°C at the surface and bottom temperatures around 5°C in the summer. Aragonite and calcite saturation states were <1.00 and <1.56, respectively, below 50 m, indicating that the deep bottom waters are chemically challenging for shell-forming organisms, which provide important fisheries for this coastal region. Samples collected from three nearby rivers were acidic ($pH_T < 5$), which is typical of fresh surface waters in the Southern Uplands of Nova Scotia. eDNA sampling detected a consistent assemblage of fish species commonly occurring in coastal NS across sampling years, including Atlantic Herring, Atlantic Mackerel, Cunner, Tomcod, and Winter Flounder, while also identifying additional species unique to individual sampling years, including some sharks and cetaceans. In 2023, seasonal eDNA sampling revealed distinct fish and invertebrate communities in spring, summer, and fall. Together, these results highlight the ability of eDNA approaches to capture both seasonal and interannual variation in marine community composition, providing a valuable tool for detecting ecological change over time. This study establishes a baseline of oceanographic conditions and biodiversity patterns within the AOI and demonstrates the potential for repeat water sampling as an effective ecosystem monitoring approach to track future changes associated with climate variability and other environmental pressures.

RÉSUMÉ

Jeffery, N.W., Gabriel, C-E., Newhook, M., Childs, D., Pettitt-Wade, H., McBride, M., Cronmiller E., Yaroshewski, V., Heaslip, S.G., Gavel, H., Azetsu-Scott, K., Stanley, R.R.E. 2026. Baseline chemical properties and biodiversity monitoring using environmental DNA in the Eastern Shore Islands Area of Interest. Can. Tech. Rep. Fish. Aquat. Sci. 3828: x + 83 p.
https://doi.org/10.60825/ntyk-c735

Les îles de la côte Est forment un archipel d'une densité exceptionnelle, composé d'îles, d'éléments côtiers et d'habitats subtidaux variés, situé sur la côte est de la Nouvelle-Écosse (N.-É.). Cette diversité physique et écologique a mené à la désignation de la région comme site d'intérêt en vue d'une éventuelle désignation comme zone de protection marine en vertu de la *Loi sur les océans* du Canada. Afin de favoriser une compréhension globale du site d'intérêt et d'éclairer les futures mesures de gestion, nous avons recueilli des données océanographiques physiques et chimiques de référence ainsi que des échantillons d'ADN environnemental (ADNe) le long de quatre transects s'étendant des milieux côtiers jusqu'aux limites extérieures du site d'intérêt, afin de caractériser les conditions des habitats et la biodiversité qu'ils abritent. Des prélèvements de suivi d'ADNe effectués en 2022 et 2023 ont permis d'établir une série chronologique permettant de suivre l'évolution des communautés de poissons, d'invertébrés et d'algues. Les profils de température et de salinité dans le site d'intérêt étaient caractéristiques de la zone côtière atlantique de la Nouvelle-Écosse, avec des températures avoisinant les 20 °C en surface et des températures au fond avoisinant les 5 °C en été. Les indices de saturation en aragonite et en calcite étaient respectivement inférieurs à 1 et à 1,56 à plus de 50 m de profondeur, ce qui indique que les eaux profondes du fond présentent des conditions chimiques difficiles pour les organismes à coquille, qui constituent une ressource importante en matière de pêches pour cette région côtière. Les échantillons prélevés dans trois rivières voisines se sont révélés acides (pHT < 5), ce qui est caractéristique des eaux de surface douces des hautes terres du sud de la Nouvelle-Écosse. L'échantillonnage d'ADNe a permis de détecter, au fil des années d'échantillonnage, un ensemble cohérent d'espèces de poissons couramment présentes sur la côte de la Nouvelle-Écosse, notamment le hareng de l'Atlantique, le maquereau de l'Atlantique, la tanche-tautogue, le poulamon et la plie rouge, tout en identifiant d'autres espèces propres à certaines années d'échantillonnage, notamment certains requins et cétacés. En 2023, des prélèvements saisonniers d'ADNe ont révélé la présence de communautés distinctes de poissons et d'invertébrés au printemps, en été et à l'automne. Dans l'ensemble, ces résultats mettent en évidence la pertinence des méthodes d'analyse de l'ADNe pour ce qui est de saisir les variations tant saisonnières qu'interannuelles de la composition des communautés marines, ce qui en fait un outil précieux pour détecter les changements écologiques au fil du temps. Cette étude établit une base de référence concernant les conditions océanographiques et les tendances en matière de biodiversité au sein du site d'intérêt et démontre que le prélèvement répété d'échantillons d'eau peut constituer une approche efficace de surveillance de l'écosystème pour suivre les changements futurs liés à la variabilité climatique et à d'autres pressions environnementales.

INTRODUCTION

The Eastern Shore Islands (ESI) Area of Interest (herein referred to as "the AOI"), located on the Eastern Shore of Nova Scotia, was announced in spring 2018 for potential future designation as a Marine Protected Area under Canada's *Oceans Act* (Jeffery et al. 2020, Heaslip et al. in prep.). Though public consultation has been on hold since 2019, the area remains an AOI and scientific research has continued to the present. The AOI is a relatively natural area of the Nova Scotia Atlantic coastline, with a high density of islands creating unique habitat that influences the oceanography of the area (Jeffery et al. 2020; Ma et al. 2024). The AOI study area extends from the low tide mark to approximately 20 km offshore (~0 – 130 m), making the area suitable and accessible for nearshore coastal and intertidal scientific research. The study area is also important to coastal communities, which commercially harvest several species, including American Lobster (*Homarus americanus*), Atlantic Herring (*Clupea harengus*), and groundfish.

The majority of ongoing scientific projects in the AOI have focused on monitoring seagrass beds and kelp forests (e.g., Krumhansl et al. 2024; Savard-Drouin et al. 2024) and the biodiversity of the area through SCUBA surveys, baited remote underwater video (BRUVs), and drop camera imagery (e.g., Goodwin et al. 2025; Paulin et al. 2025; Sajtovich et al. 2025). Since 2018, research efforts across the AOI have progressively expanded the ecological characterization of the ESI ecosystem by integrating observations from nearshore and offshore habitats. Benthic imagery studies in particular have revealed a high diversity of previously uncharacterized benthic invertebrates in offshore areas, including sponges, bryozoans, sea pens, and crinoids (Paulin et al. 2025).

Long-term management of a conservation area requires consistent data collection that is directly relevant to the conservation objectives of the site. When collected before management measures are implemented, baseline data provide an essential foundation for evaluating long-term effectiveness and attributing observed ecological changes to management actions (e.g., Moland et al. 2013). This is particularly important in areas characterized by diverse human uses, where understanding the relationship between conservation objectives and ongoing activities is central to adaptive management (Murray et al. 2025). Monitoring programs should therefore be designed around the ecological features and processes that underpin the objectives of an area, using indicators capable of detecting (measuring) meaningful changes over time (e.g., Pomeroy et al. 2005). The ability to detect change depends on a robust understanding of the baseline conditions, with the specific data collected guided by the conservation priorities of the area.

The proposed conservation priorities for the ESI AOI include the area's high degree of naturalness, diverse biogenic habitats (including eelgrass and kelp), and migratory and foraging habitat for Atlantic Salmon and marine birds (Jeffery et al. 2020, Heaslip et al. in prep.). Understanding the state of these broad, ecosystem-level features require baseline information that captures both environmental conditions and biodiversity patterns across the AOI. Measurements of oceanographic conditions provide important context on the physical environment supporting these ecosystems and help identify

potential impacts of human activities in the area (e.g., riverine influence on marine conditions). Environmental DNA (eDNA) provides a comprehensive, non-invasive approach for characterizing diversity across a range of taxonomic groups (e.g., Gold et al. 2021; He et al. 2022; Trask et al. 2025). Together, these complementary approaches provide the opportunity for an integrated characterization of baseline ecosystem conditions collected using a shared water sampling approach, where the same samples can characterize both environmental conditions and biodiversity patterns. This establishes a foundation for long-term monitoring in the AOI.

OCEANOGRAPHIC BASELINES AND THE MARINE CARBONATE SYSTEM

Physical and chemical properties of aquatic environments are essential variables that define habitat conditions and influence the physiology, behaviour, and ecological interactions of aquatic organisms (Sunday et al. 2022; Marium et al. 2023; Barclay et al. 2026), as well as the structure and function of the communities they form (e.g., O'Brien et al. 2022; Irvine et al. 2025). These environmental conditions are particularly important and complex in coastal systems, where terrestrial influences (e.g., freshwater inputs, runoff, and the physical configuration of the coastline) interact with oceanographic processes and where the influence of human activities is the most pronounced (Murphy et al. 2024; 2026). The ESI represent a particularly complex coastal environment, characterized by a dense archipelago (Jeffery et al. 2021), highly heterogeneous circulation patterns (Feng et al. 2022), and highly localized retention patterns resulting from the interaction between a complex coastline and bathymetric transitions (Ma et al. 2024). These features create unique habitat conditions that influence the distinctive biodiversity patterns that characterize the ESI.

Monitoring spatiotemporal patterns in physical and chemical conditions is therefore fundamental for understanding ecosystem status and change, including responses to anthropogenic climate change such as ocean warming, acidification, deoxygenation, and altered circulation patterns (Jeffery et al. 2021; Barclay et al. 2026). Temperature, salinity and dissolved oxygen provide key indicators for oceanographic processes, including ocean circulation, warming, and oxygen availability. Stable oxygen isotope ($\delta^{18}O$) measurements are used in hydrology and water cycle studies and to trace marine water masses through relative contributions from seawater, precipitation, river water and ice meltwater (Gramillion and Wanielsta 2000). Measurements of the partial pressure of CO_2 (pCO_2), pH, dissolved inorganic carbon (DIC), and total alkalinity (TA) characterize the marine carbonate system and provide quantitative measures of ocean acidification (Bushinsky et al. 2019).

Calcium carbonate saturation state (Ω) is a key indicator of ocean acidification. The major mineral forms of calcium carbonate are aragonite and calcite, and aragonite is more soluble than calcite. Therefore, aragonite saturation state (Ω_{arag}) is commonly used to assess the potential vulnerability of calcifying organisms to corrosive conditions.

The ecological consequences of changes in physical and chemical conditions vary widely among species and therefore cannot be inferred from environmental observations alone. Temperature, salinity, nutrients, oxygen, and carbonate chemistry influence the physiology, growth, survival, and reproductive success of organisms (Barclay et al. 2026), with responses differing among taxonomic groups and life-history phases (Hurd et al. 2020). For example, calcifying invertebrates, including bivalve molluscs, may experience reduced calcification and greater shell dissolution under increasingly corrosive conditions, while the responses of seaweeds to elevated CO_2 depend on species-specific responses to CO_2, bicarbonate/carbonate, and H^+ in the water column (van der Loos et al. 2019). Fish responses are likewise variable among species, with changes in pH and temperature affecting metabolism, homeostasis, and survival over time (Hurd et al. 2020). The impacts of climate change may be particularly complex in diadromous fishes such as salmonids as they experience different components of their life cycles in marine and freshwater habitats (Crozier and Siegel 2025 and references therein), where changing aquatic conditions compound across different extremes and cumulate as animals transition through life history stages. These varied responses demonstrate the importance of coupling measurements of physical and chemical conditions with comprehensive biological monitoring to understand how environmental change translates to shifts in biodiversity, community composition, ecosystem function and ultimately changes in ecosystem services.

ATLANTIC SALMON AND FRESHWATER CONNECTIVITY

The Southern Upland Designatable Unit (DU) of Atlantic Salmon (*Salmo salar*) is a primary species of conservation interest for the ESI AOI. As an anadromous species, survival of Atlantic Salmon depends on the health of both freshwater and marine environments, making the AOI of particular importance as a crucial transition zone for migrating juveniles and returning adults. This anadromous species migrates into rivers to spawn, and juveniles (smolts) later migrate to the marine environment to feed and mature. Although population declines have been largely attributed to acidification of freshwater habitats (Watt 1987; Bowlby et al. 2013; Montgomery et al. 2020), the marine habitat within the AOI has been identified as a conservation priority because of its importance during freshwater to marine and marine to freshwater transitional phases of the species' life history.

Atlantic Salmon are of cultural significance to the Mi'kmaq Nation, and are harvested for food and ceremonial purposes. The decline of salmon populations in Nova Scotia therefore represents not only ecological and economic losses, but also cultural losses. The Eastern Shore Islands is an area of cultural and ecological significance for the Mi'kmaq, an area of traditional land and resource use including fishing, hunting, and gathering. Where possible, places names are provided throughout this report in Mi'kmaq in bold, blue text. The lack of a Mi'kmaw equivalent should not be interpreted as the word does not exist and this document should not be used as a language reference.

Freshwater systems in the Southern Uplands of Nova Scotia are particularly vulnerable to acidification as a result of the low buffering capacity of the local granite and slate

geology, which cannot neutralize the acidic atmospheric deposition associated with burning fossil fuels (Clair et al. 2007). Juvenile salmonids are particularly sensitive to low pH, with salmon fry unable to survive at <pH 4.7 and successful smolt production occurring ≥pH 4.9 (Lacroix 1989, 1992). Such thresholds are consistent with the documentation of the disappearance of Atlantic Salmon from Nova Scotia rivers resulting from acidification (Bowlby et al. 2013). The biological impacts of acidification on salmonids arise from several interacting mechanisms including low pH which mobilizes aluminum causing respiratory dysfunction and ionoregulatory failure (Farmer 2000; Monette and McCormick 2008). Even sub-lethal exposure can impair smoltification, reducing marine survival of fish (Farmer 2000) that enter the AOI.

To mitigate acidification, both terrestrial and in-stream liming has been implemented in this area since the early 2000s (Halfyard 2008). These efforts were supported by the Nova Scotia Salmon Association and federal and provincial partners. Terrestrial liming involves aerial or ground application of dolomitic limestone to watershed soils, which can increase base saturation and reduce runoff acidity, while instream liming uses mechanical dosers to add limestone directly to water to raise pH. West River, **Weijuik** Sheet Harbour is a flagship restoration site in Nova Scotia, where an in-stream doser has operated since 2005, located 30 km upriver of the Sheet Harbour estuary and 14.5 km upstream of its largest tributary, the Killag River, which also has an operational doser. A better understanding of the carbonate system and nutrient inputs across the freshwater-marine transition is needed to determine whether the influence of river liming extends to adjacent coastal waters. This question is of particular relevance for the AOI, where the complex archipelago promotes localized water retention and heterogeneous circulation (Ma et al. 2024), thus potentially extending the spatial influence of riverine inputs on marine habitats. Understanding these processes may help inform the recovery measures for Atlantic Salmon populations and the role of the AOI, while also improving our understanding of how freshwater management actions may influence coastal and marine ecosystems.

METABARCODING AND EDNA: NON-INVASIVE TOOLS FOR BIODIVERSITY MONITORING

Environmental DNA (eDNA) analyses have proven their value for research and monitoring aquatic biodiversity in an efficient, standardizable manner (e.g., Montgomery et al. 2020; Gold et al. 2021; Capurso et al. 2023). eDNA consists of DNA shed by organisms in the environment that is concentrated through filtration of water or sediment samples. eDNA is then extracted from the filter in a laboratory and amplified through polymerase chain reaction (PCR) to select the taxon/taxa of interest. A single taxon (a species or genus) can be quantitatively detected through real-time quantitative PCR (qPCR), or a metabarcoding approach can be used to examine a greater diversity of taxa. Through the use of various DNA primers, the DNA of groups (e.g., fishes, plants, all eukaryotes) can be amplified through PCR and sequenced on a high-throughput sequencing platform. Sampling eDNA is non-invasive and effective at capturing the representative biodiversity of an area. Numerous studies have demonstrated eDNA sampling to be efficient and at least as effective as more traditional sampling techniques in coastal and offshore environments (e.g., Stoeckle et al. 2021; He et al. 2022, 2023; Maiello et al. 2024). As such, eDNA sampling can be a suitable alternative to more

invasive sampling techniques in sensitive environments, or used as a complementary tool to enhance regular survey efforts. For example, eDNA can identify zooplankton and cryptic species that net-based surveys miss and can provide information on the genetic diversity (haplotypes) of species in the area.

Monitoring programs using eDNA must be sensitive enough to detect changes in indicator species of interest, including the introduction of non-indigenous species, the loss of indicator species, the loss of indicator taxa, or shifts or changes in species richness or community structure over time. eDNA results can vary widely across relatively small spatial and temporal scales, and thus the scale and objectives of the sampling should be considered early on during project planning (Jensen et al. 2022). In contrast, communities revealed by metabarcoding may show stability temporally and spatially if represented by a few dominant species. However, variation among communities and species richness can still be detected when eDNA sampling corresponds with species-specific spawning events, diurnal behaviour, or migration (Lolivier et al. 2025). As such, eDNA sampling can serve as a valuable tool for both baseline information and monitoring, if implemented for the system of interest.

The objectives of this study were to collect a baseline of chemical and physical oceanographic properties and examine eukaryote diversity of the AOI entirely from water sampling. Samples were first collected in 2021 to help fill knowledge gaps about the AOI outlined by Jeffery et al. (2020). We then collected eDNA samples in 2022 and 2023 to test several field sampling protocols and to compare fish and invertebrate communities between years to identify temporal stability or turnover. The data presented here can serve as baseline information for ongoing monitoring of the conservation priorities identified for the AOI, including habitat for Atlantic Salmon and the biodiversity supported by the diversity of habitats in the ESI, should it become a conservation area in the future. The information presented here will also be valuable for coastal communities and commercial fisheries in the region who experience firsthand changes in the environment, including shifting water masses, increasing ocean temperatures and water corrosiveness, and changes in biological community structure.

MATERIALS AND METHODS

DATA AVAILABILITY

Metadata and code for eDNA bioinformatics and statistical analyses are available at https://github.com/NickJeff13/eDNA-for-MPAs. Raw eDNA sequence reads are available as Fastq files in the National Center for Biotechnology Information at https://www.ncbi.nlm.nih.gov/bioproject/PRJNA1378225. Discrete water chemistry and oceanographic data are archived in the Fisheries and Oceans Canada BioChem database (Devine et al. 2014; https://www.dfo-mpo.gc.ca/science/data-donnees/biochem/index-eng.html).

WATER SAMPLING

From August 9 to 14, 2021, a total of 88 seawater samples were collected using 4 L Niskin bottles on a Sea-Bird Scientific SBE 19plus CTD integrated with an SBE 55 ECO

water sampler rosette. Niskin bottles were closed at prescribed depths at regular intervals aboard the Canadian Coast Guard Ship (CCGS) *M. Perley* along 4 transects starting near the coast to 20 km offshore (**Winipukwejk** Jeddore (ESI-13 to ESI-16), **Ketmenipukwek** Ship Harbour (ESI-9 to ESI-12), **Weijuik** Sheet Harbour (ESI-00 and ESI-5 to ESI-8) and **Nukumkiaq** Moser River (ESI-1 to ESI-4)) and from three third-order river sites (**Napu'saqnuk** St. Mary's River; **Nukumkiaq** Moser River; and West River, **Weijuik** Sheet Harbour) in the AOI (Figure 1, Table 1). These transects are separated longitudinally across the AOI, but also correspond to areas offshore of river systems known to support Atlantic Salmon. Measured parameters from water sampled at these locations included dissolved inorganic carbon (DIC), total alkalinity (TA), pCO_2 (partial pressure of carbon dioxide), methane (CH_4), salinity, dissolved oxygen, dissolved inorganic nutrients (nitrate+nitrite, ammonium, silicate, and phosphate) and oxygen isotope composition ($\delta^{18}O$) (along the **Weijuik** Sheet Harbour transect and the three rivers). Temperature and pH (pH_{NBS}) at the three river sites were measured with handheld digital units, but other sampling followed protocols presented in the following section for marine samples. River chemistry measured on August 13, 2021 reflects in-river conditions at the time of sampling, and carbonate and freshwater signals at the marine stations in the AOI (August 9 to 14, 2021) integrate inputs of the West River system from approximately August 7 to 13, 2021, given the consideration of the timing of a storm event on august 7, 2021, the pre- and post-event summertime baseflow conditions, and the long hydraulic residence of **Weijuik** Sheet Harbour Lake (Gregory et al. 1993), but should not be interpreted as a contemporaneous upstream to downstream continuum.

Niskin bottles dedicated to eDNA filtration were also collected at the bottom and surface of each CTD rosette profile. The CTD also profiled depth, temperature, and conductivity at each sampling station. In 2021 and 2022, 1 L water samples were frozen in Nalgene bottles until later thawing and filtration in a laboratory setting. In 2023, eDNA was collected from filtering 3 L of seawater directly from the Niskin bottle while aboard the vessel. Detailed eDNA sampling methods are described below.

OCEAN CHEMISTRY ANALYSES

The sampling protocols followed Standard Operating Procedures as outlined by GO-SHIP protocols (http://www.go-ship.org/) and the Guide to Best Practices for Ocean CO_2 Measurements (Dickson et al. 2007). DIC and TA samples were collected in 500 mL gas-tight borosilicate bottles and preserved with 100 µl of saturated mercuric chloride following SOP 1 in Dickson et al. 2007. Samples were stored at room temperature until analysis. DIC was determined using gas extraction and coulometric titration with photometric endpoint detection (Johnson et al., 1985). TA was measured by open-cell potentiometric titration with full curve Gran Point determination using a Titrando dosimat with Tiamo software in conjunction with a sample delivery system built in-house. DIC and TA samples were calibrated with measurements of a secondary internal standard, verified against a certified seawater reference material (Batch # 186) supplied by Andrew Dickson (Scripps Oceanographic Institution, San Diego, USA). The

precision of DIC and TA measurements was ±2.4 and ±3.5 μmol kg^{-1}, respectively. Dissolved CH_4 and pCO_2 samples were collected in 125 mL serum bottles, preserved by the addition of 50 µl saturated mercuric chloride solution, and immediately crimp sealed with butyl rubber septa. Dissolved CH_4 and pCO_2 were later measured with a static headspace equilibrium method modified from Neill et al. (1997), where equilibrated headspace samples were injected into a gas chromatograph equipped with a catalytic methanizer and a flame ionization detector (Punshon et al. 2014). Methane saturation was calculated using the Bunsen solubility coefficients of Wiesenburg and Guinasso (1979). The analytical uncertainty for dissolved CO_2 and CH_4 is of ±0.8 % or better. The *in situ* pCO_2, pH on the total scale,(pH_T) and the saturation state of aragonite (Ω_{arag}) and calcite (Ω_{calc}), indices of corrosiveness, were calculated from DIC and TA using CO2SYS v.3 (Lewis et al. 1998) using the following constants: the first and second dissociation constants for carbonic acid, K_1 and K_2, computed on the total scale of Lueker et al. (2000), the hydrogen sulfate constant K_{HSO_4} of Dickson (1990), the hydrogen fluoride constant $K_{f\ of\ (}$Perez and Fraga (1987), and total boron of Lee et al. (2010). For the river samples, *in situ* pCO_2 and calculated TA (TA_{calc}) were calculated from pH and pCO_2 at salinity of 0 (Freshwater option) using CO2SYS v.3 (Lewis et al. 1998) using the following constants: *K1* and *K2,* computed on the total scale of Millero (1979), the hydrogen sulfate constant *KHSO4 of* Dickson (1990).

Salinity samples were analysed using a Guildline Autosal salinometer using Guildline salinity standards from series P163, with a standard deviation of 0.0001 on all samples. Samples for dissolved oxygen were drawn into gravimetrically calibrated 125 mL iodine flasks and immediately fixed with Winkler reagents (1 ml of manganese chloride and 1 ml of alkaline iodide), then stored in the dark until analysis within 24 hours. Dissolved oxygen concentrations were determined using a computer-controlled Winkler titration with colorimetric endpoint detection after Jones et al. (1992). Standard deviation on standards and duplicates were always better than 0.01 mL L^{-1}. The apparent oxygen utilization (AOU) was calculated using the *oce* R package (Kelley and Richards 2024). The $\delta^{18}O$ was measured at the University of Ottawa's Jan Veizer Stable Isotope Laboratory using mass spectrometry for samples collected along the **Weijuik** Sheet Harbour transect and for the three river sites only. Analytical precision was 0.06 ‰. Nutrient samples were measured at 22 °C with a segmented flow auto analyser following the methods described in Strickland and Parsons (1972) for nitrate, phosphate, and silicate, and the fluorometric method of Kerouel and Aminot (1997) for ammonium. For these analyses, pooled duplicate precision for nitrate, phosphate, silicate and ammonium were 0.06, 0.113, 0.03, and 0.35 μmol L^{-1}, respectively.

ENVIRONMENTAL DNA SAMPLING

Offshore eDNA Transects

Four offshore eDNA transects were sampled within the AOI in 2021 and 2022 aboard the CCGS *M. Perley* to gain baseline and time series information on fish species in the AOI (Figure 1). In 2021 and 2022 triplicate 1 L water samples were collected from surface and bottom water at each station, and captured eDNA on 0.22 µm Sterivex filters using a peristaltic pump. This sampling involved freezing collected water samples in Nalgene bottles, and later thawing and filtering the samples in the lab at BIO, which was labour-intensive and may have caused DNA damage and breakage with the freeze-thaw cycle.

In 2023, we updated our sampling strategy, instead filtering triplicate 3 L water samples using 1.2 µm Smith-Root filters using an on-board vacuum pump. The larger pore size selected enabled some microbes to pass through the filter, reducing non-target eDNA amplification, and allowed for efficient filtering of a larger water volume to capture more eukaryotic eDNA. However, we were only able to sample one transect (four stations directly off **Weijuik** Sheet Harbour, ESI-05 to ESI-08) in spring, summer, and fall due to vessel priorities in St. Anns Bank MPA. No offshore transects were sampled in 2024 or 2025 because of a lack of dedicated research vessel time.

eDNA Sequencing

The eDNA filters from 2021 and 2022 were shipped on ice to the Centre for Environmental Genomics Applications (CEGA; St. John's, Newfoundland) for DNA extraction and sequencing. Briefly, each Sterivex filter was removed from its housing and digested in lysis buffer. Captured DNA was extracted from each filter, after which the DNA underwent PCR amplification for the specific marker region being targeted. Nucleotide barcodes were added to the DNA from each filter to identify the sample during bioinformatic processing, and Illumina adapters were also added to enable next-generation sequencing on an Illumina platform. Amplified, barcoded DNA from each sample is then pooled into a sequencing library and sequenced on an Illumina instrument. In 2021 and 2022, libraries were sequenced at CEGA on an Illumina NovaSeq 6000 machine with a sequencing depth target of 1 million reads per sample.

The eDNA samples collected in 2023 were processed and sequenced by the DFO Aquatic Biotechnology Laboratory (Dartmouth, Nova Scotia). DNA was extracted from Smith-Root filters using the Qiagen DNeasy Blood & Tissue Kit and QIAcube Connect robotic workstation (Qiagen). Extracted DNA was amplified at a region of *cytochrome c oxidase I* (COI) and *12S ribosomal RNA* (12S) with custom Ultramer DNA primers (IDT) and simultaneously indexed with a unique combination of nucleotide barcodes using PCR. The primer sets used per year are presented in Table 2. The PCR products were evaluated for quality using the Agilent 4200 TapeStation electrophoresis system with D1000 ScreenTapes and Reagents (Agilent). Successful PCR-amplified samples were purified using the AxyPrep Mag PCR Clean-up Reagent (Axygen), then quantified using the AccuClear Ultra High Sensitivity dsDNA Quantitation kit (Biotium). Equimolar amounts of each purified PCR sample were pooled to create a library (either COI or 12S). Target input amounts of DNA were 50ng/sample for the COI libraries and

25ng/sample for the 12S libraries. The completed libraries were purified again using the AxyPrep Mag PCR Clean-up Reagent, evaluated using the 4200 TapeStation with the HS D1000 assay kit, and quantified using the NEBNext Library Quant Kit for Illumina (New England Biolabs). Libraries were sequenced using the Illumina MiSeq System with either v3 600-cycle paired-end chemistry (COI libraries) or v2 500-cycle paired-end chemistry (12S libraries).

Bioinformatic Processing and Analyses

Raw sequence reads were converted to fastq format and demultiplexed. Forward and reverse primers were trimmed from all sequences using cutadapt v.4.0 (Martin 2011) with an error rate of 0.11, minimum quality score of 20, and minimum length set to 20. Demultiplexed reads were processed using the QIIME2-2024.10 pipeline (Bolyen et al. 2019). Paired-end reads were imported for each marker separately using the *import* tool, and denoised using the DADA2 plugin. For 16S, –p-trunc-len-f and –p-trunc-len-r were both set to 125, but were set to 116 and 108 respectively for 12S. A consensus method was used to detect chimeras, and the –p-min-fold-parent-over-abundance parameter was set to 2 to improve the number of reads passing the chimera filter. After denoising, the results were summarized as feature-tables including the filtered amplicon sequence variant (ASV) feature table, representative fasta sequences, and denoising statistics using the *feature-table* plugin. The taxonomy of each ASV sequence was assigned using BLASTn against the eukaryotic nucleotide database for 12S and 16S markers and a sequence match >97%, while a Ribosomal Database Project (RDP) naive Bayesian classifier v5.1.0 was used to assign the taxonomy for the COI marker at a probability >0.98 (Porter et al. 2014; Porter and Hajibabaei 2018).

ASV tables for each eDNA marker consisting of species names and read counts per species per eDNA sample were filtered for non-aquatic species (e.g., terrestrial mammals, insects, fungi) and for taxonomic identifications with a percent match <98%. After data filtration, barplots of confirmed species and their read counts were created for each marker and each year of data. Krona plots showing the relative proportion of each species by ASV count and their hierarchical taxonomy were plotted using the *taxplore* R package (Schlegel 2026). Species accumulation curves and non-metric multidimensional scaling (NMDS) plots were conducted in the *vegan* R package (Oksanen et al. 2025) to show species diversity and sample community similarities. Jaccard dissimilarities were used to create the distance matrix for the NMDS of the eDNA communities. Finally, for the 2023 dataset, alluvial plots were generated using the *ggalluvial* package (Brunson and Read 2023) to visualize the species found at each station in the **Weijuik** Sheet Harbour transect (ESI-5 to ESI-8) in different seasons (spring, summer, and fall), and whether they were found in surface or bottom samples.

RESULTS

BASELINE PHYSICAL AND CHEMICAL CHARACTERIZATION – CARBONATE SYSTEM, NUTRIENTS, AND TRACERS

Temperature measurements along all 4 transects showed evidence of stratification, with surface waters of 20°C declining rapidly below approx. 25 m to <5°C and to ~5°C at 100

m. This pattern was mirrored in salinity profiles, with fresher surface waters (< 25 m) in the nearshore (<31 psu), overlying more saline waters in the offshore sites at the end of the transects (~32-33 psu) below 50 m. (Figure 3, Figure 4, Figure 5). These sites fell into two groups when plotted on the T-S diagram: shallow nearshore coastal waters (left grouping), and a group along a mixing line, occupying more saline, colder waters (Figure 4).

Dissolved inorganic carbon (DIC) and total alkalinity (TA) in water samples ranged from 1947.06 to 2166.61 μmol kg^{-1} (mean = 2019.70 μmol kg^{-1}, SD = 67.18 μmol kg^{-1}) and from 2060.00 to 2221.90 μmol kg^{-1} (mean = 2130.10 μmol kg^{-1} , SD = 37.50 μmol kg^{-1}) respectively, increasing consistently through depth for both parameters at all sites. Total alkalinity was the lowest along the surface of the **Nukumkiaq** Moser River transect and the highest along the surface of the **Winipukwejk** Jeddore transect (Figure 6). pCO_2 (*in situ*) was lowest at the surface, increasing through depth at all sites, ranging from 402.33 to 656.97 μatm (mean = 492.8 μatm, SD = 56.4) (Figure 7). The saturation of CH_4 for most sites ranged from 110.4% to 392.5% with a mean of 182.8% (SD=64.9) with no consistent trend through the profile. Maximum CH_4 values were observed at the site in **Weijuik** Sheet Harbour (ESI-00), where the CH_4 saturation was 849% and 1840% at 2 m and 10 m, and CH_4 saturation ranged from 440.3% to 758% at the coastal station of the **Ketmenipukwek** Ship Harbour transect (ESI-09) (Figure 7). The calculated pH_T ranged from 7.77 to 7.97 with a mean of 7.89 (SD = 0.04), with the highest pH_T at the surface for most sites. Uncertainty in calculated pH values propagated through carbonate system calculations ranged from 0.0098 to 0.0016 pH units. The lowest pH_T values (7.77) were observed at the bottom of the deepest sites in the **Winipukwejk** Jeddore and **Weijuik** Sheet Harbour transects, where the highest DIC and pCO_2 values in the dataset were also measured (Figure 8). The saturation state of aragonite (Ω_{arag}) ranged from 0.85 to 1.91 across the sites (mean = 1.37, SD = 0.33) and generally decreased through depth, with the lowest values at depth offshore. Values of Ω_{arag} below 1, an indicator of corrosive water conditions, were found below 50 m at the sites farthest offshore for all four transects (ESI-4, ESI-8, ESI-12 and ESI-16) (Figure 8). Below 50 m, the saturation state of calcite (Ω_{calc}) also reached a minimum, with values between 1.37 and 1.55 (Appendix Table 2). Uncertainty in calculated Ω_{arag} and Ω_{calc} values propagated through carbonate system calculations ranged from 0.033 to 0.062 and from 0.077 to 0.153 (unitless), respectively.

Dissolved oxygen at these sites ranged from 217.82 to 306.95 μmol kg^{-1} (mean = 272.44 μmol kg^{-1}, SD = 19.95), and in general, increased through depth to a peak in each profile from 15–25 m and then declined (Figure 9). The lowest dissolved oxygen value (217.82 μmol kg^{-1}) was observed at the bottom of the deepest site of the **Winipukwejk** Jeddore transect. The apparent oxygen utilization (AOU), a proxy for remineralization of organic matter, ranged from -48.22 to 96.19 μmol kg^{-1} (mean = 7.67 μmol kg^{-1}, SD = 34.33), with the lowest (negative values) at the surface and the highest values at depth through the profiles at all sites. The lowest AOU values were

observed at the bottom of the site farthest offshore along the **Weijuik** Sheet Harbour transect (ESI-08) (Figure 9).

The alongshore perspective (closest and furthest sections; Figure 10 and Figure 11) shows lower salinity and temperature and higher dissolved oxygen and Ω_{arag} for the **Ketmenipukwek** Ship Harbour and **Nukumkiaq** Moser River transects relative to **Weijuik** Sheet Harbour and **Winipukwejk** Jeddore. The oxygen isotope composition ($\delta^{18}O$) was measured on the samples taken through depth along the **Weijuik** Sheet Harbour transect, with values ranging from -2.12 ‰ to -1.22 ‰ (mean = -1.85‰, SD = 0.25). $\delta^{18}O$ forms a strong positive relationship with salinity for the seawater sites (r^2 = 0.933, Figure 12). The most saline sites in the deepest waters offshore, therefore, displayed the highest $\delta^{18}O$ values and may represent different water masses relative to those inshore, since the correlation improves when data from nearshore are separated from offshore stations The zero-salinity intercept was -15.58 ‰ for this relationship (Figure 12).

Total nitrogen (the sum of nitrate, nitrite and ammonium) ranged from 0.063 to 12.925 $\mu mol\ kg^{-1}$ (mean = 2.814 $\mu mol\ kg^{-1}$, SD = 3.753, Figure 13). Phosphate ranged from 0.067 to 1.168 $\mu mol\ kg^{-1}$ (mean = 0.433, SD = 0.319) and silicate ranged from 0.335 to 13.76 $\mu mol\ kg^{-1}$ (mean = 3.524 $\mu mol\ kg^{-1}$, SD = 3.547). Nutrients were lowest in surface waters and generally increased with depth, with higher values offshore (Appendix Table 3). For Moser River, Ship Harbour and Jeddore sections, AOU and nitrate/nitrite and phosphate concentrations show a similar increasing trend through depth for the first three sites moving offshore. However, this changes at the furthest site at these three sections below 25 m; despite increasing positive AOU values through depth, here, the nitrate concentration decreased to near 1 $\mu mol\ kg^{-1}$ or lower, and the phosphate concentrations decreased (Appendix Table 3). At Sheet Harbour, however, the positive relationship between AOU and nutrients was maintained through depth at the furthest site from shore (i.e. ESI-8). It is here that we also see the lowest Ω_{arag} and Ω_{calc} of all the samples measured (Appendix Tables 2 and 3). Figure 14 shows a ternary plot of total nitrogen against phosphate and against silicate, where the black dot in the plot represents the idealized silicate-adjusted Redfield ratio of 16 Si: 16 N : 1 P. All seawater samples sit above this point, with nitrogen limiting relative to phosphate and silicate (Figure 14).

RIVER SAMPLES

Results for the river samples taken on August 13, 2021 are presented in Table 1. River water DIC ranged from 155.11 to 194.70 $\mu mol\ kg^{-1}$. Although it was not possible to reliably measure TA on our system, which is not configured for freshwater samples, the calculated values obtained using CO2SYS were near-zero, or nominal,, with the highest at **Napu'saqnuk** St. Mary's River. River water pCO_2 ranged from 768.5 μatm at **Nukumkiaq** Moser River to 2803.6 μatm at **Napu'saqnuk** St. Mary's River, and CH_4 saturation ranged from 503.1% at the West River, **Weijuik** Sheet Harbour to 18697.97% at **Napu'saqnuk** St. Mary's River. Dissolved oxygen ranged from 240.13 to 266.93 $\mu mol\ kg^{-1}$ across the sites. The stable isotope ratio of oxygen ($\delta^{18}O$) at these

sites were highly variable, ranging from -7.03 ‰ to -6.06 ‰, with no relationship with salinity (0.0219 to 0.024 psu), but instead are linked to watershed properties that control residence time and would affect enrichment in the heavier isotope following evaporation. The Moser River drains the smallest watershed, with the slowest flow, and the St. Mary's River drains the largest watershed and has the highest flows.

River waters were more acidic than marine samples (pH_{NBS} 4.00–4.75; Table 1) and were silicate and/or phosphate limited according to the ternary plot (Figure 14). Continuous monitoring at the West River, **Weijuik** Sheet Harbour and Killag River dosers by the Nova Scotia Salmon Association recorded the recession of a storm pulse that peaked on August 7, 2021 (West River 2.68 m^3/s, dose rate 3.54 t/day; Killag River 5.15 m^3/s, dose rate 6.81 t/day). Over the six-day sampling period (August 9–14, 2021), daily mean discharge declined 78–84% on both rivers (West River: range 0.29–1.77 m^3/s, median 0.95 m^3/s; Killag River: range 0.77–3.46 m^3/s, median 1.57 m^3/s), with lime dose rate declining proportionally at both dosers (West River: range 0.38–2.34 t/day, median 1.26 t/day; Killag River: range 1.02–4.58 t/day, median 2.07 t/day). By August 13 and 14, West River dose rates had fallen to 0.58 and 0.38 t/day respectively and Killag River dose rates to 1.22 and 1.02 t/day respectively, consistent with summer baseflow conditions and comparable to the June–August 2021 dose rate median of 0.56 t/day (West River) and 1.02 t/day (Nova Scotia Salmon Association, unpublished data).

ENVIRONMENTAL DNA – EUKARYOTIC DIVERSITY

Summary of eDNA Detections

From 2021 to 2023, including seasonal (spring, summer, fall) sampling in 2023, we detected eDNA from 73 species of vertebrates using the 12S and 16S markers, and 62 species of metazoan invertebrates and 12 species of marine algae from the COI marker. These results are those we are highly confident in, after filtering for taxonomy matches >97% match, removing non-marine organisms (e.g., insects and terrestrial mammals), and species only known to occur in the Pacific Ocean (e.g., Pacific Herring, *Clupea pallasii*), which are likely the result of laboratory contamination or misidentified reference sequences. The invasive bryozoan *Membranipora membranacea* and the invasive red algae *Bonnemaisonia hamifera* and *Dasysiphonia japonica* were detected in both 2022 and 2023, when the COI marker was used to investigate general eukaryotic diversity.

2021-2022 Results

In 2021, we detected 17 species of fish using the 12S eDNA marker, and 18 fish species with the 16S marker (Figure 15). For both markers, the surface samples largely consisted of these three pelagic species (Atlantic Saury, Mackerel, and Herring), while the benthic samples were more diverse and occupied more space in the NMDS plots (Figure 16). In 2022, we detected 27 species of fishes with 12S, and 29 species with 16S (Figure 17). Like 2021, the surface samples overlapped with the benthic samples in the two-dimensional NMDS space but occupied a broader overlapping area, indicating

similar fish communities represented by both the surface and bottom samples (Figure 18).

The samples from 2021 and 2022 show similar spatial patterns, with pelagic fishes (*Clupea harengus*, *Scomber scombrus, Scomberesox saurus*) and Cunner DNA the most prevalent and abundant in terms of eDNA reads across the samples. eDNA was captured for species common to the Eastern Scotian Shelf, including alewife, Northern and Atlantic Wolffish, Sea Raven, Redfish, Haddock, Atlantic Cod, Tomcod, and flounders. Atlantic Moonfish (*Selene setapinnis*) were detected only in 2021 in the AOI with both 12S and 16S markers. Minke Whale (*Balaenoptera acutorostrata*) were also detected in the AOI in 2021 and 2022. A diversity of sharks and skates were detected in 2022 with the 12S and 16S markers, including Thresher Shark, Porbeagle, Basking Shark, Blue Shark, and Soft Skate (*Malacoraja spinacidermis*). Soft Skate in particular were an interesting find, as they are rare and typically only found in deep water (>450 m). However, only 2485 DNA reads were detected for this species, in only one sample (ESI-16 at a depth of 110 m).

In 2022, the most common invertebrate captured in each sample (by DNA read count) was the picophytoplankton *Micromonas pusilla*, followed by several species of copepods (zooplankton) (Figure 19). The planktonic calanoid copepod genera detected include *Calanus, Pseudocalanus, Clausocalanus, Centropages, Acartia, Oithona, Metridia,* and *Tortanus.* Benthic macroinvertebrates detected included barnacles, polychaete worms, gastropods, hydrozoans, and brittle stars (Figure 19, Figure 20). Two invasive species, the red algae *Dasysiphonia japonica* and the bryozoan *Membranipora membrancea* were also detected with the COI marker in 2022. NMDS of the invertebrate communities showed greater distinction between the bottom and surface samples than the fish markers (12S and 16S) (Figure 21). Surface and bottom samples separated along NMDS axis 1, while NMDS axis 2 separated samples by depth, indicating depth stratification in invertebrate communities in the AOI.

2023 Results

In 2023, when we began sampling a greater water volume and using a self-preserving Smith-Root filter, we detected higher fish diversity along the one transect off **Weijuik** Sheet Harbour, which was sampled in spring, summer, and fall. We detected eDNA from 64 marine vertebrate species, including four cetaceans (Common Dolphin (*Delphinus delphis*), Atlantic White Sided Dolphin (*Lagenorhynchus acutus*), Common Minke Whale (*Balaenoptera acutorostrata*), and North Atlantic Right Whale (*Eubalena glacialis*)), three cartilaginous fishes (Thorny Skate (*Amblyraja radiata*), Basking Shark (*Cetorhinus maximus*), and Porbeagle (*Lamna nasus*)), and 58 bony fish species (Figure 22). The fish species detected in 2023 were similar to previous years, including river herrings (*Alosa* spp.), flounders, Pollock, Cunner, tunas, eelpouts, wrymouth, sticklebacks, Brook Trout, and Atlantic Salmon (Figure 22, Figure 23). Several freshwater fish species, including Yellow Perch (*Perca flavescens*), Brown Bullhead (*Ameiurus nebulosus*), and White Sucker (*Catostomus commersonii*), were detected along the **Weijuik** Sheet Harbour transect, primarily at ESI-05 which is closest to the mouth of the harbour and estuary (Figure 24, Figure 25).

The invertebrates detected included a diversity of copepods, green and red algae, barnacles, and a mix of other phyla, including polychaete worms, echinoderms, krill, and molluscs (Figure 22, Figure 27). Arthropods were the most common phylum detected, and mainly consisted of zooplankton (copepods and krill). Like 2022, multiple genera of calanoid copepods typical of North Atlantic zooplankton were detected in both surface and bottom samples. Polychaetes and echinoderms were the next most abundant invertebrate taxa, followed by molluscs, cnidarians (mainly hydrozoans), and sponges (Figure 27).

Alluvial plots of both the fish and invertebrate communities also showed clear differences among season, sampling station, and whether the water samples were from the surface or bottom waters (Figure 26, Figure 28). NMDS of both the 12S and COI results showed clear seasonal separation of the fish and invertebrate communities along this transect, and a distinct change in community from inshore to offshore (Figure 29). For fish with k=8 reduced dimensions, transect sites separate out along NMDS1, while seasons were separated along NMDS2. There was some overlap between spring and fall samples, while summer was entirely overlapped by spring and fall samples. For invertebrates with k=10 reduced dimensions, seasonal differences appeared along NMDS1 with complete separation of all three seasons. The different transect sites were separated along NMDS2, indicating an inshore-offshore transition in community structure (Figure 29).

DISCUSSION

Here we characterize baseline physical and chemical oceanographic properties, along with biological communities identified using environmental DNA within the ESI AOI. This study revealed potentially corrosive bottom waters in the deepest sections of the four transects conducted across the AOI, which likely originate from mixing of waters from the Gulf of St. Lawrence mixed with cold slope water entering the Scotian Shelf. We also provide spatiotemporal information on benthic and pelagic fishes and invertebrates in the AOI with three years of eDNA data, and include linkages between the physical and chemical environment with the biological communities. The data provided here are fundamental to understanding the ESI ecosystem, both as an Area of Interest and for providing scientific information to coastal commercial fisheries that depend on healthy lobster and other shellfish stocks.

COASTAL PHYSICAL ENVIRONMENT

Coastal waters of the ESI AOI area are dominated by nearshore processes, influenced locally by runoff and estuarine circulation within a complex coastline geomorphology and bathymetry, and are influenced by waters carried by the Nova Scotia Current at 40-50 m depth (Dever et al. 2016; Hachey, 1941). Temperature and salinity profiles of the Eastern Shore AOI were typical of summertime measurements of the Scotian Shelf. Vertical CTD profiles taken in the AOI showed strong stratification, with warmed surface waters reaching ~20°C and temperatures declining rapidly to <5°C between 40 and 80 m, followed by relatively uniform temperatures of 5-6°C below 80 m, consistent with subarctic oceans in the summer (Andres et al. 2024) and with reported spatiotemporal

patterns along the Scotian Shelf in 2021 (Hebert et al. 2023). The ~20°C surface temperatures are consistent with the unusually warm conditions observed across the Scotian Shelf in 2021, when surface temperatures were the second warmest on record (Cyr et al. 2022). Salinity measurements showed a similar vertical structure, with the freshest waters above 40 m across all transects out to 15-20 km, while the deepest waters farther offshore displaying the most saline waters for all 4 transects. The T-S diagram (Figure 4) constructed for these samples shows this influence of mixing with the slope waters of the Scotian Shelf carried by the Nova Scotia Current (Hachey 1941; Mclellan et al. 1953) (Figure 2).

These patterns are also supported by the $\delta^{18}O$ data (Figure 12). The most depleted values of $\delta^{18}O$ were measured in rivers (Table 1), which is then mixed with coastal nearshore waters, and $\delta^{18}O$ increases with the contribution of more saline waters at depth offshore (Figure 12, Appendix Table 3) (Azetsu-Scott et al. 2012). Note that the zero-salinity intercept of -15.58 ‰ is consistent with that measured by Kerrigan et al. (2017) (-15.55 ‰) and Fairbanks (1982) (-15.55‰).

The Nova Scotia Current travels southwest along the length of the Scotian Shelf (Figure 1b), carrying waters predominantly mixed with slope waters influenced by outflow from the Gulf of St. Lawrence (Hebert et al. 2023). These Gulf of St. Lawrence waters are a mix of terrestrial runoff and marine sources, and of increasingly warmer conditions, with persistent acidic and corrosive (Ω_{arag}) waters with hypercapnic (in situ pCO_2 >1000 μatm) and chronically low oxygen conditions, tending to hypoxia (Lizotte et al. 2026). Local variability in the circulation in the nearshore environment is evident in the alongshore view of the temperature and salinity, where freshest surface waters were measured (near 30 psu) in the surface waters directly off **Ketmenipukwek** Ship Harbour (Figure 5, Figure 10).

NUTRIENT DYNAMICS

Nutrient profiles at river and marine sample sites were consistent with expectations for these environments in the summer, with the river waters silicate and/or phosphate limited and the marine waters nitrogen limited. Silicate concentrations in rivers in the Southern Uplands are low relative to available marine silicates, which is consistent with observations in and around **Ketmenipukwek** Ship Harbour in the 1990s (Strain 2002). The coastal filter, consisting of subtidal sediments and marine plants such as seagrasses, reduces the amount of anthropogenic nutrient inputs from land into the ocean, and marine phytoplankton and plants trap nitrogen (in the form of ammonium and nitrates) through assimilation, burial, and denitrification. Eelgrass meadows are widespread in the ESI, which contribute largely to the coastal filter function and reduction of nitrogen in the water column in the summer (e.g., Aoki et al. 2020). Previous studies have also demonstrated that archipelagos are particularly effective in trapping and retaining phosphorus, which may also be expected of the dense archipelago of the ESI (Asmala et al. 2017). Marine water samples of the AOI were nitrogen limited, as is typical of Atlantic coastal waters in summer (Blais et al., 2024).

Marine samples showed near complete drawdown of nitrate in surface waters, consistent with a healthy coastal environment in summer months as biological activity uses nitrate for processes such as primary production. The nutrient data provided no evidence of coastal eutrophication in the AOI during the sampled periods.

COASTAL AND FRESHWATER CARBONATE DYNAMICS AND OCEAN ACIDIFICATION

Parameters of the marine carbonate system were used to measure and monitor ocean acidification, included TA, DIC, and $pCO_{2,}$ derived pH_T and the saturation state of aragonite and calcite (Ω_{arag} and $\Omega_{arag,}$ respectively) (Appendix Table 2) . Although there were limited observations along the Scotian Shelf in 2021, our data were consistent with measurements from nearby Scotian Shelf monitoring stations near Halifax (HL_01 and HL_02), and with regional data across the Atlantic Zone more broadly (Gibb et al. 2023). The lowest DIC and TA concentrations and highest pH and Ω_{arag} and Ω_{calc} values occurred at the surface. However, deeper waters below 50 m exhibited the lowest pH values measured and Ω_{arag} less than 1, indicating corrosive conditions for calcifying benthic organisms (Barclay et al. 2026). Overall, the measurements indicate the presence of adverse chemical conditions in bottom waters, and in particular, at the offshore end of each of the transects.

Dissolved oxygen concentrations were lower than the theoretical potential oxygen concentrations in the top 25 m, as shown by calculations of apparent oxygen utilization (AOU) (Appendix Table 3). A negative AOU above 25 m indicates a dominance of photosynthesis in surface waters above the halocline, whereas the positive AOU below 25 m, indicates a consumption of oxygen with remineralization, which also coincides with observed increases in nitrate, phosphate, DIC, and a decrease in pH_{total} and Ω_{arag} and Ω_{calc}, especially notable 15-20 km offshore. These trends are consistent with other studies (Thomas et al. 1999; Lehmann et al. 2023), and with the observed ocean acidification metrics from 2021 for the Gulf of St. Lawrence (Gibb et al 2023). The waters that flow along the Scotian Shelf are primarily derived from the warm and organic matter rich environment of the Gulf of St. Lawrence, factors which would also serve to enhance remineralization rates in the coastal waters of the Eastern Shore Islands. Despite these trends, dissolved oxygen concentrations were not low enough to be considered hypoxic.

A further consideration here is the impact of freshwater inputs on the water chemistry. Rivers carry terrestrial run-off, which can lower TA in coastal and nearshore environments, thus reducing the system's buffering capacity with respect to acidification. Local DIC concentrations can also change through uptake of CO_2 by primary producers and from coastal run-off (along with TA and nutrients). Indeed, variability was observed when comparing the alongshore patterns for the closest sampling sites for each transect (Figure 10). Notably, the lower TA observed in these two sites did not necessarily indicate a reduced buffering capacity, as these sites had higher pH and Ω_{arag} than **Weijuik** Sheet Harbour and **Winipukwejk** Jeddore. These

trends were less apparent in the farthest alongshore transect (35 km offshore) (Figure 11).

The observed reduction in salinity (freshening) and in temperature at the surface could indicate a larger influence of freshwater river inputs along these transects (**Ketmenipukwek** Ship Harbour and **Nukumkiaq** Moser River), but can also be explained by variability associated with complex nearshore ocean circulation associated with the complex coastline (e.g., Feng et al. 2022) and variable runoff. Indeed, the watersheds of the three rivers were distinct and varied in size and geomorphology, , with **Nukumkiaq** Moser River as the slowest flowing river with the smallest drainage basin dominated by wetlands, and **Napu'saqnuk** St. Mary's River at the other extreme, which drains a notable proportion of freshwater from the Eastern Nova Scotia Uplands. Of the three rivers, **Napu'saqnuk** St. Mary's River had the most depleted $\delta^{18}O$ values, which matched the value for precipitation reported by Kerrigan et al. (2017) in the Bedford Basin (~-7 ‰). In contrast, the slow moving waters of **Nukumkiaq** Moser River would reflect the ^{18}O enrichment that results from evaporation from a small watershed in a wetland-dominated system (Gramillion and Wanielsta 2000). Moreover, the transport across the land-to-ocean interface alter both DIC and TA through various processes, thus highlighting the importance of local variability in the transformations of the marine carbonate system across is continuum (Cai et al. 2011, Yin et al. 2024). Repeated sampling is recommended in order to tease out local drivers of the variability.

Methane concentrations also showed high variability along the inshore sample stations, where the concentration of CH_4 was highest in **Weijuik** Sheet Harbour, with some elevated measurements also present at nearby **Ketmenipukwek** Ship Harbour. The most extreme value was measured in the sample from the St. Mary's River (>18,000%, Table 1). Coastal nearshore environments are known to produce hotspots of this potent greenhouse gas through methane seeps and methanogenesis in estuaries and areas with high organic matter (Borges et al. 2016). We note that there may also be a connection between high nutrient concentrations and dissolved CH_4 at these sites, supported by recent research indicates that microbial processes drive increased methane emissions with high nutrient availability (Wang et al. 2026).

The pH values observed across all three rivers were highly acidic and notably within the range known to impair juvenile salmon survival. Despite the presence and contribution of lime from the West River and Killag River lime dosers, West River, **Weijuik** Sheet Harbour had the lowest pH_{NBS} (4.00) relative to **Napu'saqnuk** St. Mary's (4.75) and **Nukumkiaq** Moser (4.16) rivers at the time of sampling (Table 1). Such low pH values (an accompanying low alkalinity and DIC) are typical of freshwater systems in Nova Scotia, which are among the most acidic in North America, primarily due to extremely poor buffering capacity offered by the surficial geology (Clair et al., 2007); in fact, calculated TA based on the pH and pCO_2 was nominally zero.

The low pH at West River, **Weijuik** Sheet Harbour observed in August of 2021 reflects conditions at the time of measurement when the lime dose rate was near the seasonal minimum and proportional to the discharge of a post-storm flow recession.

If we assume a dosing rate of 1.5 tonnes of dolomite lime ($CaCO_3$, 100.09 g mol^{-1})) added per day, this equates to a contribution of ~12,000 moles of $CaCO_3$ per day, or ~24,000 equivalents of alkalinity per day. Over the 54 day residence time of the **Weijuik** Sheet Harbour estuary (Gregory et al., 1993), this daily input totals ~1.3 x 10^9 milliequivalents of alkalinity. Dividing this total by the estuary volume (1.06 x 10^8 m^3, Gregory et al, 1993) yields the potential impact on the order of 9.7 μmol alkalinity per kg seawater, a back of the envelope estimate. This value is just above the measurement precision for total alkalinity (better than 3.5 μmol kg^{-1}) and it would be therefore difficult to detect an impact. Moreover, since dosing is scaled with the rivers' discharge, the lime inputs to the estuary would vary seasonally and due to storm events, making detection of this subtle signal even more challenging given natural variability. Note that this calculation doesn't consider several important factors: the spatial heterogeneity of the freshwater plume (alkalinity would be concentrated near the river mouth), tidal mixing and dynamics of freshwater stratification, an absence of in-river transformations of the added $CaCO_3$ and an assumption of 100% solubility of the limestone. Sampling the estuary more frequently across seasons and tidal cycles would be required to help resolve whether there is a measurable impact of river liming on the marine carbonate system in the estuary and beyond.

The detection of eDNA from Atlantic Salmon in the AOI (this study), coupled with their detection in adjacent rivers and associated water quality measurements (Montgomery et al. 2020) reinforces their ongoing, seasonal use of the coastal marine zone in the AOI as migratory habitat. While marine pH levels recorded in the AOI are higher and more stable than in the freshwater environment, the transition from acidic freshwater (pH<4.5) to the marine environment can introduce a period of increased osmotic stress for out-migrating smolts. This physiological challenge is further exacerbated by the mobilization of inorganic aluminum in the rivers, which can impair gill function and reduce the success of seawater acclimation (Farmer 2000). Consequently, though the AOI includes a key transition area, survival in this zone may be impacted by the quality of freshwater habitats of contributing watersheds. Although the sampled rivers lie outside the AOI boundaries, their close proximity, including their location within the same or adjacent watersheds to rivers flowing into the AOI, suggests connectivity through freshwater discharge, which can influence coastal nutrient and carbonate dynamics and habitat conditions for migrating Atlantic Salmon and other diadromous fishes.

Similar pH and saturation state of aragonite profile patterns were observed across all transects, supporting the conclusion that terrestrial and freshwater liming efforts of the adjacent watershed did not substantially alter offshore carbonate conditions at the temporal and spatial scales that were sampled. Relatively higher pH values or increased saturation state of aragonite would have lent support for an influence of terrestrial and freshwater liming efforts nearshore at this time of year.

The sampling design was deemed adequate for resolving the variability in physical and chemical parameters through depth and along the transects. However, repeat monitoring of the site would help to disentangle the impacts of river run-off contributions to coastal carbonate chemistry from those arising from variability in ocean circulation. Moreover, this study provides evidence for the influence of slope water on nearshore waters carried by the Nova Scotia Current below 40-50 m depth (at the farthest sites, 20-30 km offshore).

EDNA METABARCODING AND BIODIVERSITY

The fish species detected by eDNA from 2021 to 2023 were consistent among years and included common species such as Atlantic Herring, Atlantic Mackerel, Atlantic Saury, Cunner, Pollock, various flatfishes, gunnels, sand lances, and other gadids. There were, however, some unique species detections in each year, including Moonfish in 2021 (detected with both the 12S and 16S markers), Grey Triggerfish and Basking Shark in 2022, and multiple unique species in 2023, such as Eelpout (*Zoarces americanus)* and several freshwater and diadromous fish species, which were detected more frequently because of the seasonal sampling coverage in 2023. The higher species richness in 2023 in general may have been because of a higher volume of water sampled relative to 2021/2022 (3 L vs. 1 L respectively), the seasonal component of our sampling, or the change in filter size (Gómez-Repollés et al. 2026). The 16S fish marker was only used in 2021 and 2022, where results were similar between 12S and 16S in 2021; however, in 2022, several shark species were detected including Blue Shark, Common Thresher Shark, Porbeagle, and Spiny Dogfish.

In 2021, the surface samples largely overlapped with the benthic samples in Jaccard community similarity, although the benthic samples showed greater variation in community composition among samples (Figure 16). In contrast, pelagic samples were more consistent in composition, reflecting the predominance of the same pelagic species across samples, particularly Atlantic Herring, Atlantic Saury, and Atlantic Mackerel. In 2022, surface and benthic samples again showed substantial overlap in community composition, although surface samples exhibited greater variation than in 2021 (Figure 18). The observed overlap between surface and benthic samples in both years suggests that sampling either layer can capture broadly similar fish communities. These small but significant interannual differences could reflect real fish community differences at the times of sampling, or could reflect potential methodological differences between years. However, both the field and laboratory methods were the same between these years, aside from in 2022 when samples were thawed and filtered sooner than in 2021, which could lead to different rates of DNA degradation (Stica et al. 2025).

The inter-annual difference in fish communities documented here demonstrate the importance of long-term time series data for identifying trends in community composition. Previous studies have shown that eDNA communities can vary significantly between year, months, and even between days sampled within a week (Sevellec et al. 2025). While detecting change at the community level among months or

seasons can be expected, interannual differences in communities sampled at the same time of year are more difficult to interpret. Ip et al. (2023) showed that eDNA is a reliable tool for detecting coral spawning events and associated fish species over a three-year time series, and could infer day- versus night-spawning species. However, as noted by Sevellec et al. (2025), eDNA sampling between years and broad spatial scales, like other sampling methods, only reflects a fraction of the total organismal diversity of the ecosystem, therefore interannual differences can be expected. For marine eDNA sampling, it is particularly important to consider the variability in ocean temperature and biochemical conditions, as well as tide cycles, currents, and storm events, all of which can impact eDNA results and the objective of creating long-term time series.

As with other ecological monitoring approaches, establishing a robust baseline for eDNA requires several years of consistent sampling. The additional influence of environmental conditions on eDNA transport, persistence, and detection, combined with natural variation in species presence within a dynamic marine system, may contribute to greater interannual variability in eDNA observations in comparison to direct sampling approaches (e.g., nets, pots, seines). Continued, standardized sampling over longer time periods will therefore be important for distinguishing natural variability from persistent changes in community composition and for determining whether meaningful trends can be detected.

In 2023, we were able to detect seasonal differences in fish communities, with spring and fall having more dissimilar communities (i.e., less overlap in the NMDS space), while the summer samples overlapped with the spring and fall. We were also able to discriminate sample stations along the **Weijuik** Sheet Harbour transect, showing an inshore-offshore transition spanning stations ESI-05 to ESI-08 (Figure 28). An alluvial plot of the most common fish species (those with >8000 eDNA reads) show which fish species were present at which sample station and in which season (Figure 25). Some species were only detected in the inshore stations (ESI-05 and ESI-06), which included Cunner, Winter Flounder, and Atlantic Salmon. White Sucker were the most abundant freshwater species detected, though they were only found at ESI-05 which is the closest to the **Weijuik** Sheet Harbour estuary. Other species were found at all stations and in all seasons, including Atlantic Herring, Atlantic Mackerel, Atlantic Cod, and Rock Gunnel (Figure 25). Our results indicate the need for consistent field and laboratory methods to capture and process eDNA to create a robust time series for monitoring. Although our field methods changed between 2021/2022 and 2023, we were able to detect the most common species each year, and were able to detect seasonal and spatial differences in fish communities with eDNA metabarcoding.

The invertebrates detected with the COI marker in 2022 and 2023 were similar, with phytoplankton and a variety of copepods being the most abundant species captured. The calanoid copepods detected with eDNA included numerous genera found in the North Atlantic Ocean, including *Acartia, Calanus, Clausocalanus, Pseudocalanus, Centropages, Metridia,* and *Tortanus,* and the cyclopoid genus *Oithona* (Beaugrand et al. 2002, Albouy-Boyer et al. 2016). Other common invertebrates detected included polychaete worms, snails, barnacles, echinoderms, and the invasive bryozoan *M. membranacea*.

M. membranacea encrusts on numerous kelp and algae species, which can lead to defoliation of macroalgae and reduce canopy cover (Attridge et al. 2022). This invasive bryozoan was detected across the AOI in 2022 and 2023, where kelps and macroalgae are abundant and widely distributed. In addition to *M. membranacea*, several invasive seaweeds were also detected. *Bonnemaisonia hamifera* and *Dasysiphonia japonica*, both invasive red algae, were found within the AOI in 2022 and 2023 when the COI marker was used. Our offshore samples in this study did not detect other invasive species previously found using eDNA in the shallow subtidal bays of the AOI, including *Botrylloides violaceus* (Violet Tunicate)*, Juxtacribrilina mutabilis* (an encrusting bryozoan), *Carcinus maenas* (European Green Crab), and *Polydora onagawaensis* (a shell-boring invasive polychaete worm) (Trask et al. 2025). Our results reinforce the use of eDNA for detecting aquatic invasive species, particularly in the offshore subtidal environment where monitoring using collection plates does not occur (e.g., Sephton et al. 2017).

While these results provide useful baseline information on biodiversity in the area, they also highlight the variability in community composition among years. Developing a long-term biodiversity time series using a new monitoring approach may therefore benefit from combining eDNA with conventional sampling approaches, particularly during the initial years of monitoring. Conventional, direct-observation methods can provide an independent reference against which early eDNA observations can be evaluated (e.g., He et al. 2022; 2023; Trask et al. 2025), helping to establish the ecological context for subsequent changes detected through eDNA. A multi-marker approach could further broaden taxonomic coverage and improve the consistency of detection across taxa. If a single fish eDNA marker is selected for cost-effectiveness, the various primers for targeting fish should be tested *in silico* or with local environmental samples to examine their efficiency for local taxa. Primer sets and markers for fish can vary vastly in their efficiency and selectivity for different fish taxa (e.g., cartilaginous versus bony fishes), which should be considered for long-term monitoring (Kumar et al. 2022).

LINKAGES BETWEEN THE ENVIRONMENT AND BIOLOGICAL COMMUNITIES

In our study, we measured chemical oceanographic parameters and ocean temperature with the goal of linking these data to the biological communities and diversity of the AOI. The AOI receives freshwater inputs from multiple rivers and water masses from the Gulf of St. Lawrence transported by the Nova Scotia Current with incursions of deep slope water. Mixing of these water masses and seasonal stratification produce spatial and temporal gradients in salinity, temperature, and pH which, along with water depth, determine the distribution of species assemblages across the AOI and broader Scotian Shelf. The low aragonite saturation levels and low pH in the deepest parts of our sampling transects are potentially corrosive to calcifying organisms, including molluscs, bryozoans, crustaceans, and calcareous sponges. The stress these conditions induce in these organisms can result in reduced growth and developmental rates, and impact shell hardness (Puerta et al. 2020). Repeat sampling of these deep portions of the AOI could help monitor the health of commercially important stocks, such as American Lobster and Sea Scallop.

Surface waters and sampling stations closer to river inputs showed lower salinity than offshore deeper waters as expected. Freshwater (e.g., White Sucker, Creek Chub, Yellow Perch, and Brown Bullhead) and estuarine fish (e.g., Tomcod, sticklebacks, and killifish) eDNA is typically only found at nearshore stations, where these species are either present or their DNA is transported by river outflows and detected during sampling. Most diadromous species, including Brook Trout, Atlantic Salmon, American Eel, and *Alosa* spp. were similarly detected at the more inshore stations (ESI-05 and -06), though *Alosa* eDNA was also detected at ESI-7 and -08 in the spring and fall.

Several marine species were found at all stations, including Mackerel, Atlantic Herring, Atlantic Cod, Silver Hake, and Rock Gunnel. Others, such as Acadian Redfish and American Plaice, were detected at all stations except the shallowest (ESI-05). Several species were only found in one season and at one site, include Haddock (*Melanogrammus aeglefinus*; detected in spring at ESI-08), Right Whale (detected in fall at ESI-05), and Basking Shark (detected in fall at ESI-07). These limited detections reflect the rarity of these species in the AOI, and also their lifestyle in the North Atlantic. Haddock are a demersal fish on the Eastern Scotian Shelf that are typically found between 30 and 180 m depth, but were depleted along with Atlantic Cod by the early 1990s and currently remain under a fisheries moratorium (Rincón and Kenchington 2016). Right Whale, which are listed as Endangered under the *Species At Risk Act*, typically migrate from southern calving grounds to foraging grounds in the Gulf of St. Lawrence, where they reside in the summer and fall and feed on Calanoid copepods (Crowe et al. 2021). Our eDNA detections in fall 2023 may have thus detected an individual migrating through the Eastern Scotian Shelf or foraging near the AOI.

RECOMMENDATIONS FOR FUTURE SAMPLING AND MONITORING

As an identified AOI, the area will benefit from monitoring of its conservation priorities to support ongoing research and conservation. Monitoring data consists of an adequate baseline and time-series to measure potential change in indicators linked to the conservation priorities. A monitoring program for the ESI could include numerous methods and data sources, but would likely focus on the animal diversity associated with the diverse habitats within the area, its biogenic habitats including kelp forests and Eelgrass meadows, and monitoring abundance of Atlantic Salmon. Offshore eDNA samples have not been collected in the ESI since 2023, though nearshore sampling associated with beach seining has continued at reference stations at Little Harbour, Taylor Head Provincial Park, and Moosehead Cove. This study provides an important and novel baseline for coastal eDNA biodiversity monitoring and a foundation for developing future long-term monitoring in the coastal area, including within the AOI. Ideally, future eDNA sampling would be conducted consistently at the same transect locations to build a time series of species richness and community composition, tracking changes from inshore to offshore and providing a basis for detecting and interpreting change over time.

Sensors and autonomous samplers are now available for both monitoring ocean chemistry (e.g., the carbonate system, temperature, salinity, etc.) and for collecting eDNA samples, which could reduce the need for research vessel time, especially in remote areas. At an international scale, the Biogeochemical Argo project is developing

and deploying a network of autonomous profiling Argo floats, which include physical, chemical, and optical sensors to measure ocean properties at the surface and various depths (Chai et al. 2020). Van Wyngaarden et al. (2024) have demonstrated the application of autonomous eDNA samplers developed in Nova Scotia, Canada, for multi-week sampling in the coastal ocean. Combining autonomous eDNA samplers with oceanographic instruments could be a cost-effective method for long-term monitoring in the coastal ocean, with minimal input from personnel beyond deploying and retrieving equipment. In areas such as the Eastern Shore Islands, these approaches could complement traditional vessel-based surveys by enabling more frequent sampling and continuous or fine-scale temporal observations, providing greater capacity to capture seasonal dynamics and short-term changes in environmental conditions and biodiversity.

Of note, the COI assays applied in this study did not detect commercially important macroinvertebrates that are known to occur in the AOI, including Sea Scallop, Lobster, Rock Crab, and Jonah Crab. Lobster, which support a key commercial fishery in the Eastern Shore, in particular are prevalent throughout the AOI. Their lack of eDNA detection is likely the result of numerous factors, including primer-template mismatches, where these decapod and bivalve species are not amplified, or their eDNA is not amplified due to the hyper-abundance of phytoplankton and zooplankton using the majority of primer oligos and PCR reagents (Ren et al. 2025). eDNA from thick-shelled benthic invertebrates, including decapods, seems to be less abundant in the water column relative to soft-bodied animals, and so detections of these species of interest may be more reliable from sediment samples or during moulting and spawning periods when cells, larvae, and gametes are in the water column (Crane et al. 2021). Different sampling strategies or more targeted eDNA primers will be required if detections of these species are a priority.

The Nova Scotia Salmon Association operates lime dosers on the West River, **Weijuik** Sheet Harbour and the Killag River, which include hydrology monitoring. Integration of these datasets with future AOI surveys would improve the ability to attribute coastal carbonate variability to upstream liming relative to natural hydrological variability. Future surveys aimed at detecting a liming influence on coastal carbonate chemistry should be timed to cover additional seasons to assess the influence of different discharge levels, dose rates, and lake residence time. For example, depending on dose rates, sampling during the spring freshet, when the river system discharge is highest and the effective lake residence of **Weijuik** Sheet Harbour Lake is shorter as a result of high flow, could provide a more sensitive detection period for inshore stations (i.e., ESI-00 and ESI-5).

This study provides baseline characterization of the physical and chemical environment in the AOI alongside a multi-year environmental DNA time series describing biological communities. Together, these results demonstrate how discrete water sampling can provide integrated information on both environmental conditions and biological community composition. Establishing a baseline for TA and DIC, alongside temperature, salinity, nutrients, and other environmental variables, provides a foundation for characterizing natural variability, including seasonal influences such as spring freshets, and for detecting longer-term changes associated with anthropogenic ocean acidification and other environmental pressures. Ocean chemistry data have not been

collected in the offshore portion of the AOI since this 2021 mission, aside from temperature and conductivity profiles available from CTD casts in subsequent years. Repeat sampling for chemical properties at regular intervals (e.g., 5 year cycle) could help assess changes in temperature, nutrient levels, aragonite saturation, and other physical and chemical ocean properties over time. Although no clear relationships were detected between eDNA-derived animal communities and the environmental properties of the water, collecting physical, chemical, and biological data remains valuable because it provides a more integrated picture of ecosystem state and establishes the environmental context needed to interpret changes in biodiversity and marine communities over time. The ongoing effects of a changing climate further emphasize the importance of tracking both environmental conditions and biological communities together, allowing changes in ecosystem state to be detected and interpreted within the context of a changing marine environment.

ACKNOWLEDGEMENTS

We thank the crews of the CCGS *M. Perley* for their assistance with at-sea sampling operations; staff at the Centre for Environmental Genomics Applications (St. John's, Newfoundland) and the Aquatic Biotechnology Laboratory (DFO, Dartmouth, Nova Scotia) for eDNA sequencing; and the Nova Scotia Salmon Association for providing liming and hydrology monitoring data. We are grateful to Lindsay Beazley and Elise Will (DFO Maritimes Region) for their helpful comments to improve the initial draft.
This research was funded by the DFO Marine Conservation Targets program.

TABLES

*Table 1. Physical and chemical data for 3 rivers (**Napu'saqnuk** St. Mary's River, Sherbrooke; West River, **Weijuik** Sheet Harbour; and **Nukumkiaq** Moser River) located within the Eastern Shore Islands Area of Interest on August 13, 2021. Sampling locations are shown in Figure 1. DIC = total inorganic carbon, TA = total alkalinity, AOU = apparent oxygen utilization.*

Parameter	Napu'saqnuk St. Mary's River	West River, Weijuik Sheet Harbour	Nukumkiaq Moser River
Temperature (°C)	25.7	23.9	22.7
Salinity (psu)	0.024	0.022	0.022
pH (NBS scale)	4.752	4.004	4.156
DIC (μmol kg^{-1})	191.34	155.11	194.70
TA_{calc} (μmol kg^{-1})	nominal	nominal	nominal
pCO_2 in situ (μatm)	2964.6	789.9	1200.5
CH_4 Saturation (%)	18698.0	3084.2	503.1
Dissolved Oxygen (μmol kg^{-1})	240.1311	266.9341	251.9496
AOU (μmol kg^{-1})	15.5556	-2.6971	18.2418
$\delta\ ^{18}O$ (‰)	-7.30	-6.06	-6.63

Table 2. The eDNA primer sets, their target taxa, and references for each year of eDNA analyses.

Primers	Year(s)	Target Taxa	Reference
MiFish-U-F/R	2021, 2022	Fish (12S gene)	Miya et al. 2015
MiFish-U-248_F/R	2023	Fish (12S gene)	He et al. 2022
16SFish	2021, 2022	Fish (16S gene)	McInnes et al. 2016
LerayXT	2022	Eukaryotes (COI gene)	Wangensteen et al. 2018
Leray	2023	Eukaryotes (COI)	Leray et al. 2013

FIGURES

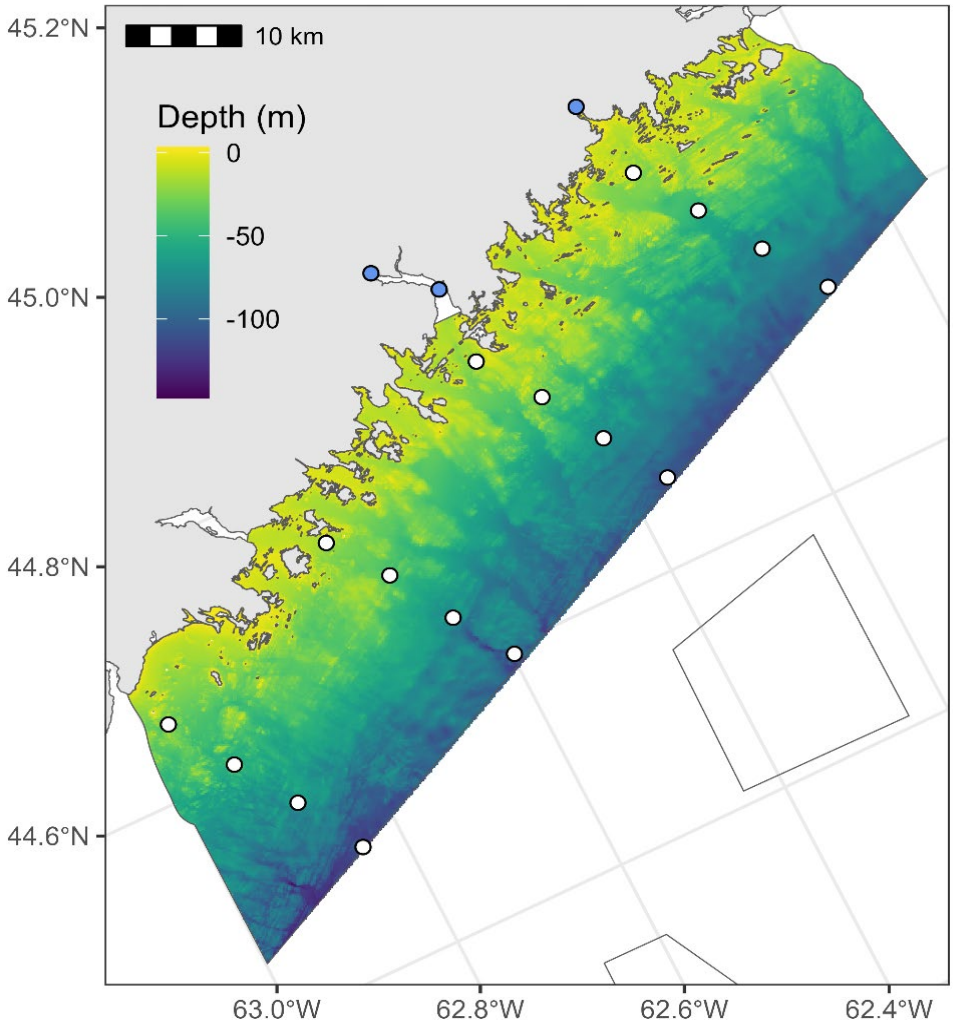


*Figure 1. Location of seawater sampling sites taken between August 9 and 14, 2021 following a 4x4 transect design spaced 65km alongshore and 20km from the nearshore to the outer boundary of the AOI (white circles). The same four transects were sampled in 2022 and 2023 for environmental DNA only. Additional samples were taken from three third-order river sites (**Napu'saqnuk** St. Mary's River (not shown, 45.1742° N, -61.9797° W); **Nukumkiaq** Moser River; and West River,**Weijuik** Sheet Harbour and ESI-00; blue circles) in the Eastern Shore Islands Area of Interest (AOI). Locations overlaid on a 10 m resolution bathymetry raster masked to the extent of the AOI. Draft network sites denoted by polygons with black borders.*

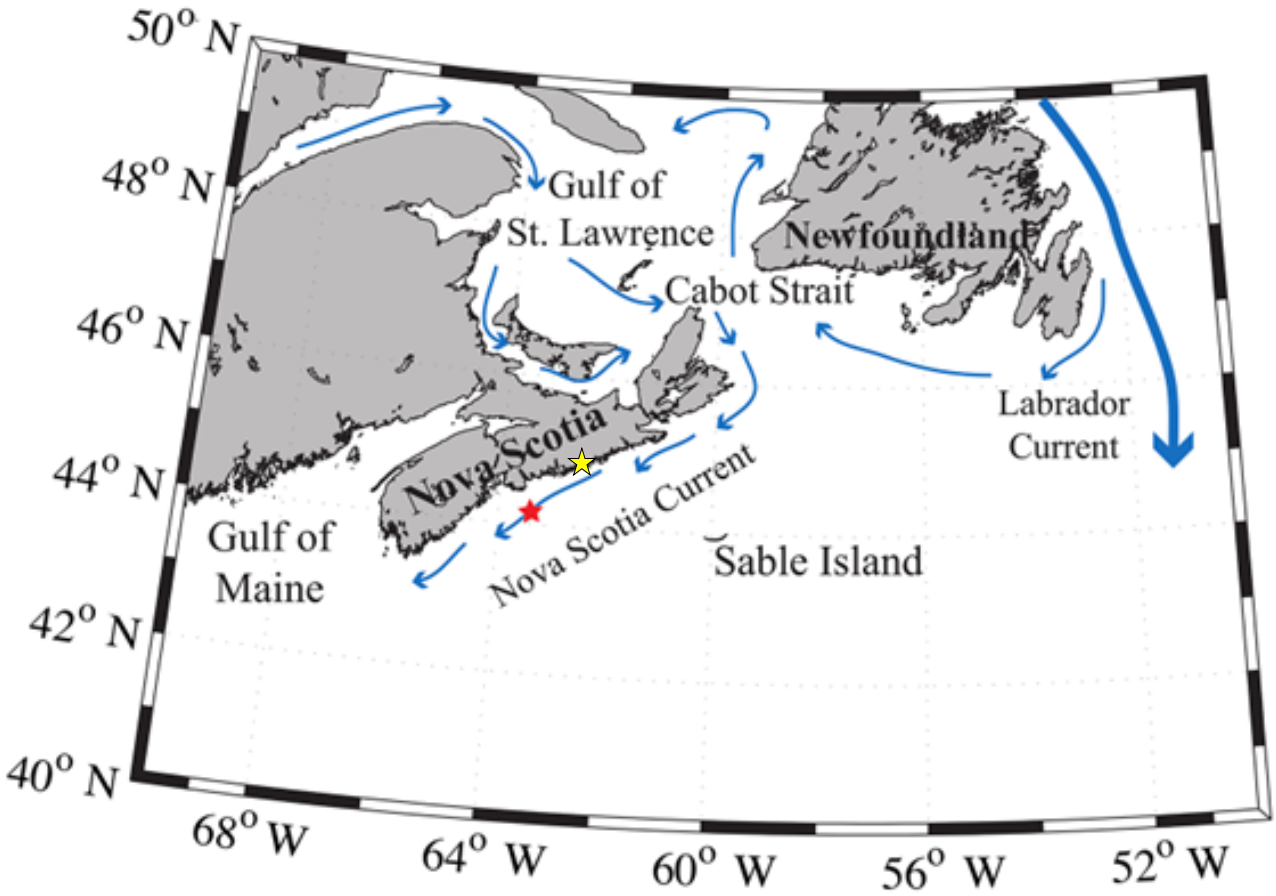


*Figure 2. Map of the Atlantic Zone of Eastern Canada, showing ocean currents in blue. A yellow star indicates the location of the Eastern Shore Islands Area of Interest (AOI), and a red star at HL_2, fixed station monitoring site off **Kjipuktuk** Halifax, Nova Scotia. Figure modified from Lemay et al. (2018).*

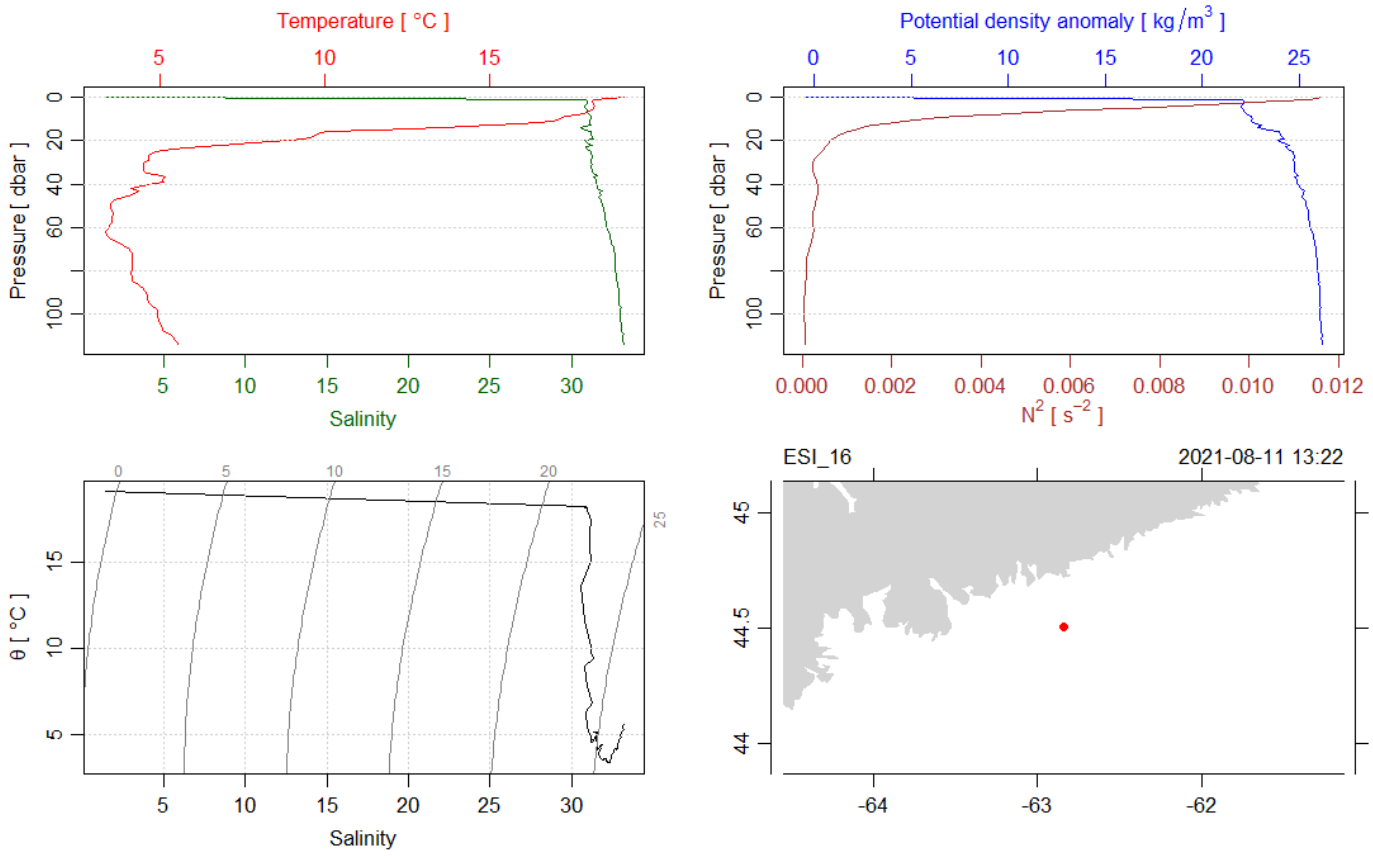


Figure 3. An example CTD profile from August 11, 2021, at station ESI_16. The top left panel shows the temperature and salinity profiles with depth, while the top right panel shows the potential density anomaly of water and the square of buoyancy frequency (N^2) profiles with pressure. The bottom left panel shows conservative temperature (θ) plotted against salinity, and the bottom right panel shows the CTD profile location offshore of Nova Scotia. All plots are derived from the oce R package (Kelley and Richards 2024).

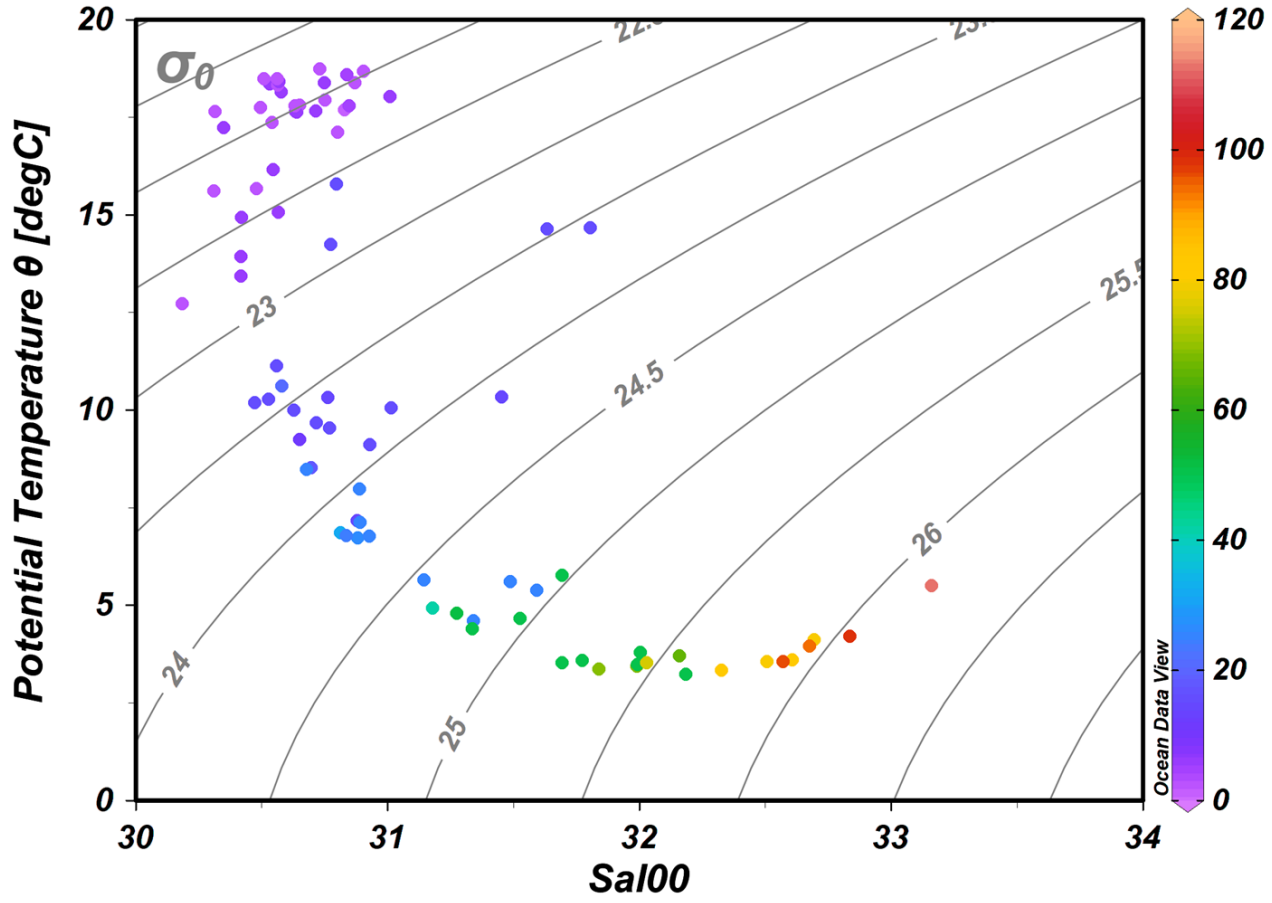


Figure 4. T-S diagram with isopycnals for data from all stations sampled between August 9 to 14, 2021 from the along the Eastern Shore Islands AOI transects in Figure 1. Each point's colour represents the depth the sample was collected (legend at right).

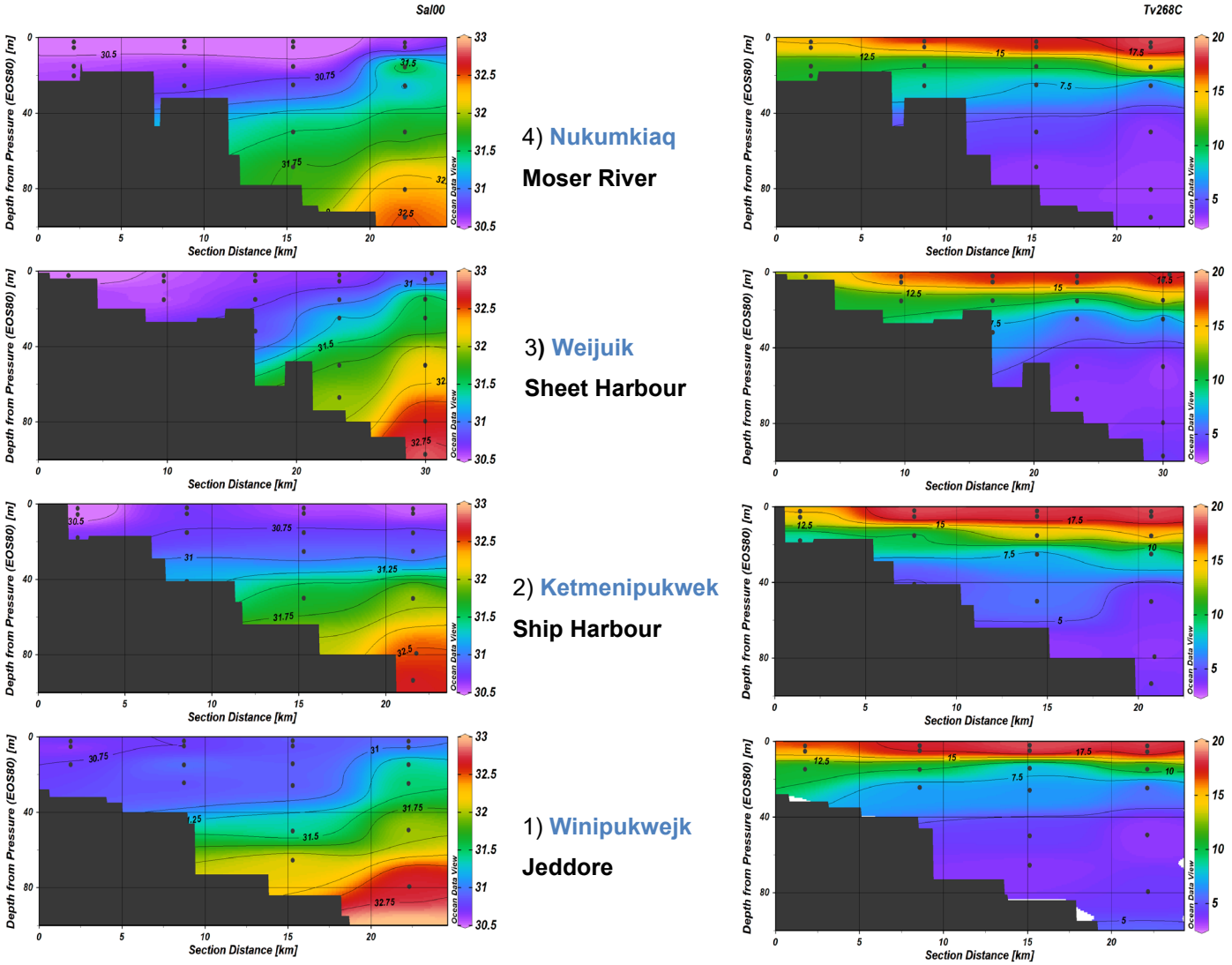


Figure 5. Section plots of salinity (Sal00, left) and temperature (Tv268C, right) data, including bathymetry, for 4 transects sampled between August 9 and 14, 2021. The discrete sample locations through depth are indicated with black dots. The x-axis denotes the section distance along the transect, extending from inshore to offshore. Salinity is lowest at the surface and highest in the deepest areas of the transects, while temperature is highest at the surface. Evidence of a cold intermediate layer is shown in the temperature plots as purple colouring.

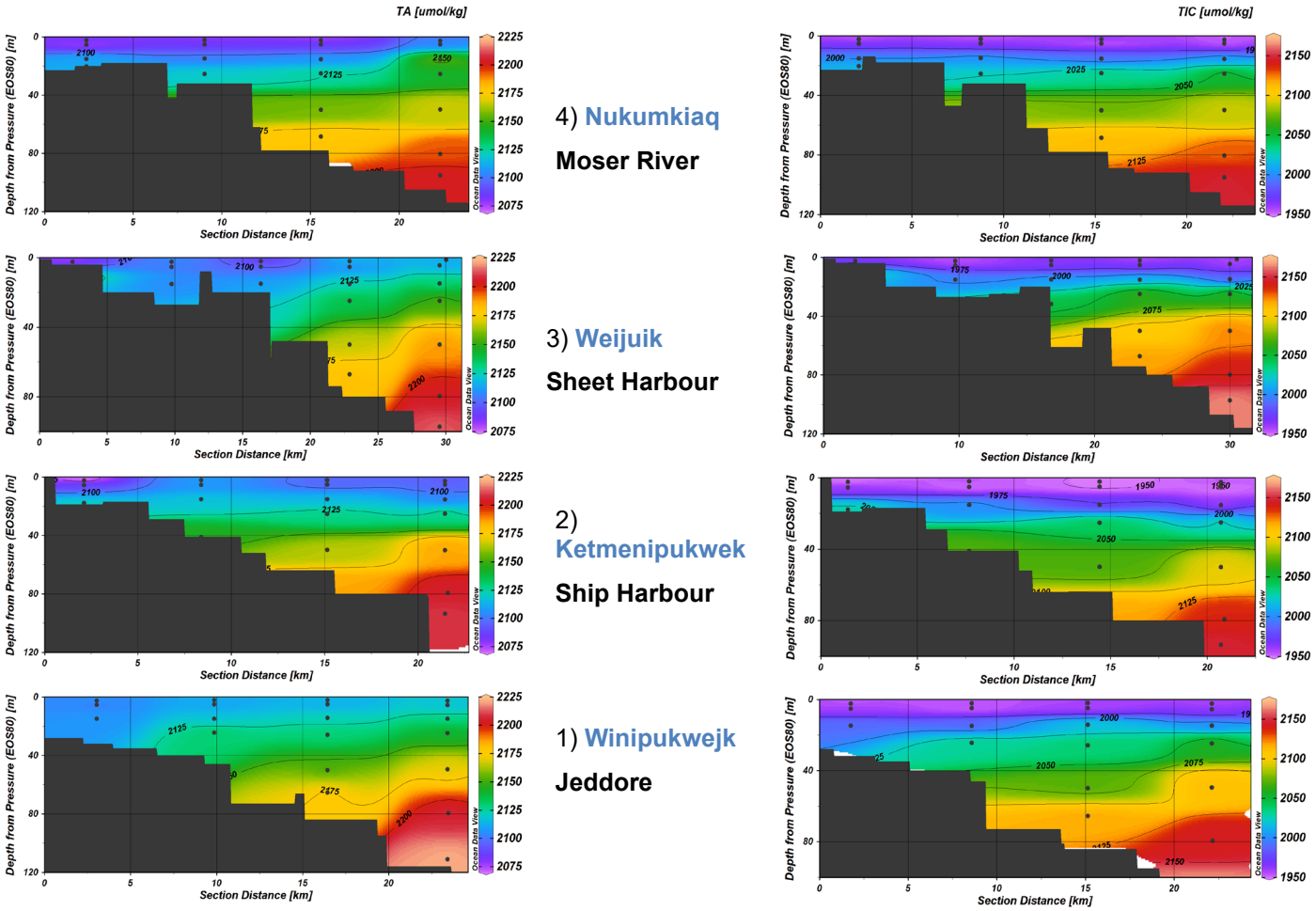


Figure 6. Section plots of total alkalinity (TA, left) and total dissolved inorganic carbon (TIC, right) data, including bathymetry, for 4 transects sampled between August 9 and 14, 2021. The discrete sample locations through depth are indicated with black dots. The x-axis denotes the section distance along the transect, extending from inshore to offshore. A general increase in both TA and TIC as depth increases is shown.

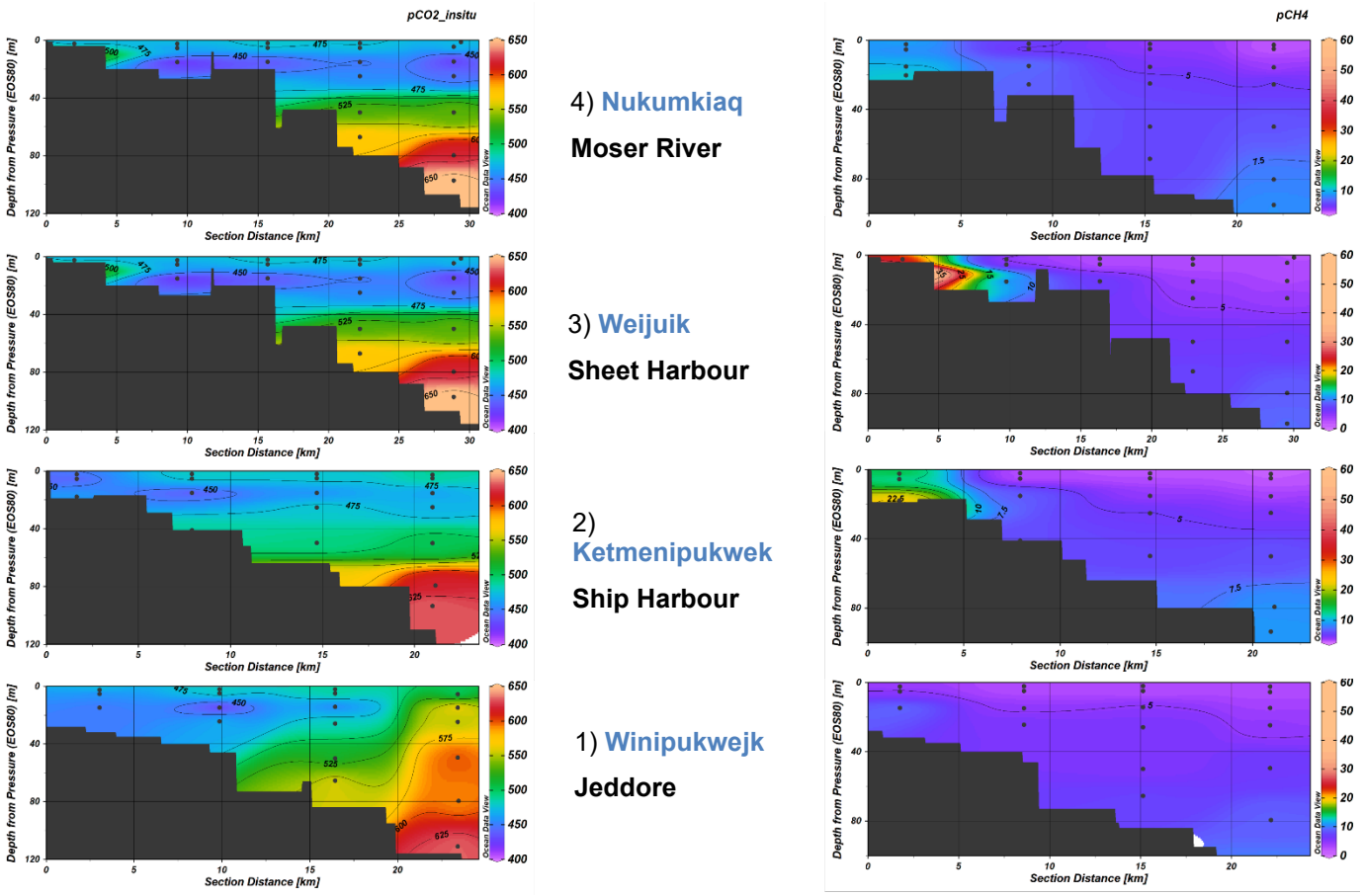


Figure 7. Section plots of data, including bathymetry, for 4 transects sampled between August 9 and 14, 2021 showing pCO_2 (left) and CH_4 (right) along the 4 study transects, enumerated on each plot. The discrete sample locations through depth are indicated with black dots.

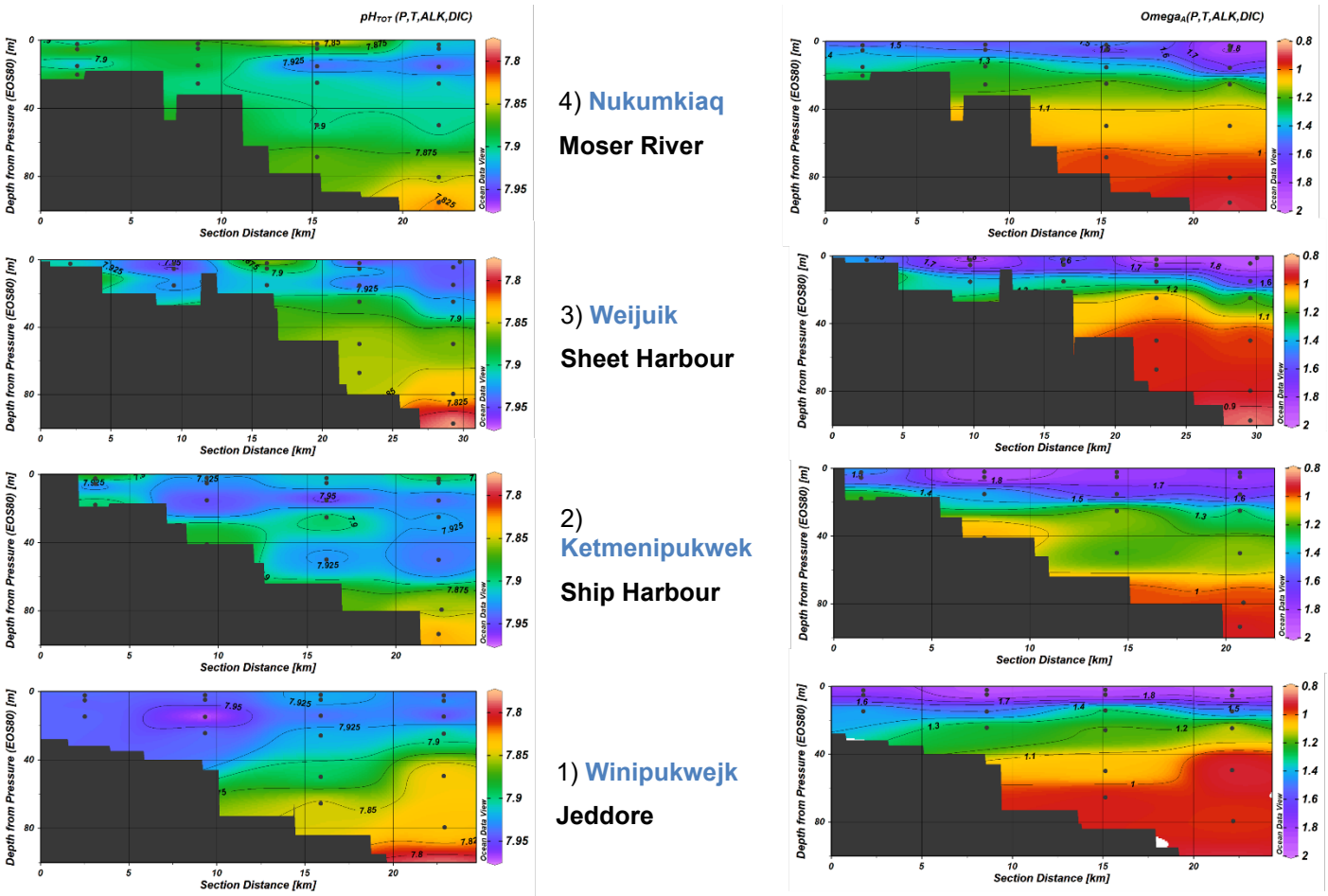


Figure 8. Section plots of data, including bathymetry, for 4 transects sampled between August 9 and 14, 2021 showing pH (left) and Ω aragonite saturation (right) along the 4 study transects, enumerated on each plot. The discrete sample locations through depth are indicated with black dots.

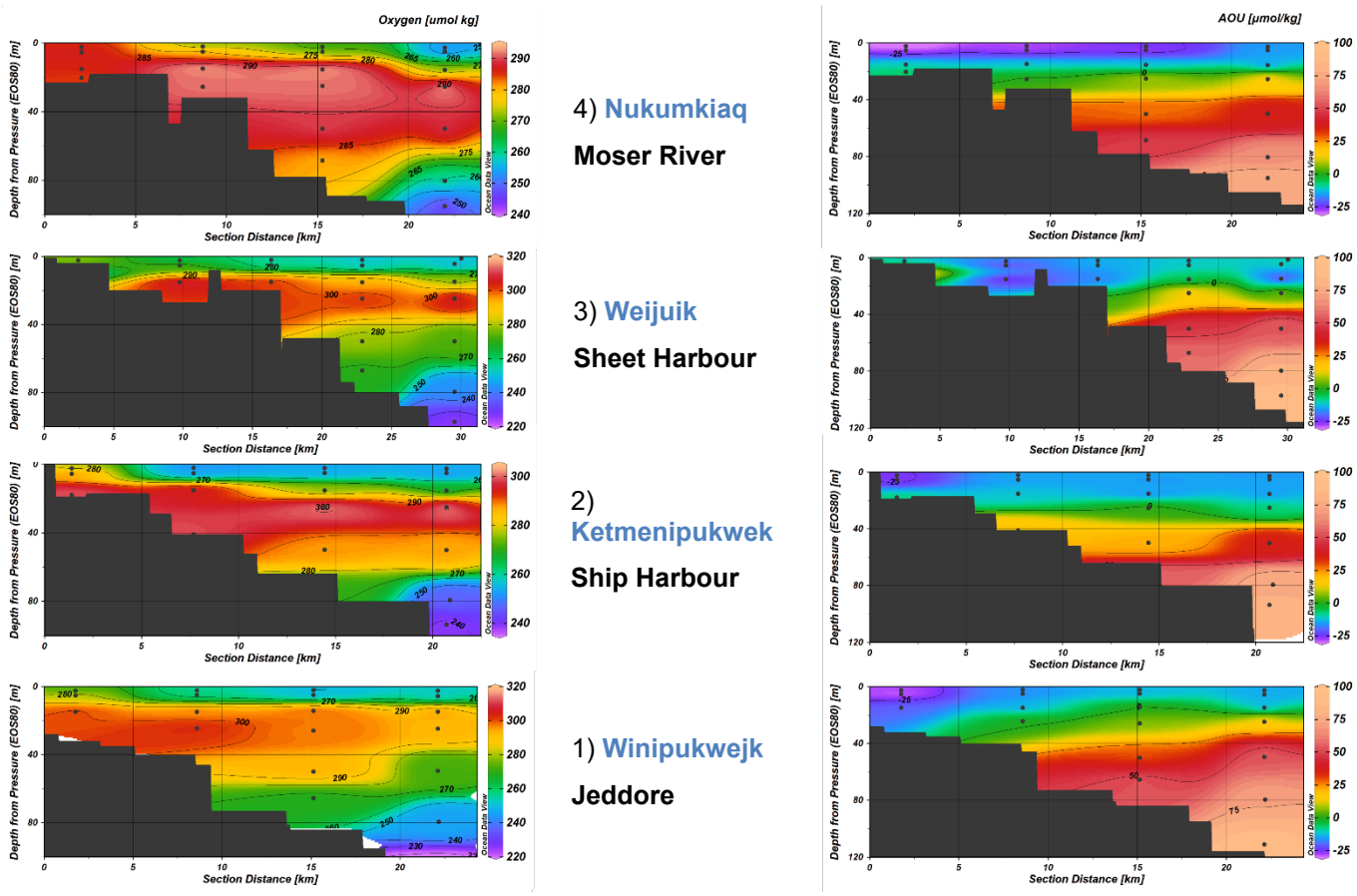


Figure 9. Section plots of data, including bathymetry, for 4 transects sampled between August 9 and 14, 2021 showing Dissolved oxygen and AOU along the 4 study transects, enumerated on each plot. The discrete sample locations through depth are indicated with black dots.

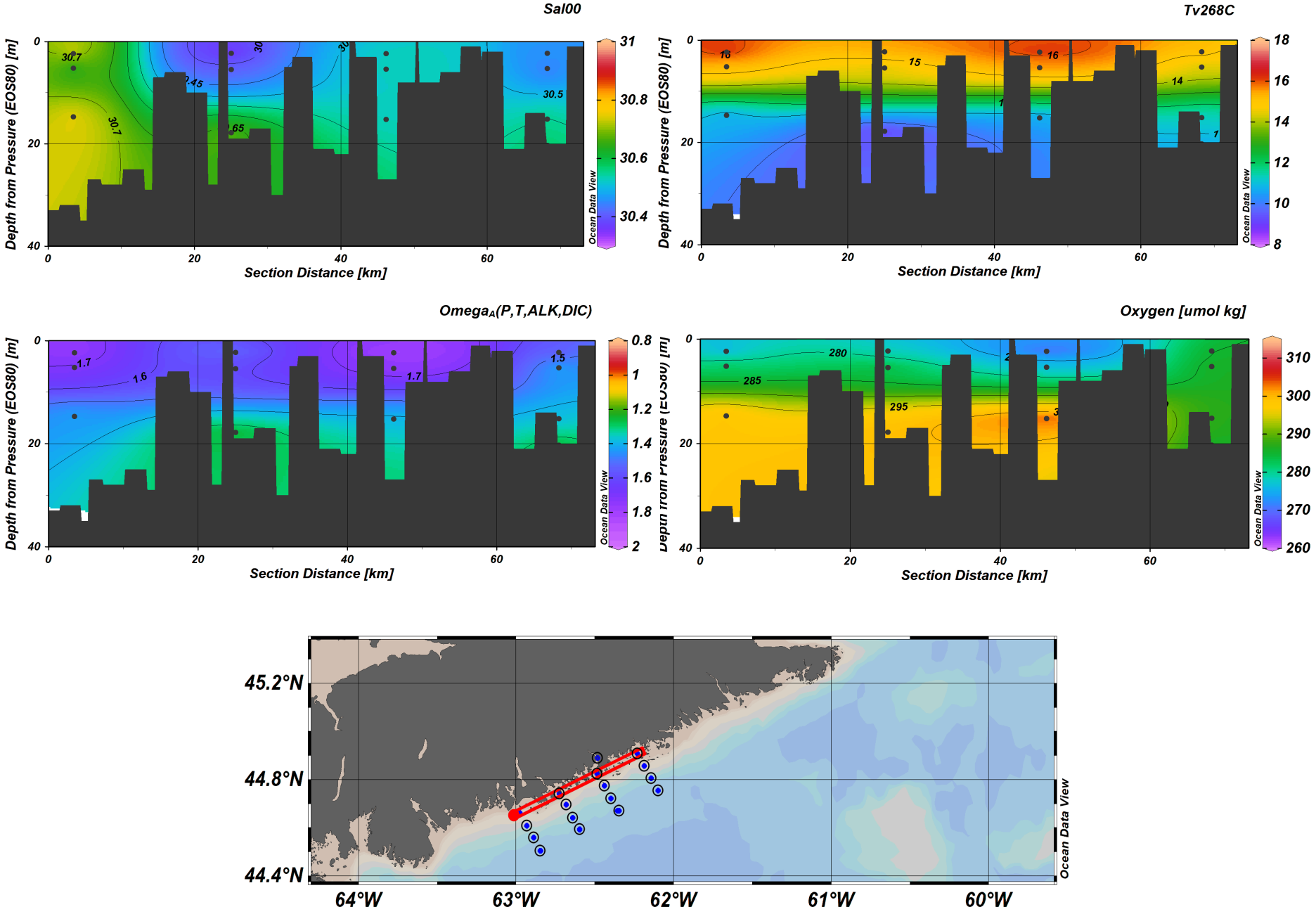

Sal00
Depth from Pressure (EOS80) [m]
Section Distance [km]
Ocean Data View
Tv268C
Depth from Pressure (EOS80) [m]
Section Distance [km]
Ocean Data View
Omega$_A$(P,T,ALK,DIC)
Depth from Pressure (EOS80) [m]
Section Distance [km]
Ocean Data View
Oxygen [umol kg]
Depth from Pressure (EOS80) [m]
Section Distance [km]
Ocean Data View
45.2°N
44.8°N
44.4°N
64°W
63°W
62°W
61°W
60°W
Ocean Data View

Figure 10. Alongshore section plots with bathymetry for salinity, temperature, saturation state of aragonite (W_{arag}) and dissolved oxygen data from sites sampled August 9 to 14, 2021, for the most nearshore sites of each of the 4 study transects: ***Nukumkiaq*** *Moser River (ESI-1 to ESI-4),* ***Weijuik*** *Sheet Harbour (ESI-00 and ESI-5 to ESI-8),* ***Ketmenipukwek*** *Ship Harbour (ESI-9 to ESI-12), and* ***Winipukwejk*** *Jeddore (ESI-13 to ESI-16). The discrete sample locations through depth are indicated with black dots.*

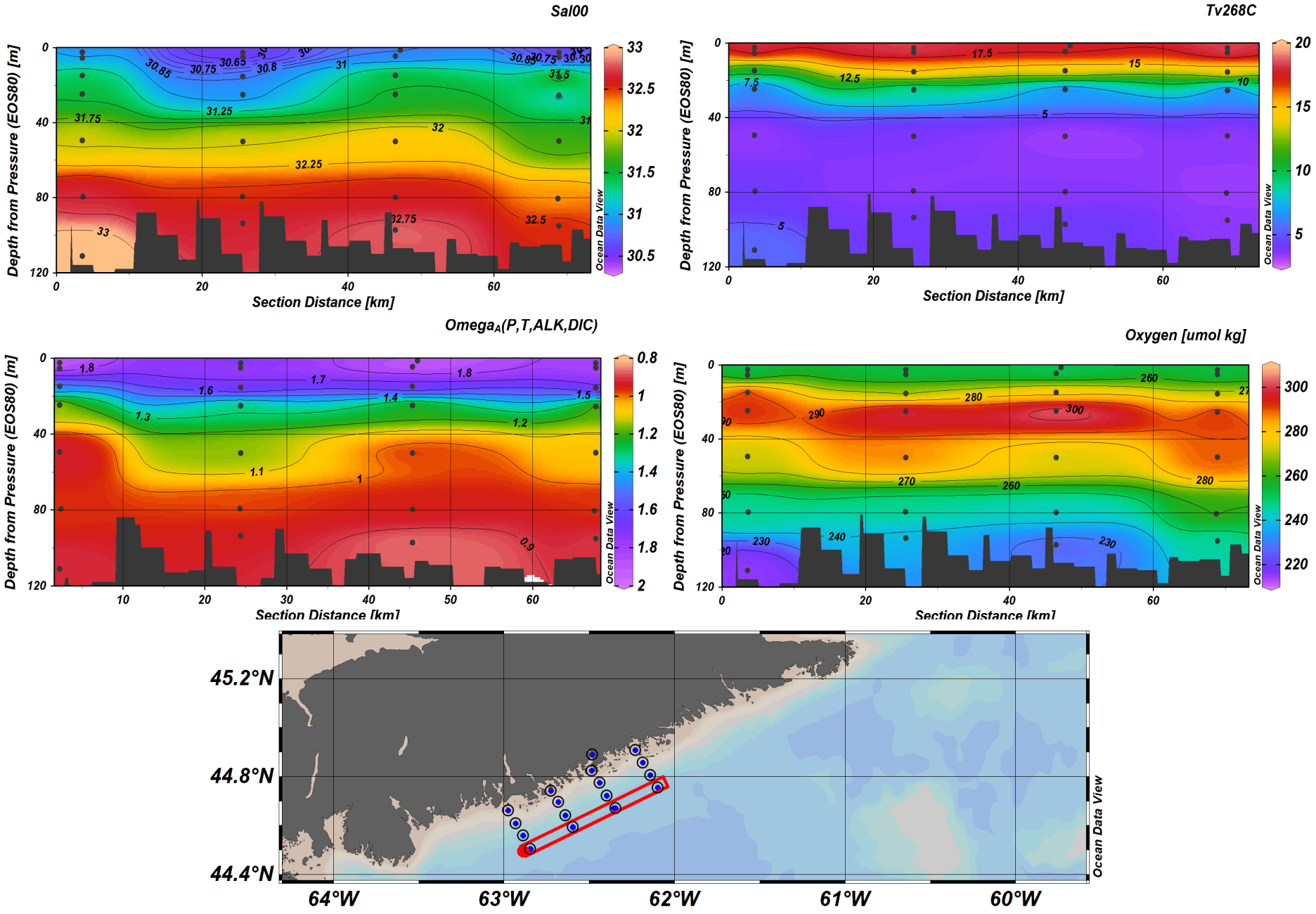

Sal00
Depth from Pressure (EOS80) [m]
Section Distance [km]
Ocean Data View
Tv268C
Depth from Pressure (EOS80) [m]
Section Distance [km]
Ocean Data View
Omega$_A$(P,T,ALK,DIC)
Depth from Pressure (EOS80) [m]
Section Distance [km]
Ocean Data View
Oxygen [umol kg]
Depth from Pressure (EOS80) [m]
Section Distance [km]
Ocean Data View
45.2°N
44.8°N
44.4°N
64°W
63°W
62°W
61°W
60°W
Ocean Data View

Figure 11. Alongshore section plots with bathymetry for salinity, temperature, saturation state of aragonite (Ω_{arag}) and dissolved oxygen data from sites sampled August 9 to 14, 2021, for the farthest offshore sites of each of the 4 study transects: ***Nukumkiaq*** *Moser River (ESI-1 to ESI-4),* ***Weijuik*** *Sheet Harbour (ESI-00 and ESI-5 to ESI-8),* ***Ketmenipukwek*** *Ship Harbour (ESI-9 to ESI-12), and* ***Winipukwejk*** *Jeddore (ESI-13 to ESI-16). The discrete sample locations through depth are indicated with black dots.*

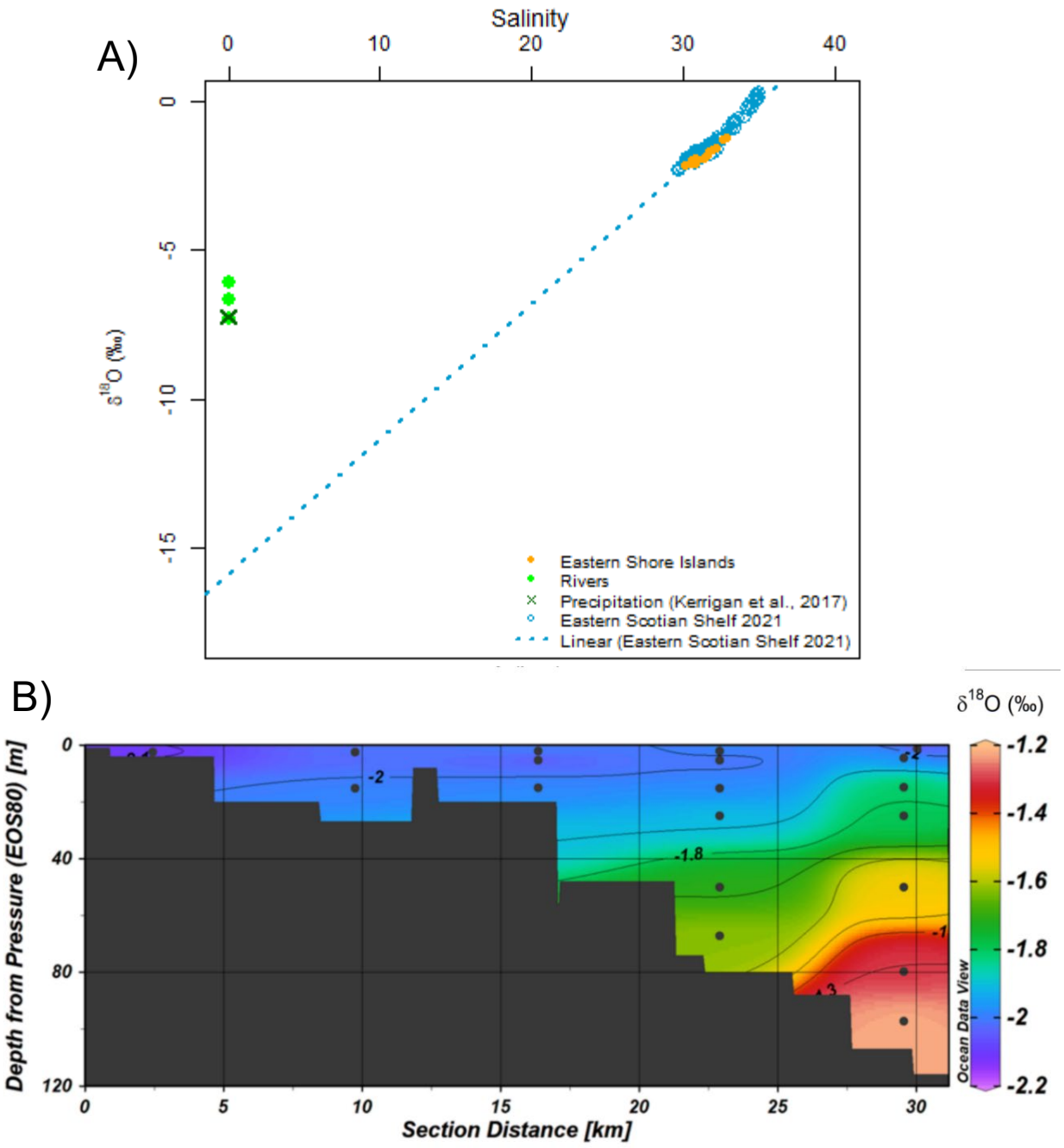


Figure 12. A) Scatterplot of δ ^{18}O plotted against salinity for the marine samples along the ***Weijuik*** *Sheet Harbour transect. The river samples range from -6.06 to -7.30 ‰ and are not shown here. The relationship between these variables is linear, with high correlation (r^2 = 0.933), which improves (r^2 = 0.996) when the shallow nearshore samples (ESI-0, ESI-5 and ESI-6) are treated separately. B) Section plot of δ ^{18}O for the* ***Weijuik*** *Sheet Harbour transect. Note the influence of river samples, located near the coast, and the higher salinity slope water influence offshore.*

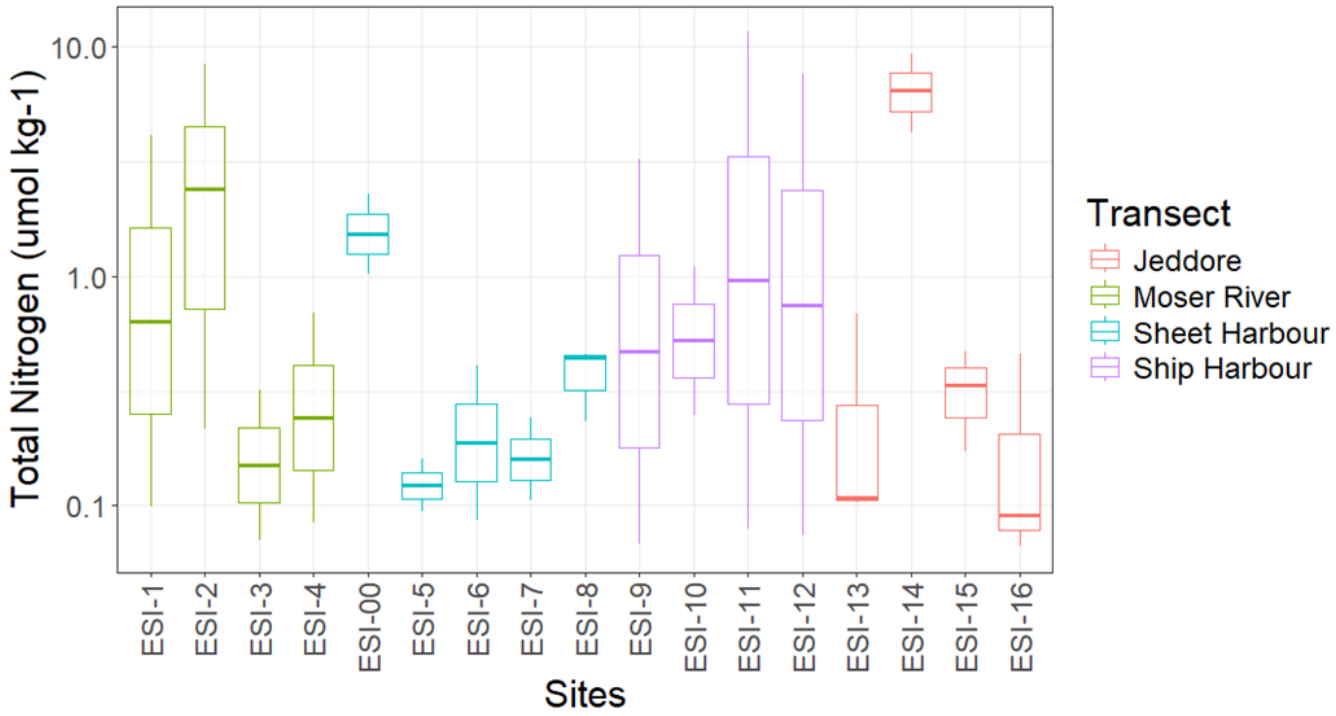


*Figure 13. Box plot of total inorganic nitrogen (nitrate + nitrite + ammonium) along sections through depth for the **Nukumkiaq** Moser River (ESI-1 to ESI-4), **Weijuik** Sheet Harbour (ESI-00 and ESI-5 to ESI-8), **Ketmenipukwek** Ship Harbour (ESI-9 to ESI-12), and **Winipukwejk** Jeddore (ESI-13 to ESI-16) transects in order of sampling between August 9 and 14, 2021. The colour corresponds to the transect name (legend) and within each transect, the sites (left to right) are ordered inshore to offshore.*

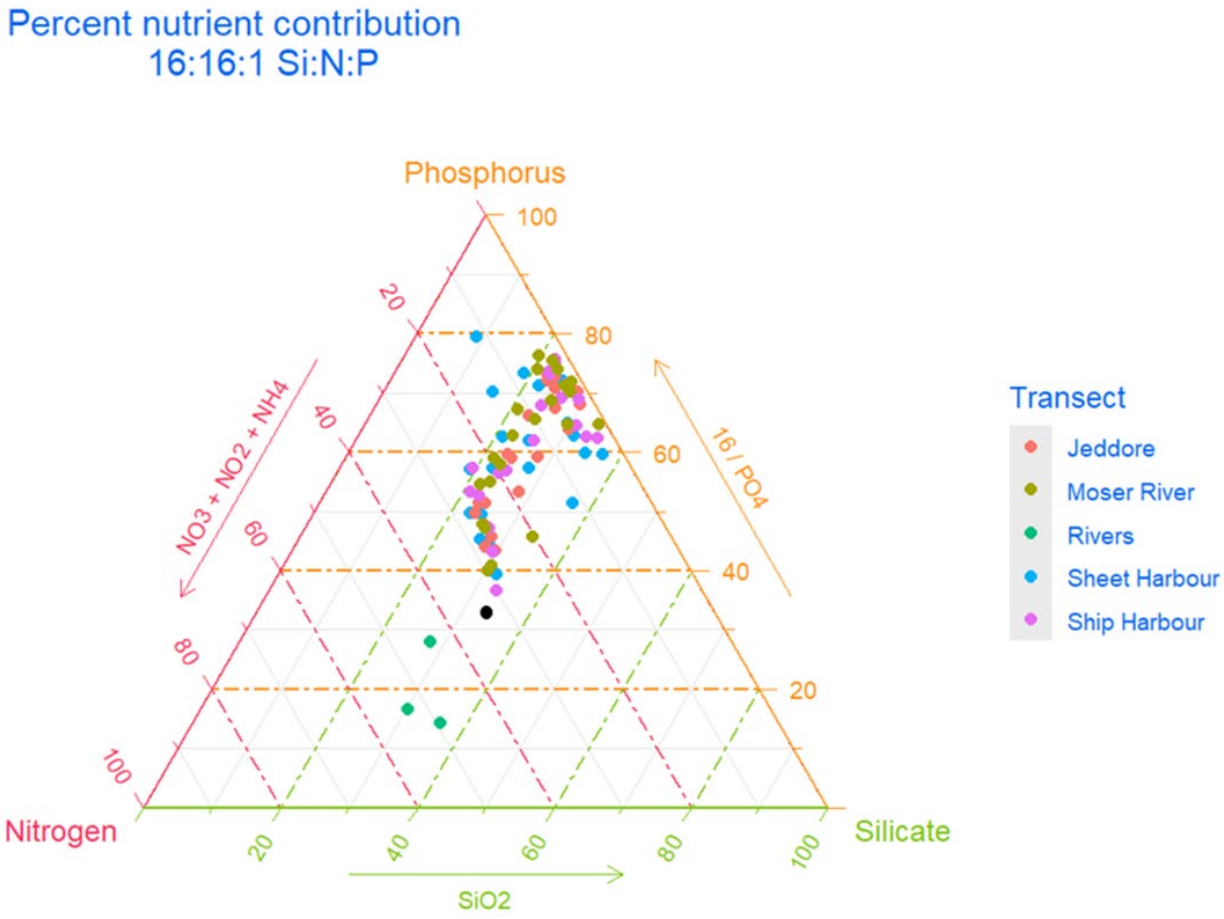


Figure 14. Ternary plot of the % nutrient contribution (% silicate versus % total nitrogen vs. % phosphate) for all sites sampled for all depths. The black dot represents reference point of the idealized Redfield Ratio (16:16:1 Si:N:P). The marine sites are nitrogen limited, whereas the river sites (in green) are silicate and/or phosphate limited.

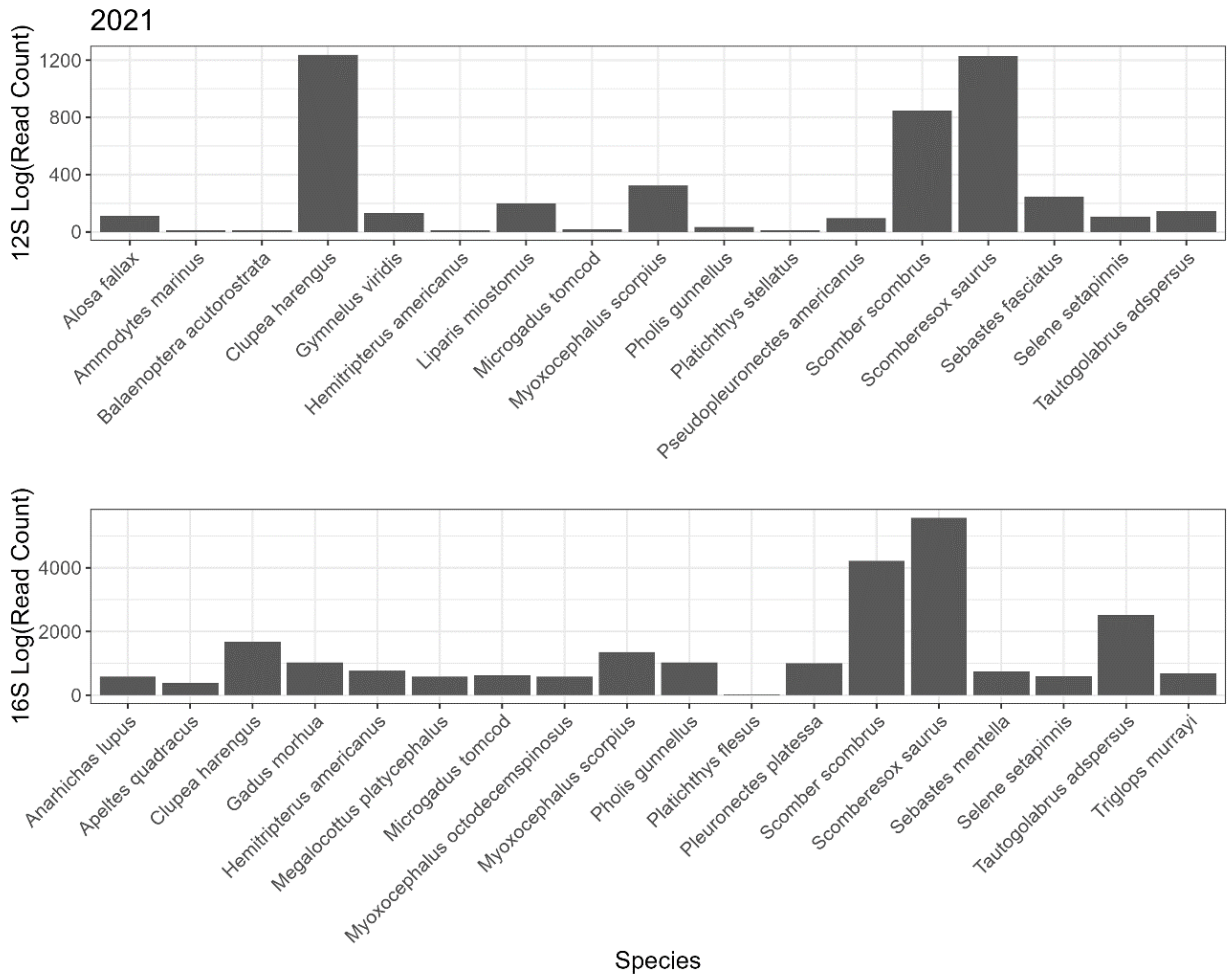


Figure 15. Fish species detected in eDNA using the 12S (top) and 16S (bottom) mitochondrial markers across 16 sites (4 offshore transects with 4 sites each) sampled from the CCGS M. Perley in summer 2021.

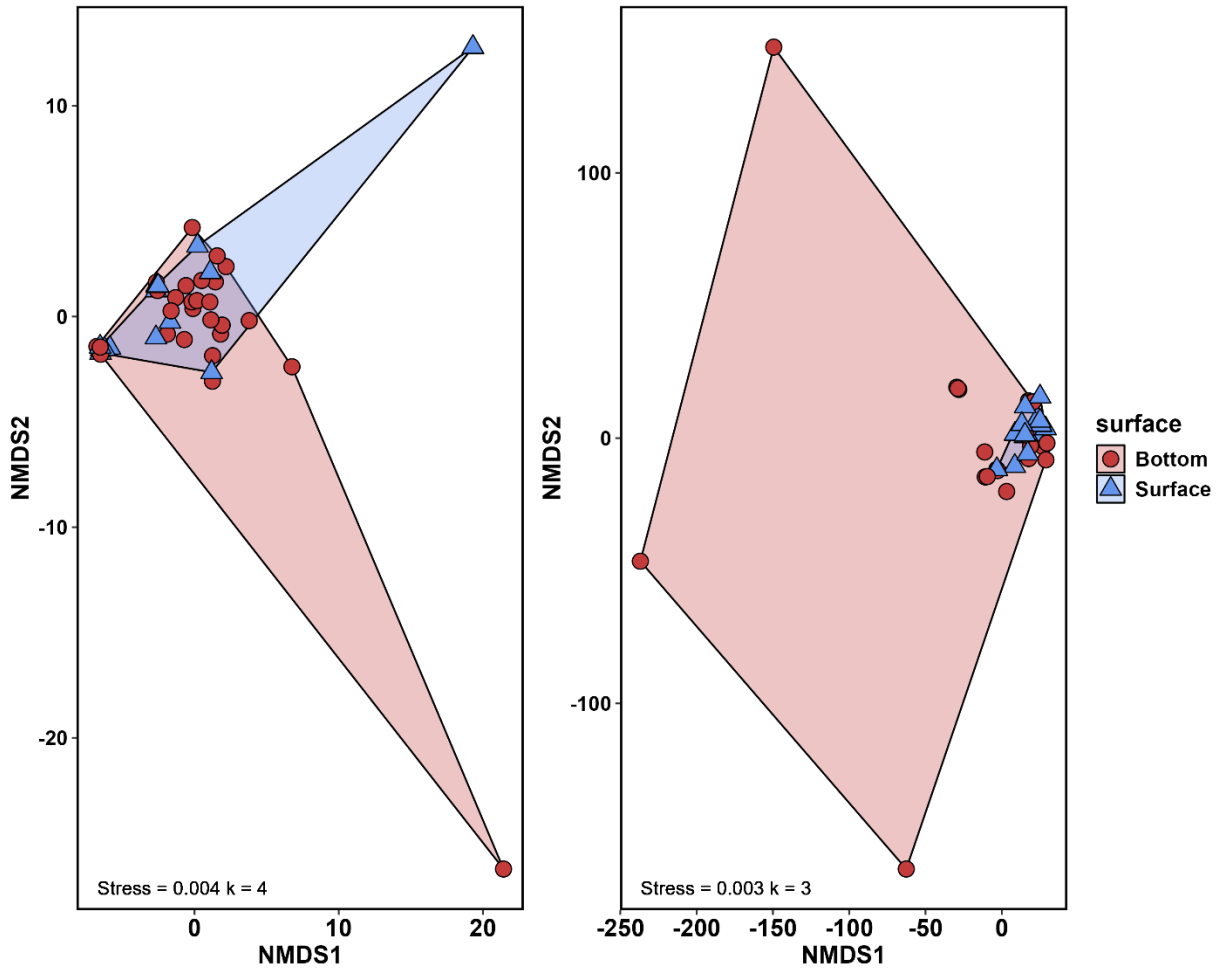


Figure 16. Non-metric multidimensional scaling plot of 2021 Perley eDNA fish data (12S = left, 16S = right). Surface samples generally clustered close together regardless of station, while benthic samples were more dispersed.

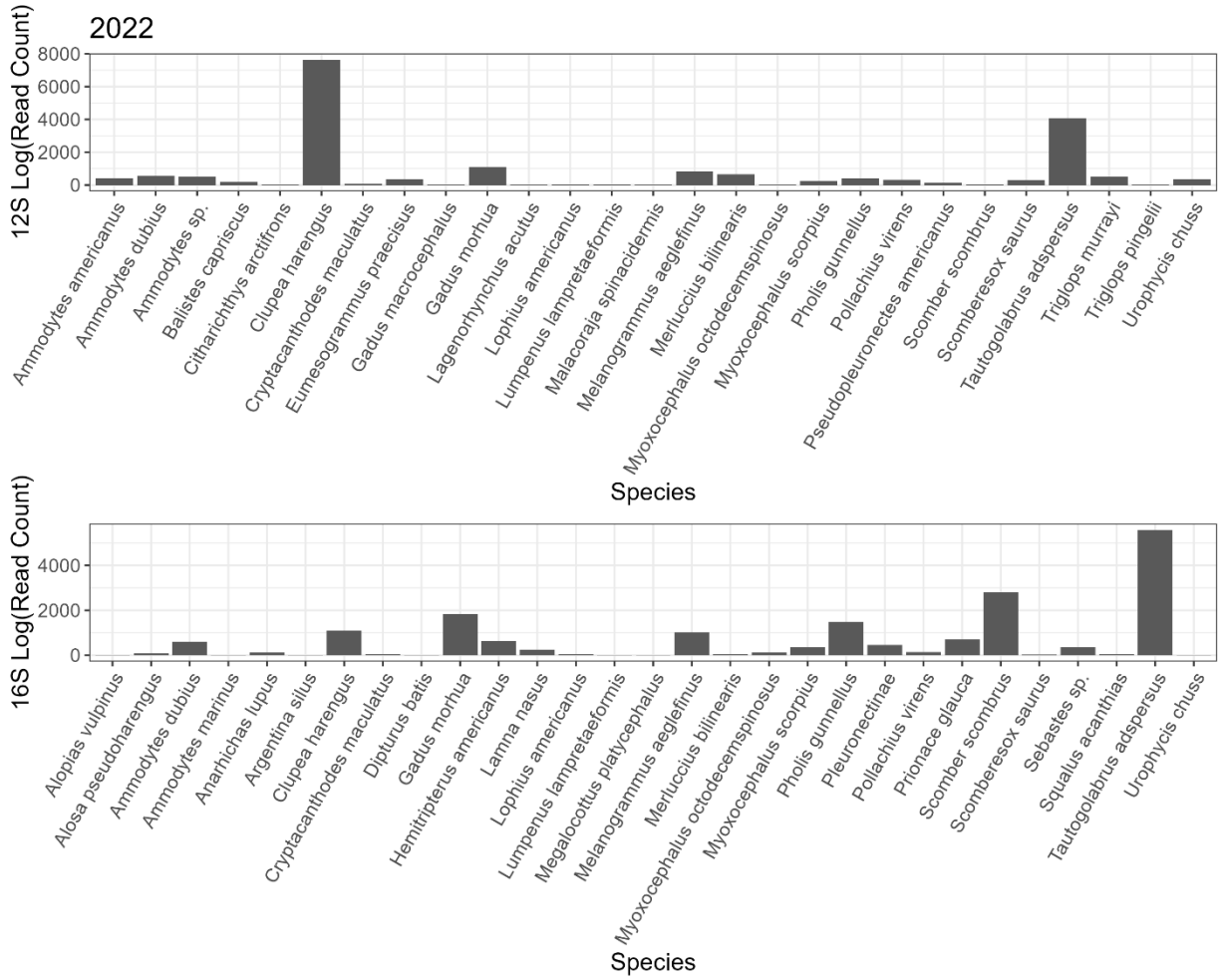


Figure 17. Fish species detected from the offshore in 2022 using the 12S (top) and 16s (bottom) eDNA markers. The log-transformed read count is shown on the y-axis for each species. While there is substantial overlap in fish species detected between the two marker types, more species of elasmobranchs (sharks and skates) were identified using the 16S marker.

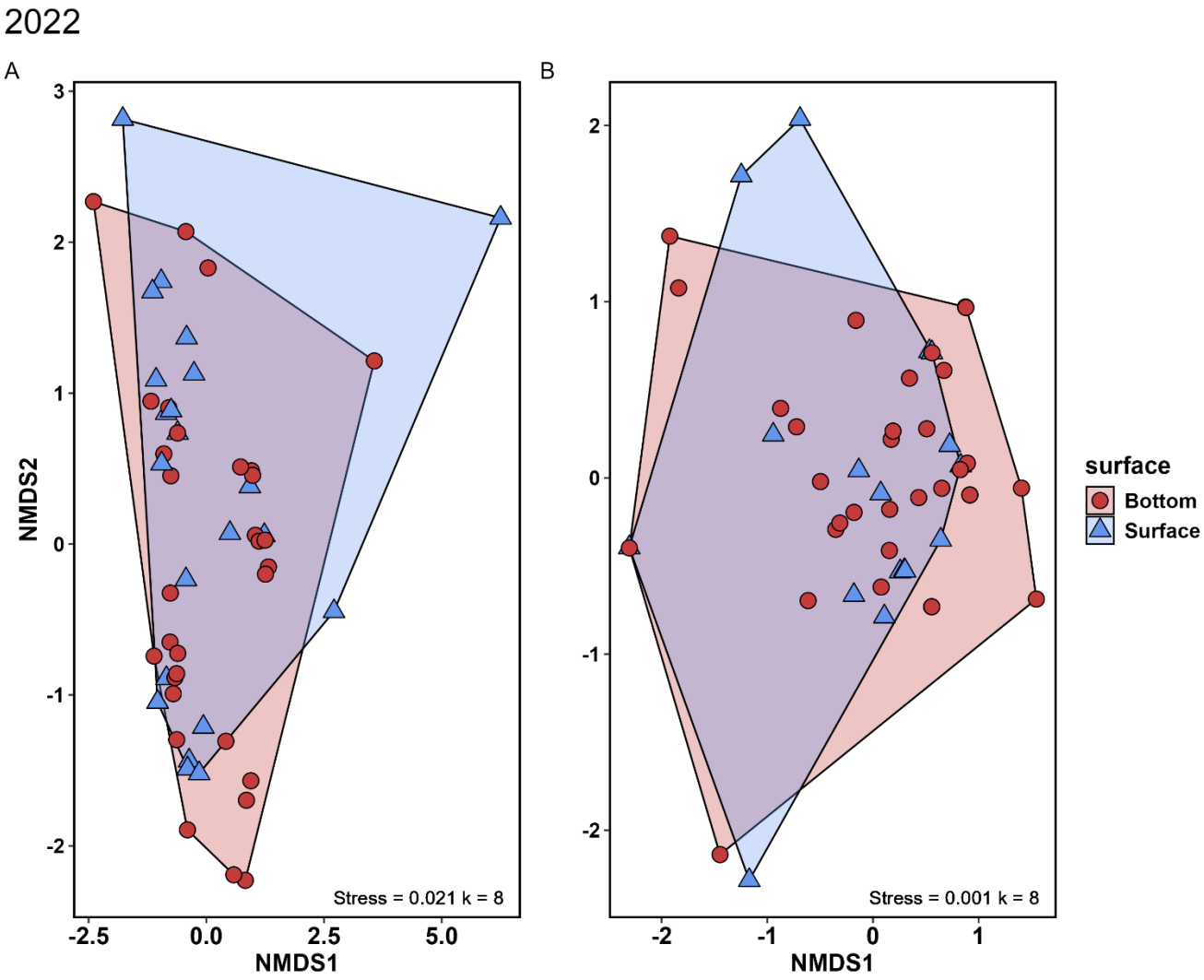


Figure 18. Non-metric multidimensional scaling plot of fish eDNA samples collected in 2022 using Jaccard distances (12S = left, 16S = right). For both markers there was substantial overlap between surface and benthic eDNA samples suggesting similarity in the communities recovered by eDNA metabarcoding.

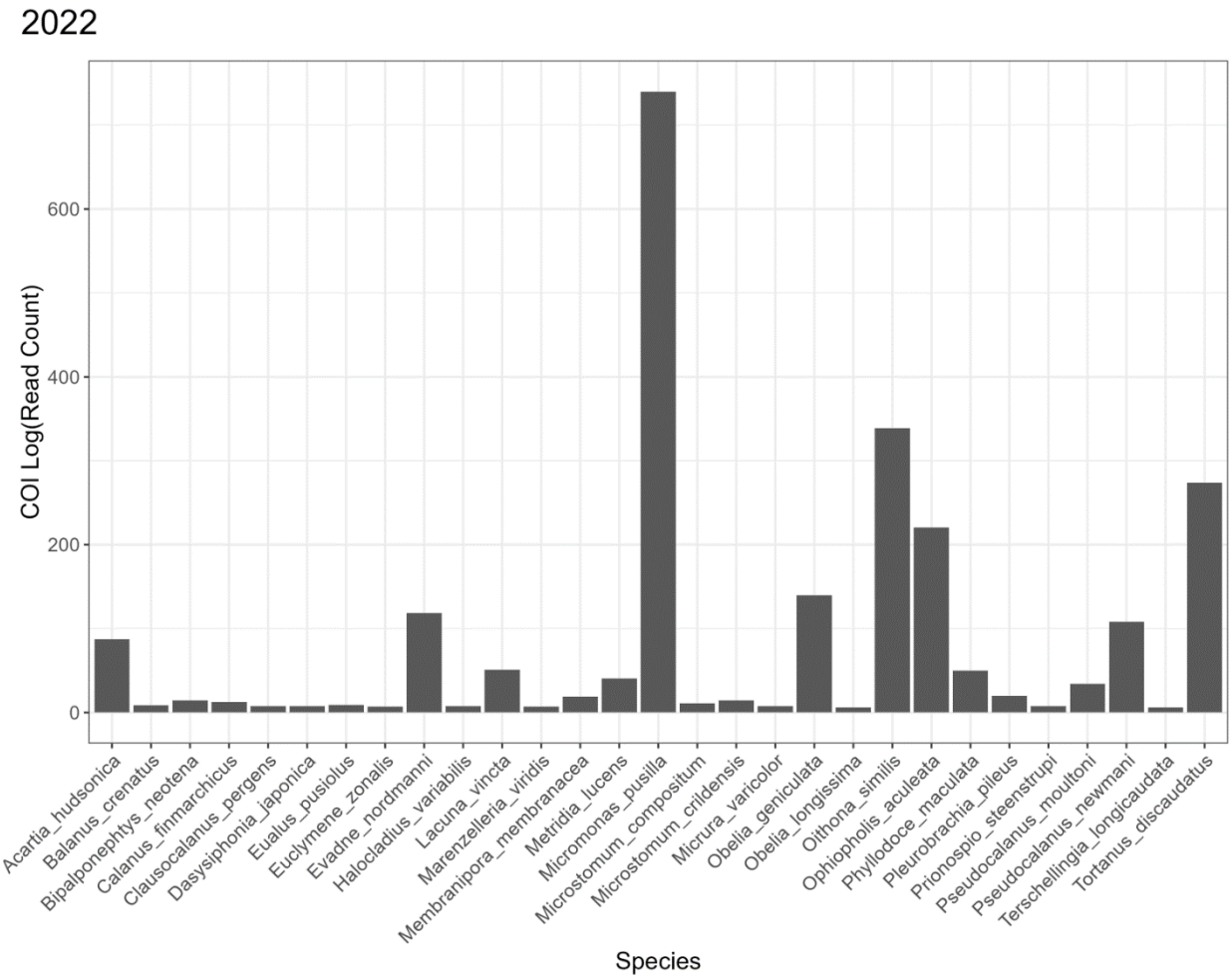


Figure 19. Invertebrate and algal species detected from the offshore in 2022 using the COI eDNA marker. The log-transformed read count is shown on the y-axis for each species. The most abundant species is the picophytoplankton Micromonas pusilla, followed by several species of copepods (Oithona similis and Tortanus discaudatus).

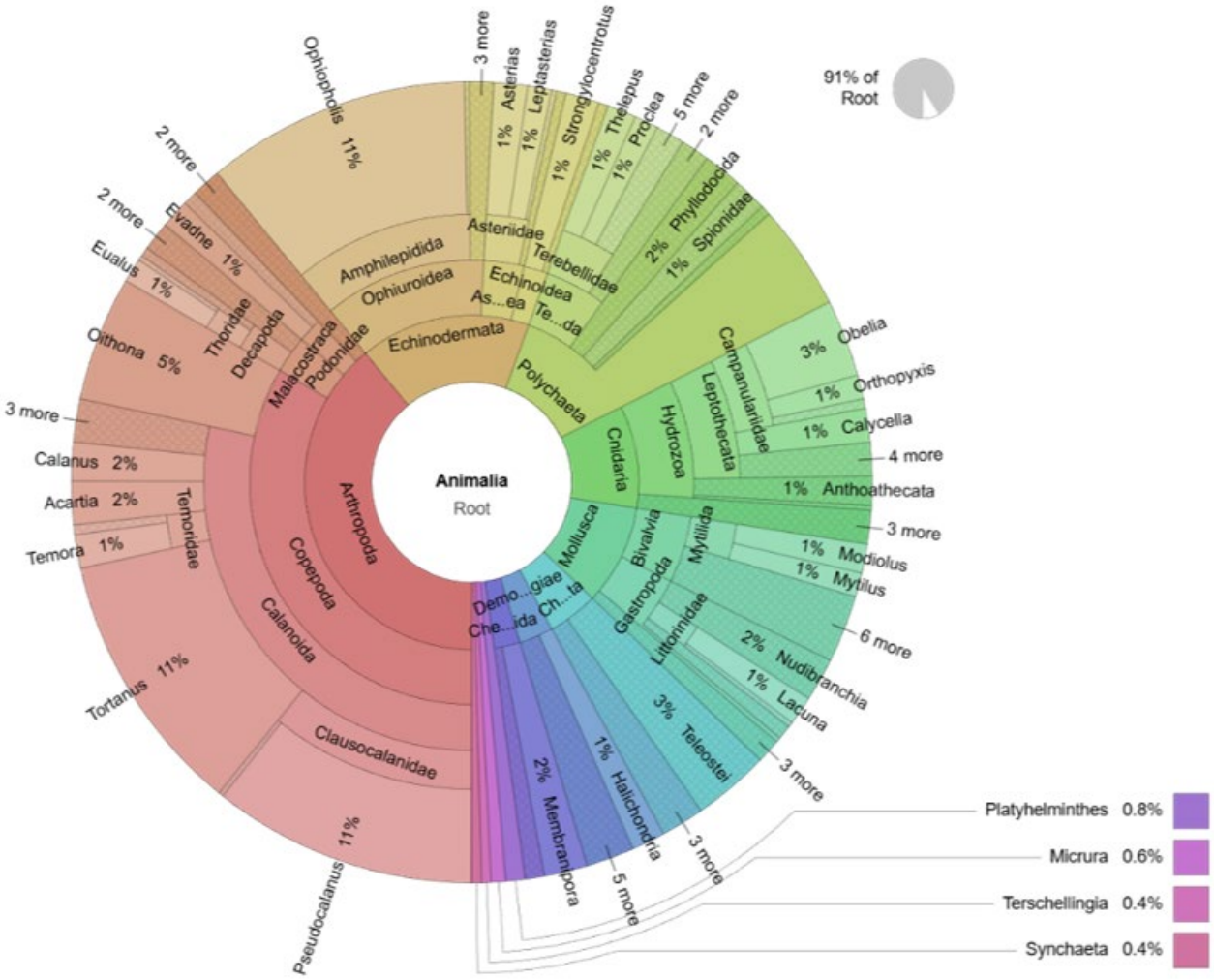


Figure 20. Krona plot of animal diversity at the genus level detected by the 2022 COI eDNA marker. The percentages beside each genus name refer to the diversity of amplicon sequence variants (ASV) that make up the total proportion of the total ASVs found in the samples (i.e., higher percentages mean more ASVs are found in that species). The phytoplankton Micromonas pusilla was removed from the plot because it made up the majority of eDNA reads.

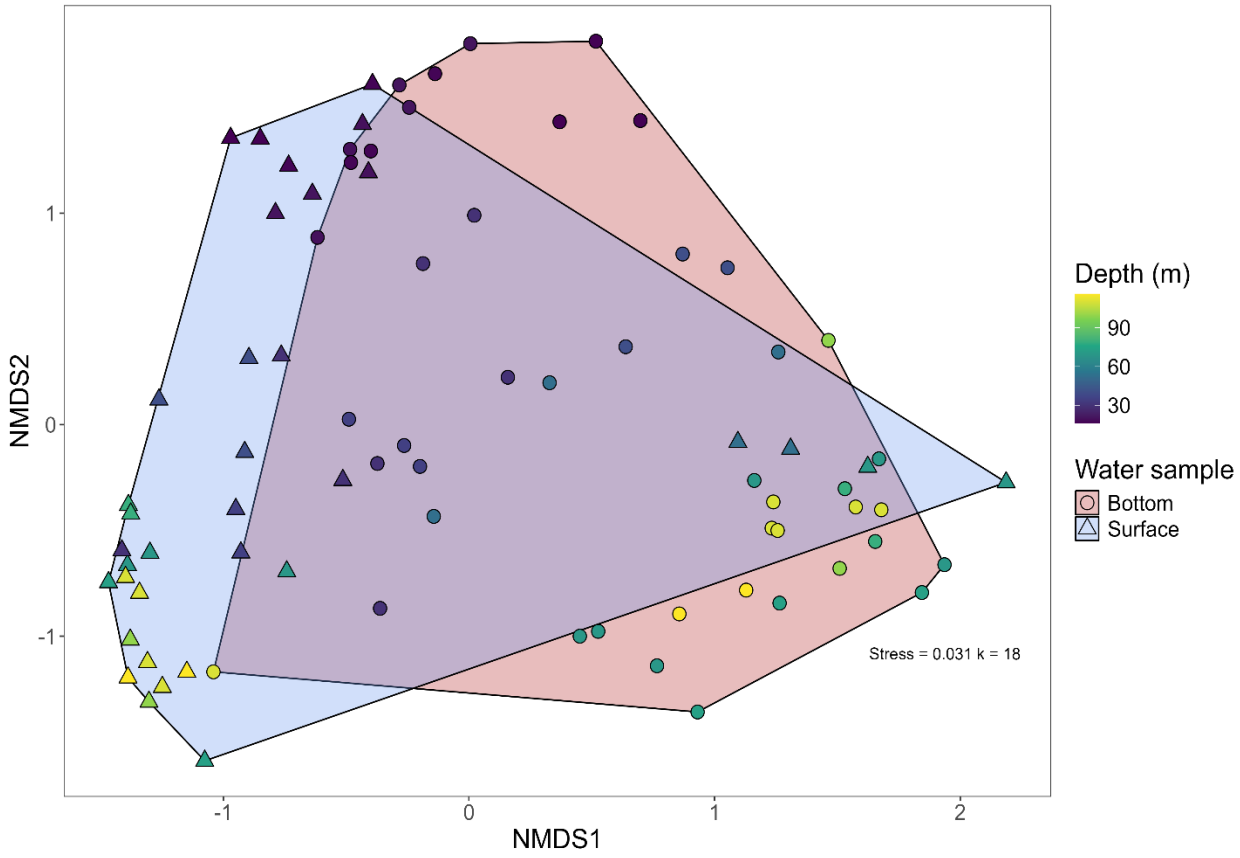


Figure 21. NMDS of 2022 COI data with points coloured by water depth. For the COI data, the bottom and surface samples largely separate along NMDS1, with the exception of four samples. There is significant clustering of samples by water depth, with deeper samples separating from shallower samples along NMDS2.

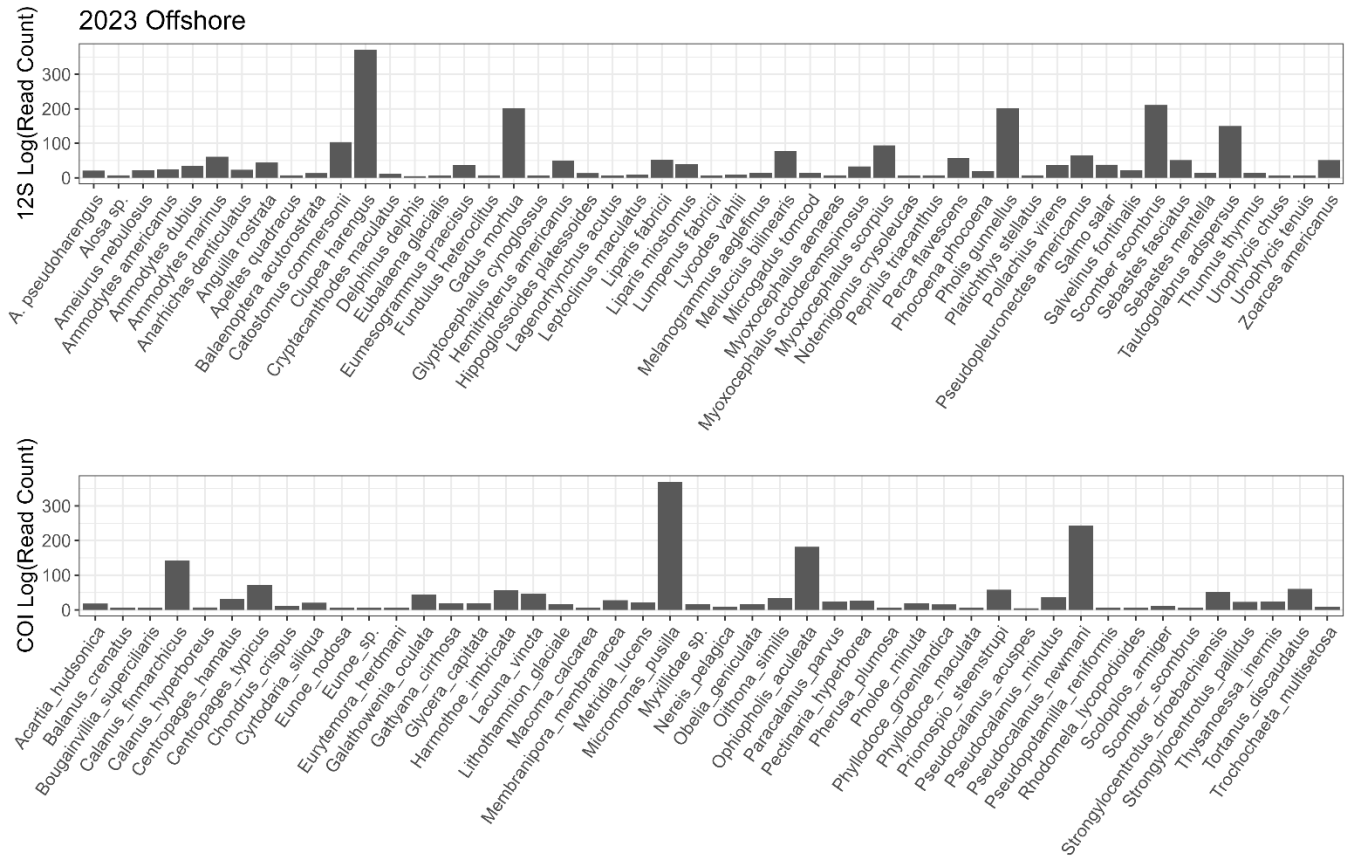


Figure 22. Fish (top panel) and invertebrate species (bottom) detected from the offshore in 2023 using the 12S (top) and COI (bottom) eDNA markers. The log-transformed read count is shown on the y-axis for each species.

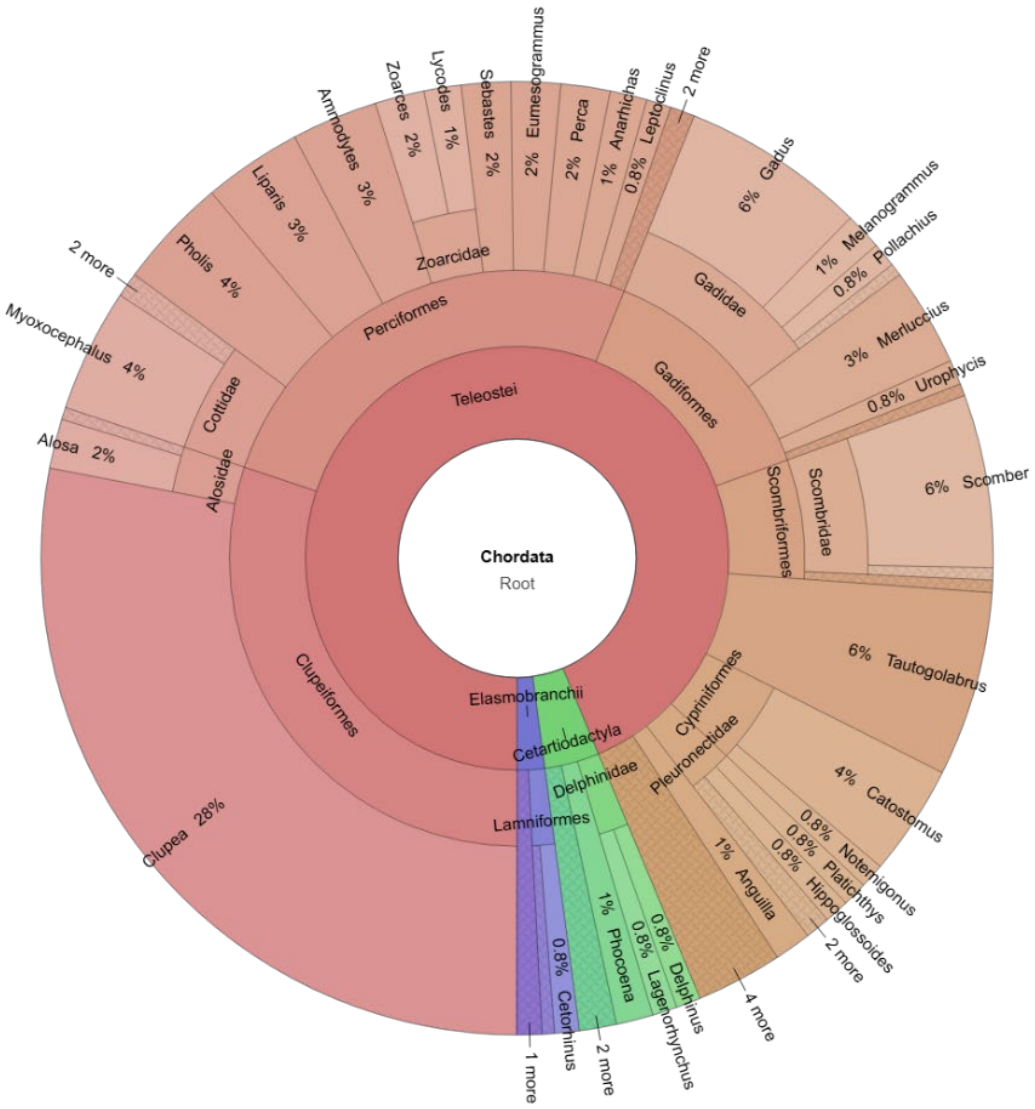


Figure 23. Krona plot of chordate diversity at the genus level detected by the 2023 12S eDNA marker. The percentages beside each genus refer to the diversity of amplicon sequence variants (ASV) that make up the total proportion of the total ASVs found in the samples (i.e., higher percentages mean more ASVs are found in that species). Bony fishes (Teleostei) make up the majority of detections, while elasmobranchs (blue) and cetaceans (green) make up smaller proportions of detected genera.


spring
fall
Species
Zoarces americanus
Urophycis tenuis
Thunnus thynnus
Tautogolabrus adspersus
Semotilus atromaculatus
Sebastes mentella
Scomber scombrus
Salvelinus fontinalis
Salmo salar
Pseudopleuronectes americanus
Pollachius virens
Pholis gunnellus
Phocoena phocoena
Perca flavescens
Notemigonus crysoleucas
Myoxocephalus scorpius
Myoxocephalus octodecemspinosus
Microgadus tomcod
Merluccius bilinearis
Lumpenus fabricii
Liparis spp.
Lagenorhynchus acutus
Hemitripterus americanus
Gadus morhua
Fundulus heteroclitus
Eumesogrammus praecisus
Delphinus delphis
Cryptacanthodes maculatus
Clupea harengus
Cetorhinus maximus
Catostomus commersonii
Balaenoptera acutorostrata
Apeltes quadracus
Anguilla rostrata
Anarhichas denticulatus
Ammodytes marinus
Ammodytes dubius
Ameiurus nebulosus
Alosa sp.
A. pseudoharengus
ESI_05
ESI_06
ESI_07
ESI_08
Station
Read count
10000
20000
30000
40000
Sample depth (m)
30
60
90

*Figure 24. Bubble plot of all fish species detected in surface eDNA samples collected along the **Weijuik** Sheet Harbour transect in spring and fall 2023. The size of the bubble is proportional to the number of eDNA reads for that species, while the colour corresponds to the water depth of the station.*



*Figure 25. Bubble plot of all fish species detected in bottom eDNA samples collected along the **Weijuik** Sheet Harbour transect in spring, summer, and fall 2023. Only station ESI-06 was sampled in the summer. The size of the bubble is proportional to the number of eDNA reads for that species, while the colour corresponds to the water depth of the station.*

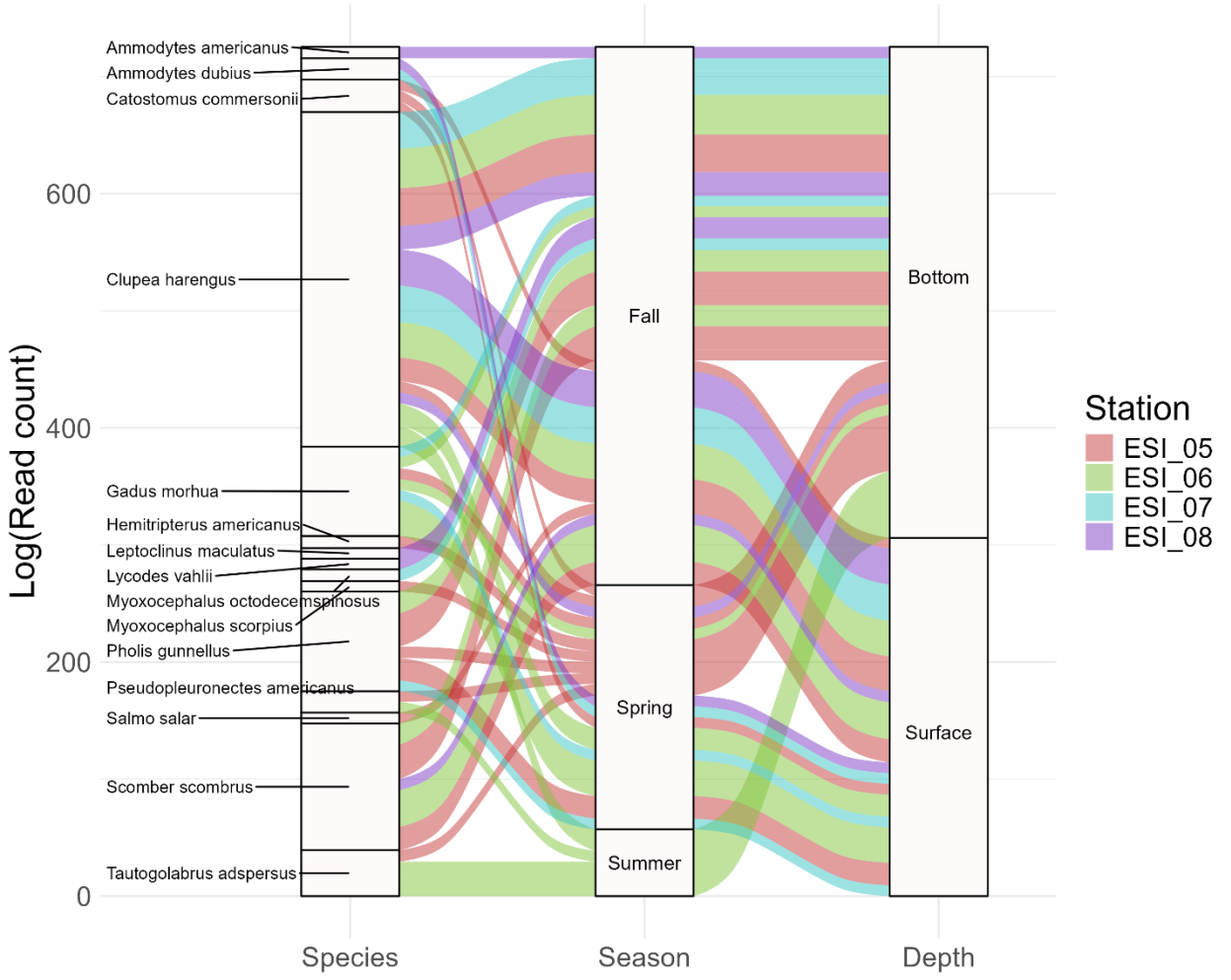


*Figure 26. Alluvial plot showing the most commonly detected (>8000 DNA reads) fish species using eDNA metabarcoding (12S marker) along a single transect south of **Weijuik** Sheet Harbour aboard the CCGS M. Perley in 2023. The plot shows the seasons and water sample location (surface vs. benthic samples) each species of fish was found in, and the colours represent the sampling station in the transect – ESI-05 is closest to the mouth of **Weijuik** Sheet Harbour, while ESI_08 is farthest offshore. Atlantic Herring (Clupea harengus) are the most abundant fish detected, and they are found in all sample stations, seasons, and in both surface and bottom samples.*

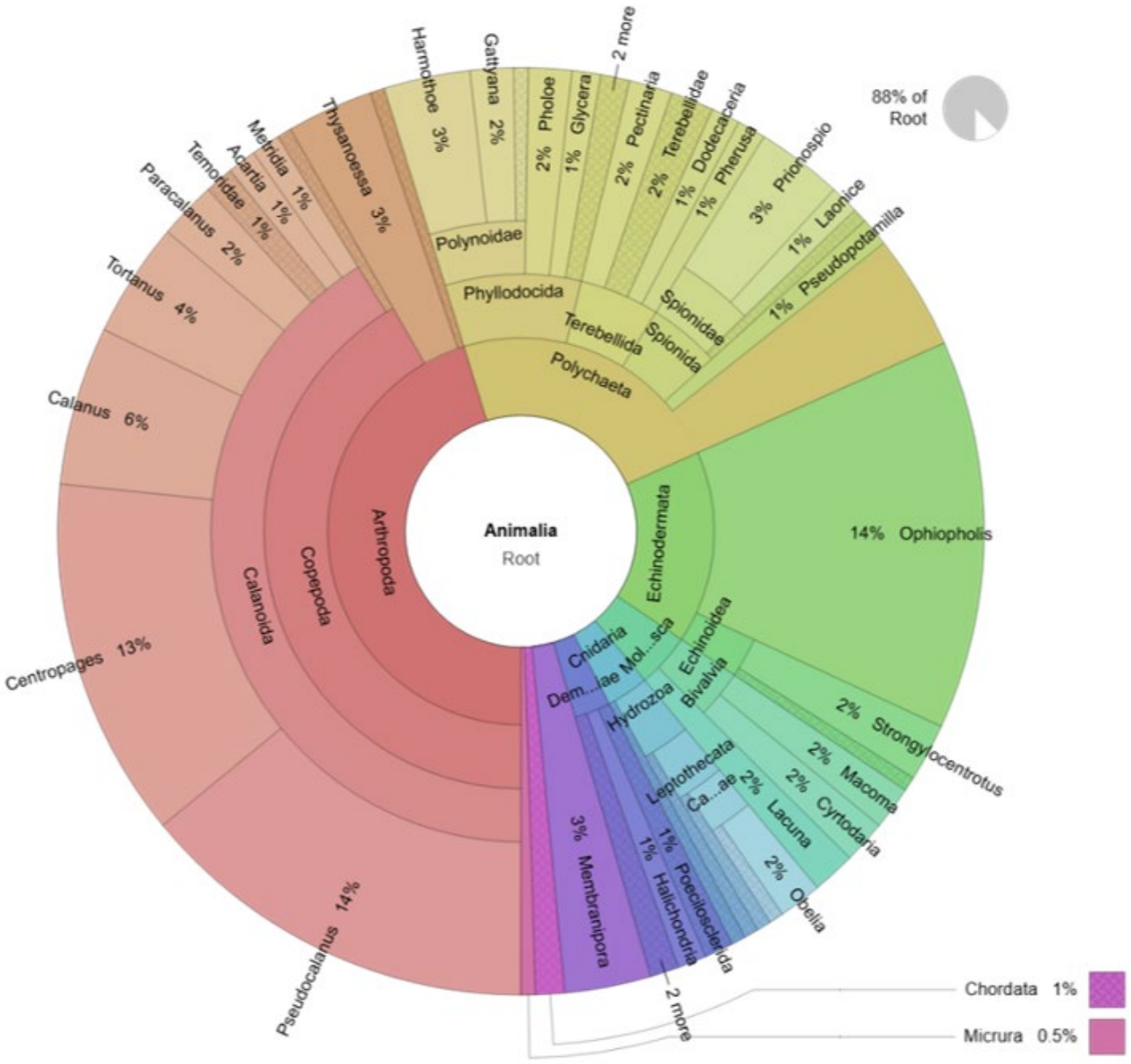


Figure 27. Krona plot of animal diversity at the genus level detected by the 2023 COI eDNA marker. The percentages beside each genus refer to the diversity of amplicon sequence variants (ASV) that make up the total proportion of the total ASVs found in the samples (i.e., higher percentages mean more ASVs are found in that species).

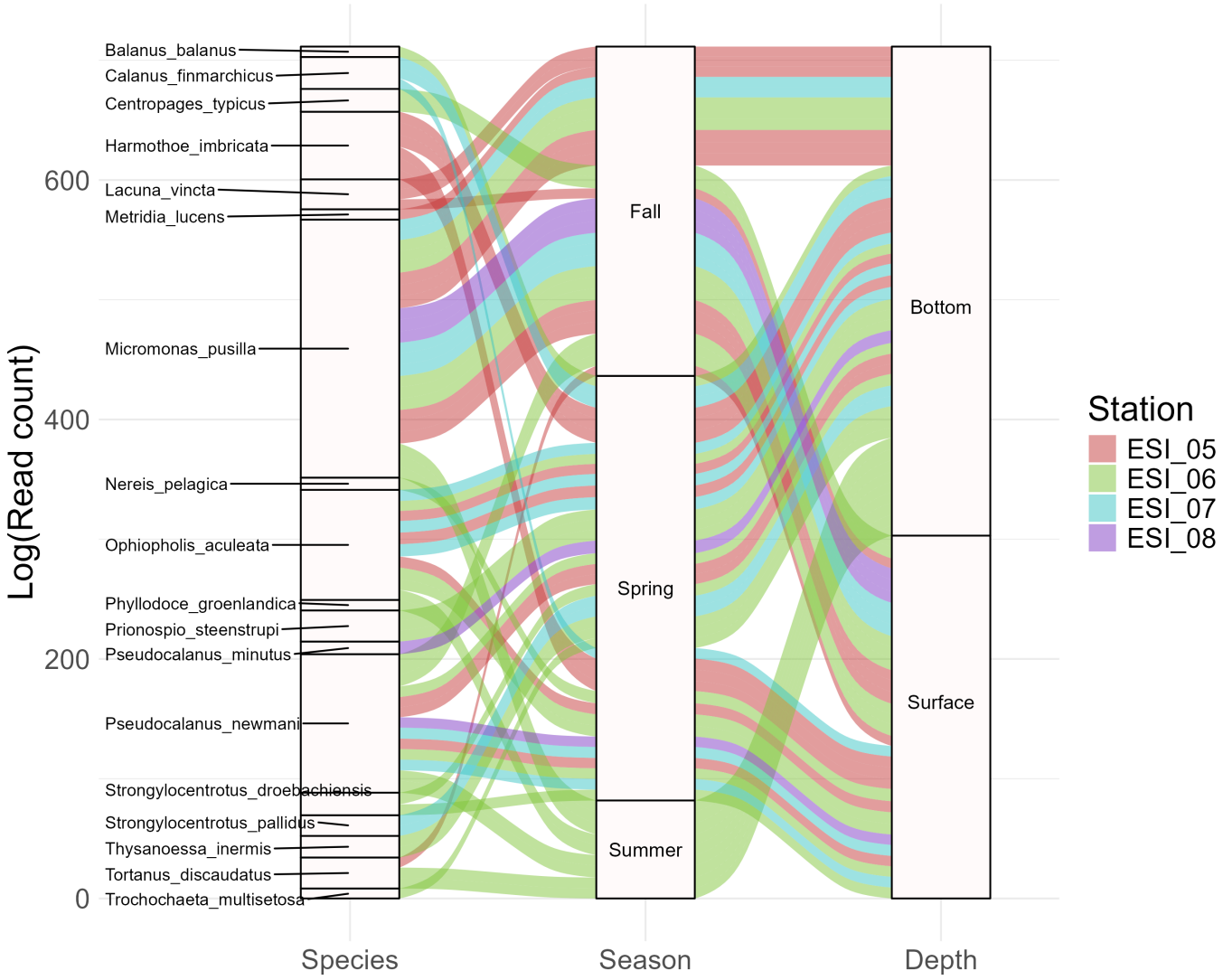


*Figure 28. Alluvial plot showing the most commonly detected (>4000 DNA reads) invertebrates using eDNA metabarcoding (12S marker) along a single transect south of **Weijuik** Sheet Harbour aboard the CCGS M. Perley in 2023. The plot shows the seasons and water sample location (surface vs. benthic samples) each invertebrate was found in, and the colours represent the sampling station in the transect – ESI_05 is closest to the mouth of **Weijuik** Sheet Harbour, while ESI_08 is farthest offshore.*

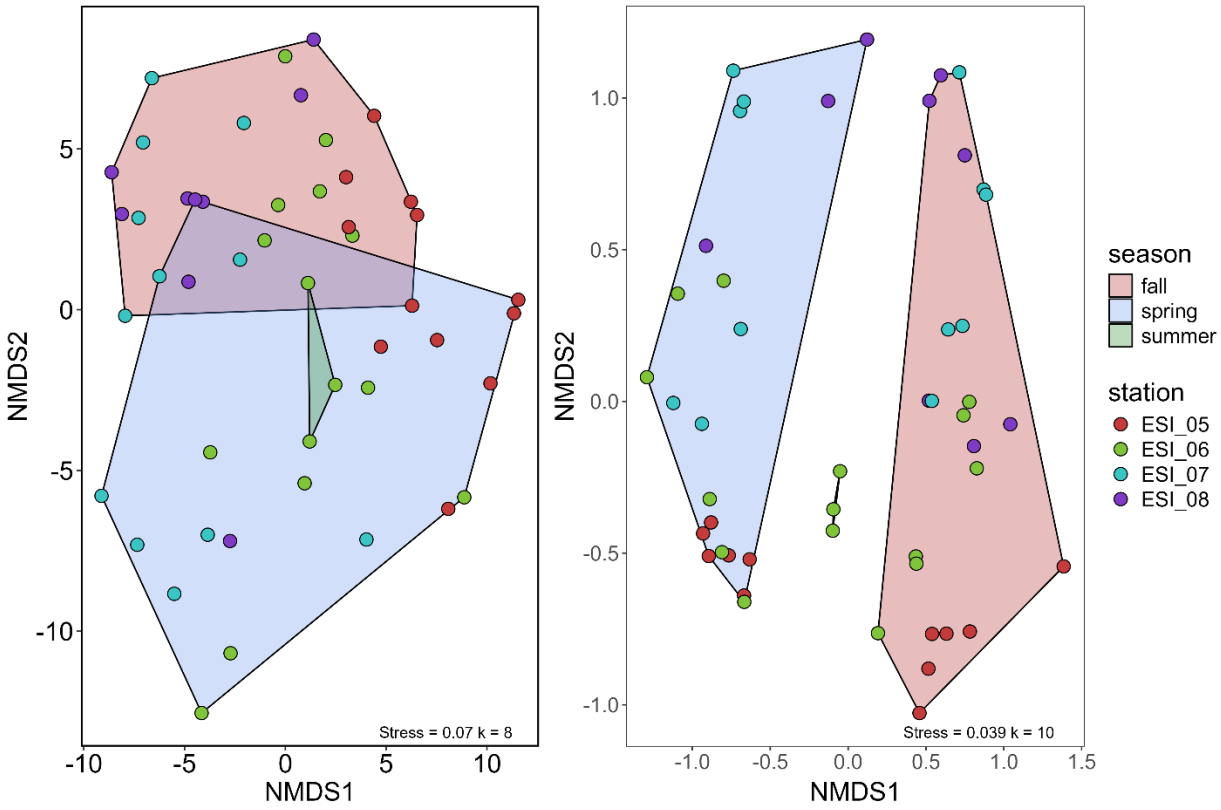


Figure 29. NMDS of Perley 2023 seasonal data (12S=left, COI=right). Only one station was sampled in summer (ESI-6). The polygons represent the season the samples were collected (spring, summer, and fall), while the point colours correspond to the sampling sites. Both markers show a clear separation of spring and fall fish and invertebrate communities, with summer being intermediate to both seasons.

REFERENCES

Albouy-Boyer, S., Plourde, S., Pepin, P., Johnson, C.L., Lehoux, C., Galbraith, P.S., Hebert, D., Lazin, G. and Lafleur, C. 2016. Habitat modelling of key copepod species in the Northwest Atlantic Ocean based on the Atlantic Zone Monitoring Program. J. Plankton Res. 38(3): 589-603.

Andres, H.J., Soontiens, N., Penney, J., and Cyr, F. 2024. Seasonal variations of the cold intermediate layer on the Newfoundland and Labrador Shelf. Progr. Oceanog. 229: 103379.

Aoki, L.R., McGlathery, K.J., and Oreska, M.P. 2020. Seagrass restoration reestablishes the coastal nitrogen filter through enhanced burial. Limnol. Oceanogr. 65(1): 1-12.

Asmala, E., Carstensen, J., Conley, D.J., Slomp, C.P., Stadmark, J. and Voss, M., 2017. Efficiency of the coastal filter: Nitrogen and phosphorus removal in the Baltic Sea. Limnol. Oceanogr. 62(S1), S222-S238.

Attridge, C.M., Metaxas, A., and Denley, D. 2022. Wave exposure affects the persistence of kelp beds amidst outbreaks of the invasive bryozoan *Membranipora membranacea*. Mar. Ecol. Prog. Ser. 702:39-56 https://doi.org/10.3354/meps14191

Azetsu-Scott, K., Petrie, B., Yeats, P., and Lee, C. 2012. Composition and fluxes of freshwater through Davis Strait using multiple chemical tracers. J. Geophys. Res. Oceans 117(C12).

Barclay KM, Gurney-Smith HJ, Ahmed M, Christian JR, Cyr F, Duke PJ, Else BGT, Gimenez I, Lizotte M, Reader MC, Roth M, Rutherford K, Starr M, Steiner NS, Turner J, VanderZwaag, DL, and Evans, W. 2026. Ocean acidification in Canada: the current state of knowledge and pathways for action. Front. Mar. Sci. 13:1761703. https://doi.org/10.3389/fmars.2026.1761703

Beaugrand, G., Ibañez, F., Lindley, J.A., and Reid, P.C. 2002. Diversity of calanoid copepods in the North Atlantic and adjacent seas: species associations and biogeography. Mar. Ecol. Prog. Ser. 232: 179-195.

Blais, M., Galbraith, P.S., Lizotte, M., Clay, S.A. and Starr, M. 2024. Chemical and Biological Oceanographic Conditions in the Estuary and Gulf of St. Lawrence During 2023. Can. Tech. Rep. Hydrogr. Ocean Sci. 385: v + 84 p.

Bolyen E, Rideout JR, Dillon MR, Bokulich NA, Abnet CC, Al-Ghalith GA, Alexander H, et al. 2019. Reproducible, interactive, scalable and extensible microbiome data science using QIIME 2. Nat. Biotechnol. 37: 852–857. https://doi.org/10.1038/s41587-019-0209-9

Borges, A., Champenois, W., Gypens, N., Delille, B., and Harlay, J. 2016. Massive marine methane emissions from near-shore shallow coastal areas. Sci. Rep. 6: 27908. https://doi.org/10.1038/srep27908

Bowlby, H.D., Mitchell, S., Horsman, T.L., and Gibson, A.J.F. 2013. Recovery Potential Assessment for Southern Upland Atlantic salmon: Habitat requirements and status, threats to populations, and potential mitigation options. DFO Canada. Can. Sci. Advis. Sec. Res. Doc. 2013/006.

Brunson, J.C., and Read, Q.D. 2023. ggalluvial: Alluvial Plots in 'ggplot2'. R package version 0.12.5. http://corybrunson.github.io/ggalluvial/

Bushinsky, S.M., Takeshita, Y., and Williams, N.L. 2019. Observing changes in ocean carbonate chemistry: our autonomous future. Curr. Clim. Change Rep. 5: 207-220.

Cai, W.-J., Feely, R.A., Testa, J.M., Li, M., Evans, W., Alin, S.R., Xu, Y.-Y., Pelletier, G., Ahmed, A., Greeley, D.J., Newton, J.A., and Bednaršek, N. 2021. Natural and anthropogenic drivers of acidification in large estuaries. Annu. Rev. Mar. Sci. 13:23–55. https://doi.org/10.1146/annurev-marine-010419-011004

Callahan, B.J., McMurdie, P., Rosen, M.J., Han, A.W., Johnson, A., and Holmes, S.P. 2016. Dada2: high-resolution sample inference from Illumina amplicon data. Nat. Methods 13(7):581 doi:10.1038/nmeth.3869

Capurso, G., Carroll, B., and Stewart, K.A. 2023. Transforming marine monitoring: Using eDNA metabarcoding to improve the monitoring of the Mediterranean Marine Protected Areas network. Mar. Policy 156: 105807.

Chai, F., Johnson, K.S., Claustre, H., Xing, X., Wang, Y., Boss, E., Riser, S., Fennel, K., Schofield, O., and Sutton, A. 2020. Monitoring ocean biogeochemistry with autonomous platforms. Nat. Rev. Earth Environ. 1(6): 315-326.

Clair, T.A., Dennis, I.F., Scruton, D.A., and M. Gilliss. 2007. Freshwater acidification research in Atlantic Canada: a review of results and predictions for the future. Environ. Rev. 15: 153-167.

Crane, L. C., Goldstein, J. S., Thomas, D. W., Rexroth, K. S., and Watts, A.W. 2021. Effects of life stage on eDNA detection of the invasive European green crab (*Carcinus maenas*) in estuarine systems. Ecol. Indic. 124: 107412.

Crowe, L.M., Brown, M.W., Corkeron, P.J., Hamilton, P.K., Ramp, C., Ratelle, S., Vanderlaan, A.S., and Cole, T.V. 2021. In plane sight: a mark-recapture analysis of North Atlantic right whales in the Gulf of St. Lawrence. Endanger. Species Res. 46: 227-251.

Crozier, L.G., and Siegel, J.E. 2025. From threats to solutions: A literature review of climate adaptation in anadromous salmon and trout. Ecosphere 16: e70054.

Cyr, F., Galbraith, P., Layton, C., Hebert, D., Chen, N., Han, G. 2022. Environmental and Physical Oceanographic Conditions on the Eastern Canadian Shelves (NAFO Subareas 2, 3, and 4) during 2021. NAFO SCR Document 22/020.

Cyr, F., Gibb, O., Azetsu-Scott, K., Chassé, J., Galbraith, P., Maillet, G., Pepin, P., Punshon, S., Starr, M. 2022. Ocean carbonate parameters on the Canadian Atlantic Continental Shelf. Federated Research Data Repository. https://doi.org/10.20383/102.0673

Devine, L., Kennedy, M.K., St-Pierre, I., Lafleur, C., Ouellet, M., and Bond, S. 2014. BioChem: the Fisheries and Oceans Canada database for biological and chemical data. Can. Tech. Rep. Fish. Aquat. Sci. 3073: iv + 40 pp.

Dever, M., Hebert, D., Greenan, B. J. W., Sheng, J., and Smith, P. C. 2016. Hydrography and Coastal Circulation along the Halifax Line and the Connections with the Gulf of St. Lawrence. *Atmosphere-Ocean*, *54*(3), 199–217. https://doi.org/10.1080/07055900.2016.1189397

DFO. 2022. Oceanographic Conditions in the Atlantic Zone in 2021. DFO Can. Sci. Advis. Sec. Sci. Advis. Rep. 2022/025.

Dickson, A.G. 1990. Standard potential of the reaction AgCl(s) + 1/2 H2(g) = Ag(s) + HCl(aq), and the standard acidity constant of the ion $HSO4^-$ in synthetic seawater from 273.15 to 318.15 K. J. Chem. Thermodyn. 22(2):113–127. https://doi.org/10.1016/0021-9614(90)90074-Z

Dickson, A.G., Sabine, C.L., and Christian, J.R. (Eds.) 2007. Guide to best practices for ocean CO_2 measurements. PICES Special Publication 3. 191 pp.

Fairbanks, R. G. 1982. The origin of continental shelf and slope water in the New York Bight and Gulf of Maine: Evidence from $H_2\,^{18}O/H_2\,^{16}O$ ratio measurements, *J. Geophys. Res.*, 87(C8), 5796–5808, doi:10.1029/JC087iC08p05796.

Farmer, G.J. 2000. Effects of low environmental pH on Atlantic salmon (*Salmo salar* L.) in Nova Scotia. Fisheries and Oceans Canada. Can. Stock Assess. Sec. Res. Doc. 2000/050.

Feng, T., Stanley, R.R., Wu, Y., Kenchington, E., Xu, J., and Horne, E. 2022. A high-resolution 3-D circulation model in a complex archipelago on the coastal Scotian Shelf. J. Geophys. Res. Oceans 127(3): e2021JC017791.

Gibb, O., Cyr, F., Azetsu-Scott, K., Chassé, J., Childs, D., Gabriel, C.E., Galbraith, P.S., Maillet, G., Pepin, P., Punshon, S. and Starr, M., 2023. Spatiotemporal variability in pH and carbonate parameters on the Canadian Atlantic continental shelf between 2014 and 2022. Earth Syst. Sci. Data 15(9): 4127-4162.

Ginn, B.K., Cumming, B.F., and Smol, J.P. 2007). Assessing pH changes since pre-industrial times in 51 low-alkalinity lakes in Nova Scotia, Canada. Can. J. Fish. Aquat. Sci. 64(8): 1043-1054.

Gold, Z., Sprague, J., Kushner, D.J., Zerecero Marin, E., and Barber, P.H. 2021. eDNA metabarcoding as a biomonitoring tool for marine protected areas. PLoS One 16(2): e0238557.

Gómez-Repollés, A., Sigsgaard, E.E., Jensen, M.R., and Thomsen, P.F. 2026). Filter pore size influences taxonomic composition of retained eDNA from seawater samples—evidence from shotgun sequencing. Metabarcod. Metagenom. 10: e164232.

Goodwin, C., Cooper, J.A., Lawton, P., Brydges, T., Teed, L.L., Jeffery, N., and Stanley, R.R.E. 2025. Characterisation of sponge sublittoral habitats for the Eastern Shore Islands Area of Interest, Nova Scotia, Canada. Can. Tech. Rep. Fish. Aquat. Sci. 3679: xii + 115 p. https://doi.org/10.60825/1vcv-bs96

Gregory, D., Petrie, B., Jordan, F., and Langille, P. Oceanographic, geographic and hydrological parameters of the Scotia-Fundy and Southern Gulf of St. Lawrence Inlets. 1993. Can. Tech. Rep. Hydrogr. Ocean Sci., No. 143.

Gremillion, P. and Wanielsta, M. 2000. Effects of evaporative enrichment on the stable isotope hydrology of a central Florida (USA) river, Hydrol. Process. 14:1465-1484

Hachey, H.B. 1941. The Waters of the Scotian Shelf. J. Fish. Res. Bd. Can. 5b (4) 377-397

Halfyard, E.A. 2008. Initial results of an Atlantic salmon river acid mitigation program. Acadia University, M.Sc. Thesis. 164 p.

Heaslip, S.G., Jeffery, N.W., Pettitt-Wade, H., and Stanley, R.R.E. In prep. Review and Update of the State of Knowledge for the Eastern Shore Islands Area of Interest (AOI). DFO Can. Sci. Advis. Sec. Res. Doc. 2026/nnn

Hebert, D., Layton, C., Brickman, D. and Galbraith, P.S. 2023. Physical Oceanographic Conditions on the Scotian Shelf and in the Gulf of Maine during 2021. DFO Can. Sci. Advis. Sec. Res. Doc. 2023/044. iv + 65 p

He, X., Stanley, R.R., Rubidge, E.M., Jeffery, N.W., Hamilton, L.C., Westfall, K.M., Gilmore, S.R., Roux, L.-M., Gale, K.S.P., Heaslip, S.G., Steeves, R., and Abbott, C.L. 2022. Fish community surveys in eelgrass beds using both eDNA metabarcoding and seining: implications for biodiversity monitoring in the coastal zone. Can. J. Fish. Aquat. Sci. 79(8): 1335-1346.

He, X., Jeffery, N.W., Stanley, R.R.E., Hamilton, L.C., Rubidge, E.M. and Abbott, C.L., 2023. eDNA metabarcoding enriches traditional trawl survey data for monitoring biodiversity in the marine environment. ICES J. Mar. Sci. 80(5): 1529-1538.

Hurd, C.L., Beardall, J., Comeau, S., Cornwall, C.E., Havenhand, J.N., Munday, P.L., Parker, L.M., Raven, J.A. and McGraw, C.M. 2020. Ocean acidification as a multiple driver: how interactions between changing seawater carbonate parameters affect marine life. Mar. Freshw. Res. 71: 263-274.

Ip, Y.C.A., Chang, J.J.M., Tun, K.P.P., Meier, R., and Huang, D. 2023. Multispecies environmental DNA metabarcoding sheds light on annual coral spawning events. Mol. Ecol. 32(23): 6474-6488.

Irvine, A.L., Reygondeau, G., Stanley, R.R.E., Egorova, Y., and Tittensor, D.P. 2025. Future Climate-Driven Ecological Disruption in a Network of Marine Protected Areas on Canada's East Coast. Conserv. Lett. 18: e13123. https://doi.org/10.1111/conl.13123

Jeffery, N.W., Heaslip, S.G., Stevens, L.A., and Stanley, R.R. 2020. Biophysical and ecological overview of the Eastern Shore Islands Area of Interest (AOI). DFO Can. Sci. Advis. Sec. Res. Doc. 2019/025. xiii + 138 p.

Jeffery, N.W., Stanley, R.R.E., and Heaslip, S.G. 2021. Monitoring connectivity and climate change in the Gully Marine Protected Area. Can. Tech. Rep. Fish. Aquat. Sci. 3453: vii + 52 p.

Jensen, M.R., Sigsgaard, E.E., Ávila, M.D.P., Agersnap, S., Brenner-Larsen, W., Sengupta, M.E., Xing, Y., Krag, M.A., Knudsen, S.W., Carl, H. and Møller, P.R., 2022. Short-term temporal variation of coastal marine eDNA. Environmental DNA 4(4): 747-762.

Johnson, K., King, A.E., and Sieburth, J.M. 1985. Coulometric TCO2 analysis for marine studies: an introduction. Mar. Chem.16(1): 61-82

Jones, E.P., Zemlyak, F. and Stewart, P. 1992. Operating manual for the Bedford Institute of Oceanography automated dissolved oxygen titration system. Can. Tech. Rep. Hydrogr. Ocean Sci. 138: iv + 51 pp.

Kelley, D. and Richards, C. 2024. oce: Analysis of Oceanographic Data. https://doi.org/10.32614/CRAN.package.oce, R package version 1.8-3

Kérouel, R., and Aminot, A. 1997. Fluorometric determination of ammonia in sea and estuarine waters by direct segmented flow analysis. Mar. Chem. 57(3-4): 265-275.

Kerrigan, E.A., Kienast, M., Thomas, H., and Wallace, D.W.R. 2017. Using oxygen isotopes to establish freshwater sources in Bedford Basin, Nova Scotia, a Northwestern Atlantic fjord. Est Coast and Shelf Sci 199: 96-104

Krumhansl, K.A., Brooks, C.M., Lowen, J.B., O'Brien, J.M., Wong, M.C., DiBacco, C. 2024. Loss, resilience and recovery of kelp forests in a region of rapid ocean warming. Ann. Bot. 133: 73–92, https://doi.org/10.1093/aob/mcad170

Kumar, G., Reaume, A.M., Farrell, E., and Gaither, M.R. 2022. Comparing eDNA metabarcoding primers for assessing fish communities in a biodiverse estuary. PLoS One 17(6): e0266720.

Lacroix, G.L. 1989. Ecological and physiological responses of Atlantic salmon in acidic organic rivers of Nova Scotia, Canada. Water Air Soil Pollut. 46(1): 375-386.

Lacroix, G.L. 1992. Mitigation of low stream pH and its effects on salmonids. Environ. Pollut. 78(1-3): 157-164.

Lee, K., Kim, T.-W., Byrne, R.H., Millero, F.J., Feely, R.A., and Liu, Y.-M. 2010. The universal ratio of boron to chlorinity for the North Pacific and North Atlantic oceans. Geochim. Cosmochim. Acta 74(6):1801–1811. https://doi.org/10.1016/j.gca.2009.12.027

Lehmann, N., Reed, D. C., Buchwald, C., Lavoie, D., Yeats, P. A., Mei, Z.-P. Wang, Z. and Johnson, C., 2023. Decadal variability in subsurface nutrient availability on the Scotian Shelf reflects changes in the Northwest Atlantic Ocean. *Journal of Geophysical Research: Oceans*, 128, e2023JC019928. https://doi.org/10.1029/2023JC019928

Lemay, J., Thomas, H., Craig, S.E., Burt, W.J., Fennel, K. and Greenan, B.J. 2018. Hurricane Arthur and its effect on the short-term variability of pCO2 on the Scotian Shelf, NW Atlantic. Biogeosciences 15(7): 2111-2123.

Leray, M., Yang, J.Y., Meyer, C.P., Mills, S.C., Agudelo, N., Ranwez, V., Boehm, J.T. and Machida, R.J. 2013. A new versatile primer set targeting a short fragment of the mitochondrial COI region for metabarcoding metazoan diversity: application for characterizing coral reef fish gut contents. Front. Zool. 10(1), 34.

Lewis, E., Wallace, D., Allison, L.J. 1998. Program developed for CO2 system calculations.", Feb. 1998. https://doi.org/10.2172/639712

Lizotte, M., Blais, M., Chassé, J., Galbraith, P. S., Hébert, A.-J., and Starr, M. 2026. Acidification and CO2-Driven Conditions in the Estuary and Gulf of St. Lawrence During 2024. Can. Tech. Rep. Hydrogr. Ocean. Sci. 410 : vi + 71 p. https://doi.org/10.60825/rj0q-3t94

Lolivier, M., Cornelis, I., Maes, S., Mortelmans, J., Polet, H., and Derycke, S. 2025. Monthly eDNA metabarcoding data from the coastal North Sea area align with fish species-specific life cycle events. Environmental DNA 7(4): e70175.

Lueker, T.J., Dickson, A.G., and Keeling, C.D. 2000. Ocean pCO2 calculated from dissolved inorganic carbon, alkalinity, and equations for K1 and K2: validation based on laboratory measurements of CO2 in gas and seawater at equilibrium. Mar. Chem. 70(1–3):105–119. https://doi.org/10.1016/S0304-4203(00)00022-0

Ma, Y., Wu, Y., Jeffery, N.W., Horwitz, R., Xu, J., Horne, E. and Stanley, R.R., 2024. Simulating dispersal in a complex coastal environment: the Eastern Shore Islands archipelago. ICES J. Mar. Sci. 81(1): 178-194.

Maiello, G., Talarico, L., Brodie, C., Carpentieri, P., Sbrana, A., Shum, P., Mariani, S. and Russo, T. 2024. Net gain: Low-cost, trawl-associated eDNA samplers upscale ecological assessment of marine demersal communities. Environmental DNA 6(1): e389.

Marium, A., Chatha, A.M.M., Naz, S., Khan, M.F., Safdar, W., and Ashraf, I. 2023. Effect of temperature, pH, salinity, and dissolved oxygen on fishes. J. Zool. Systemat. 1: 1-12.

Martin, M. 2011. Cutadapt removes adapter sequences from high-throughput sequencing reads. EMBnet J. 17(1): 10-12.

McInnes, J.C., Jarman, S.N., Lea, M.A., Raymond, B., Deagle, B.E., Phillips, R.A., Catry, P., Stanworth, A., Weimerskirch, H., Kusch, A., Gras, M., Cherel, Y., Maschette, D., and Alderman, R. 2017. DNA metabarcoding as a marine conservation and management tool: A circumpolar examination of fishery discards in the diet of threatened albatrosses. Front. Mar. Sci. 4: 277.

Mclellan, H.J., Lauzier, L., and Bailey, W.B. 1953. The Slope Water off the Scotian Shelf, J. Fish. Res. Bd. Can. 10(4) 155- 176 https://doi.org/10.1139/f53-012

Millero, F.J., 1979. The thermodynamics of the carbonate system in water. Geochem. Cosmo. Acta 43:1651-1661.

Miya, M., Sato, Y., Fukunaga, T., Sado, T., Poulsen, J.Y., Sato, K., Minamoto, T., Yamamoto, S., Yamanaka, H., Araki, H. and Kondoh, M., 2015. MiFish, a set of universal PCR primers for metabarcoding environmental DNA from fishes: detection of more than 230 subtropical marine species. R. Soc. Open Sci. 2(7): 150088.

Moland, E., Olsen, E.M., Knutsen, H., Garrigou, P., Espeland, S.H., Kleiven, A.R., André, C. and Knutsen, J.A., 2013. Lobster and cod benefit from small-scale northern marine protected areas: inference from an empirical before–after control-impact study. Proc. R. Soc. B: Biol. Sci. 280(1754): 20122679.

Monette, M.Y., Björnsson, B.T., McCormick, S.D. 2008. Effects of short-term acid and aluminum exposure on the parr-smolt transformation in Atlantic salmon (*Salmo salar*): Disruption of seawater tolerance and endocrine status. Gen. Comp. Endocrinol. 158(2): 122-130. doi:10.1016/j.ygcen.2008.05.014.

Montgomery, F.A., Rutherford, R.J., and Halfyard, E.A. 2020. Characterizing water chemistry and the distribution of Atlantic Salmon on Nova Scotia's eastern shore based on environmental DNA (eDNA). Nova Scotia Salmon Association. 20 p.

Murphy, G.E.P., Stock, A., and Kelly, N.E. 2024. From Land to Deep Sea: A Continuum of Cumulative Human Impacts on Marine Habitats in Atlantic Canada. Ecosphere 15(9): e4964. https://doi.org/10.1002/ecs2.4964

Murphy, G.E.P., Agbayani, S., Nelson, J.C., Rubidge, E.M., Stanley, R.R.E., Murray, C.C., and Kelly, N.E. 2026. A Coast-to-Coast Assessment of Cumulative Impacts and Protection Potential in Canadian Marine Conservation Networks. Environ. Manag. 76: 158 https://doi.org/10.1007/s00267-026-02427-y

Murray, C.C., Dunham, A., Rubidge, E., Francis, F.T., Hunter, K.L. and Hannah, L.C., 2025. Safeguarding marine protected areas from cumulative effects: a review of methods, best practices, and applications. Environ. Manag. 75(11): 3010-3024.

Neill, C., Johnson, K.M., Lewis, E., and Wallace, D.W. 1997. Accurate headspace analysis of fCO_2 in discrete water samples using batch equilibration. Limnol. Oceanogr. 42(8): 1774-1783.

O'Brien, J.M., Stanley, R., Jeffery, N.W., Heaslip, S.G., DiBacco, C., and Wang, Z. 2022. Modeling Demersal Fish and Benthic Invertebrate Assemblages in Support of Marine Conservation Planning. Ecol. Appl. 32(3): e2546. https://doi.org/10.1002/eap.2546

Oksanen J, Simpson G, Blanchet F, Kindt R, Legendre P, Minchin P, O'Hara R, Solymos P, Stevens M, Szoecs E, Wagner H, Barbour M, Bedward M, Bolker B, Borcard D, Borman T, Carvalho G, Chirico M, De Caceres M, Durand S, Evangelista H, FitzJohn R, Friendly M, Furneaux B, Hannigan G, Hill M, Lahti L, Martino C, McGlinn D, Ouellette M, Ribeiro Cunha E, Smith T, Stier A, Ter Braak C, Weedon J 2025). vegan: Community Ecology Package. <https://doi.org/10.32614/CRAN.package.vegan>, R package version 2.7-1

Paulin, N., Murillo, F.J., Goodwin, C., Rodriguez, E., Nozères, C., and Kenchington, E. 2025. Photo Catalogue of the Epibenthic Megafauna of Eastern Shore Islands (Nova Scotia, Canada) Identified from In Situ Images. Can. Tech. Rep. Fish. Aquat. Sci. 3723: iv +307 p. https://doi.org/10.60825/w0t5-rp42

Perez, F.F., and Fraga, F. 1987. Association constant of fluoride and hydrogen ions in seawater. Mar. Chem. 21(2):161–168. https://doi.org/10.1016/0304-4203(87)90036-3

Pomeroy, R. S., Watson, L. M., Parks, J. E., and Cid, G.A. 2005. How is your MPA doing? A methodology for evaluating the management effectiveness of marine protected areas. Ocean & Coastal Management 48: 485-502.

Porter, T.M., and Gibson, J.F., Shokralla, S., Baird, D.J., Golding, G.B., and Hajibabaei, M. 2014. Rapid and accurate taxonomic classification of insect (class Insecta) cytochrome c oxidase subunit 1 (COI) DNA barcode sequences using a naive Bayesian classifier. Mol. Ecol. Res. 14: 929-942.

Porter, T.M., and Hajibabaei, M. 2018. Automated high throughput animal CO1 metabarcode classification. Sci. Rep. 8: 4226.

Puerta, P., Johnson, C., Carreiro-Silva, M., Henry, L.-A., Kenchington, E., Morato, T., Kazanidis, G., Rueda, J.L., Urra, J., Ross, S., Wei, C.-L., González-Irusta, J.M., Arnaud-Haond, S., and Orejas, C. 2020. Influence of Water Masses on the Biodiversity and Biogeography of Deep-Sea Benthic Ecosystems in the North Atlantic. Front. Mar. Sci. 7:239. doi: 10.3389/fmars.2020.00239

Punshon, S., Azetsu-Scott, K., and Lee, C.M. 2014. On the distribution of dissolved methane in Davis Strait, North Atlantic Ocean. Mar. Chem. 161: 20-25.

Ren, W., Zhou, P., and Zhang, D. 2025. Assessing the efficiency of COI primers in eDNA metabarcoding for marine metazoan biodiversity. Mar. Environ. Res. 107450.

Rincón, B., and Kenchington, E. L. 2016. Influence of benthic macrofauna as a spatial structuring agent for juvenile haddock (*Melanogrammus aeglefinus*) on the Eastern Scotian Shelf, Atlantic Canada. PLoS One 11(9): e0163374.

Sajtovich, J., Tsao, J., Kirchhoff, S., and Brown, C.J. 2025. Development and application of BRUVS-Lite: A stereo-BRUV system with integrated lighting for benthic marine monitoring in northern latitudes. Methods Ecol. Evol. 16

Savard-Drouin, A., Ulrick, A., and Metaxas, A. 2024. Wave exposure influences kelp morphological and biomechanical phenotypic plasticity. Mar. Ecol. Prog. Ser. 748: 1-15.

Sephton, D., Vercaemer, B., Silva, A., Stiles, L., Harris, M. and Godin, K. 2017. Biofouling monitoring for aquatic invasive species (AIS) in DFO Maritimes Region (Atlantic shore of Nova Scotia and southwest New Brunswick): May – November, 2012 - 2015. Can. Tech. Rep. Fish. Aquat. Sci. 3158: ix + 172p.

Sevellec, M., Lacoursière-Roussel, A., Normandeau, E., Bernatchez, L., and Howland, K.L. 2025. Effect of eDNA metabarcoding temporal sampling strategies on detection of coastal biodiversity. Front. Mar. Sci. 12: 1522677.

Schlegel, M. 2026. taxplore: Create and display interactive hierarchical Krona charts. R package version 0.1.0, commit a008eadfb340fed04d223c68ea509088b3f58f02, <https://github.com/markschl/taxplore>.

Stica, P.V., Pie, M.R., Horodesky, A., DalPont, G., Cozer, N., Biernaski, V., Netto, O.S.M., Szortyka, A., Baldissera, A. and Ostrensky Neto, A., 2025. Effects of freezing duration and speed on environmental DNA (eDNA) degradation in water samples: a controlled mesocosm study. Hydrobiologia 853: 337-351

Stoeckle, M.Y., Adolf, J., Charlop-Powers, Z., Dunton, K.J., Hinks, G., and VanMorter, S.M. 2021. Trawl and eDNA assessment of marine fish diversity, seasonality, and relative abundance in coastal New Jersey, USA. ICES Journal of Marine Science, 78(1), 293-304.

Strain, P.M. 2002. Nutrient dynamics in ship harbour, Nova Scotia. Atmosphere-Ocean, 40(1), 45-58.

Strickland, J.D.H. and Parsons, T.R., 1972. A practical handbook of seawater analysis. Fish. Res. Board Can. 167: 310 pp.

Sunday, J. M., Howard, E., Siedlecki, S., Pilcher, D. J., Deutsch, C., MacCready, P., Newton, J., and Klinger, T. 2022. Biological sensitivities to high-resolution climate change projections in the California current marine ecosystem. Global Change Biology, 28, 5726–5740. https://doi.org/10.1111/gcb.16317

Thomas, H., Ittekkot, V., Osterroht, C. and Schneider, B., 1999. Preferential cycling of nutrients – the ocean's way to increase new production and to pass nutrient limitation?

Trask, C.G., Jeffery, N.W., Stanley, R.R., Van Wyngaarden, M., McBride, M.C., He, X., Abbott, C.L. and Rawlings, T.A., 2025. Applying eDNA metabarcoding to assess invertebrate biodiversity of eelgrass (*Zostera marina*) meadows across Nova Scotia. Can. J. Fish. Aquat. Sci. 82: 1-18.

van der Loos, L.M., Schmid, M., Leal, P.P., McGraw, C.M., Britton, D., Revill, A.T., Virtue, P., Nichols, P.D. and Hurd, C.L., 2019. Responses of macroalgae to CO_2 enrichment cannot be inferred solely from their inorganic carbon uptake strategy. Ecol. Evol. 9: 125-140.

Van Wyngaarden, M., Jeffery, N.W., Horne, E., Clemente-Carvalho, R.B., Lemay, M., Grundke, I., Luy, E., Hendricks, A., Sonnichsen, C., Sieben, V., Laroche, J., Beiko, R.G., Furlong, A., Knox, T., Pettitt-Wade, H., and Stanley, R.R. 2024. Evaluating an autonomous eDNA sampler for marine environmental monitoring: Short-and long-term applications. IEEE Xplore OCEANS 2024-Halifax 1-8.

Wangensteen, O.S., Palacín, C., Guardiola, M., and Turon, X. 2018). DNA metabarcoding of littoral hard-bottom communities: High diversity and database gaps revealed by two molecular markers. PeerJ, 6, e4705. https://doi.org/10.7717/peerj.4705

Wang, J., Xia, X., Liu, S., Zhang, S., Dong, J., Wang, G., Xu, W., Zhang, L., Zheng, W., Zhang, Z., Chen,X., Yuan, L., Liu, J., Zhang, J., Xin, Y., McDowell, W.H., Tian, H., Bastviken, D., Yang, Z. 2026. Globally doubled methane emissions from nutrient-enriched rivers, *National Science Review*, 13(8) nwag192. https://doi.org/10.1093/nsr/nwag192

Watt, W.D. 1987. A summary of the impact of acid rain on Atlantic salmon (*Salmo salar*) in Canada. Water Air Soil Pollut. 35:27-35.

Wiesenburg, D. A., and Guinasso Jr, N.L. 1979. Equilibrium solubilities of methane, carbon monoxide, and hydrogen in water and sea water. J. Chem. Eng. Data 24(4): 356-360.

Wolf-Glarow, D.A., Zeebe, R.E., Klaas C., Körtzinger A., Dickson A. 2007. Total alkalinity: The explicit conservative expression and its application to biogeochemical processes. Mar. Chem. 106: 287-300.

APPENDICES

Appendix Table 1. A list of all species detected in the Eastern Shore Islands using environmental DNA metabarcoding at three markers (12S, 16S, COI) from 2021 to 2023. The 12S marker was used in all three years, while 16S was only used in 2021 and 2022, and COI was only used in 2022 and 2023.

Species Name	Common Name	eDNA Marker(s)	Year(s)
Vertebrates			
Alopias vulpinus	Common Thresher Shark	16S	2022
Alosa spp.*	Shads/River Herring	12S, 16S	2021, 2022, 2023
Amblyraja radiata	Thorny Skate	12S	2022, 2023
Ameiurus nebulosus	Brown Bullhead	12S	2023
Ammodytes americanus	Sandlance	12S	2022, 2023
Ammodytes dubius	Sandlance	12S, 16S	2021, 2022, 2023
Ammodytes marinus	Sandlance	12S, 16S	2021, 2022, 2023
Anarhichas denticulatus	Northern Wolffish	12S, 16S	2022, 2023
Anarhichas lupus	Atlantic Wolffish	16S	2021, 2022

Species Name	Common Name	eDNA Marker(s)	Year(s)
Anguilla rostrata	American Eel	12S	2023
Apeltes quadracus	Fourspine Stickleback	12S, 16S	2021, 2023
Argentina silus	Atlantic Argentine	16S	2022
Balaenoptera acutorostrata	Common Minke Whale	12S, COI	2021, 2022, 2023
Balistes capriscus	Grey Triggerfish	12S	2022
Brevoortia tyrannus	Atlantic Menhaden	12S	2023
Catostomus commersonii	White Sucker	12S	2023
Cetorhinus maximus	Basking Shark	12S	2023
Citharichthys arctifrons	Gulf Stream Flounder	12S	2022
Clupea harengus	Atlantic Herring	12S, 16S	2021, 2022, 2023
Cryptacanthodes maculatus	Wrymouth	12S, 16S	2022, 2023
Delphinus delphis	Common Dolphin	12S	2023
Dipturus batis	Blue Skate	16S	2022
Dipturus laevis	Barndoor Skate	12S	2022
Enchelyopus cimbrius	Fourbeard Rockling	12S	2023
Eubalaena glacialis	North Atlantic Right Whale	12S	2023
Eumesogrammus praecisus	Fourline Snakeblenny	12S	2022, 2023
Fundulus diaphanus	Banded Killifish	12S	2023
Fundulus heteroclitus	Mummichog	12S	2023
Gadus morhua	Atlantic Cod	12S, 16S	2021, 2022, 2023

Species Name	Common Name	eDNA Marker(s)	Year(s)
Glyptocephalus cynoglossus	Witch Flounder	12S	2023
Gymnelus viridis	Fish Doctor	12S	2021
Gymnocanthus tricuspis	Arctic Staghorn Sculpin	12S	2023
Hemitripterus americanus	Sea Raven	12S, 16S	2021, 2022, 2023
Hippoglossoides platessoides	American Plaice	12S	2023
Lagenorhynchus acutus	Atlantic White-Sided Dolphin	12S	2022, 2023
Lamna nasus	Porbeagle	12S, 16S	2022, 2023
Leptoclinus maculatus	Daubed Shanny	12S, 16S	2022, 2023
Liparis spp.*	Snailfish	12S	2021, 2023
Lophius americanus	Monkfish	12S, 16S	2022
Lumpenus fabricii	Slender Eelblenny	12S	2023
Lumpenus lampretaeformis	Snakeblenny	16S	2022
Lycodes vahlii	Vahl's Eelpout	12S	2023
Mallotus villosus	Capelin	12S	2023
Melanogrammus aeglefinus	Haddock	12S, 16S	2022, 2023
Merluccius bilinearis	Silver Hake	12S, 16S	2022, 2023
Microgadus tomcod	Tomcod	12S, 16S	2021, 2023
Myoxocephalus octodecemspinosus	Longhorn Sculpin	16S	2021, 2022, 2023
Myoxocephalus scorpius	Shorthorn Sculpin	12S, 16S	2021, 2022, 2023
Notemigonus crysoleucas	Golden Shiner	12S	2023

Species Name	Common Name	eDNA Marker(s)	Year(s)
Osmerus mordax	Rainbow Smelt	12S	2022, 2023
Perca flavescens	Yellow Perch	12S	2023
Phocoena phocoena	Harbour Poropoise	12S	2023
Pholis gunnellus	Rock Gunnel	12S, 16S	2021, 2022, 2023
Platichthys spp.*	Flounder	12S, 16S	2021, 2022, 2023
Pleuronectes platessa	European Plaice	16S	2021
Pollachius virens	Pollock	12S, 16S	2022
Prionace glauca	Blue Shark	16S, COI	2022
Pseudopleuronectes americanus	Winter Flounder	12S, COI	2021, 2022, 2023
Salmo salar	Atlantic Salmon	12S	2023
Salvelinus fontinalis	Brook Trout	12S	2023
Scomber scombrus	Mackerel	12S, 16S, COI	2021, 2022, 2023
Scomberesox saurus	Atlantic Saury	12S, 16S	2021, 2022, 2023
Sebastes fasciatus	Acadian Redfish	12S	2021, 2022, 2023
Sebastes mentella	Deepwater Redfish	16S	2021, 2023
Selene setapinnis	Atlantic Moonfish	12S, 16S	2021
Semotilus atromaculatus	Creek Chub	12S	2023
Squalus acanthias	Spiny Dogfish	16S	2022
Tautogolabrus adspersus	Cunner	12S, 16S	2021, 2022, 2023

Species Name	Common Name	eDNA Marker(s)	Year(s)
Thunnus thynnus	Atlantic Bluefin Tuna	12S	2021, 2023
Triglops murrayi	Moustache Sculpin	12S, 16S	2021, 2022, 2023
Triglops pingelii	Ribbed Sculpin	12S	2022
Urophycis chuss	Red Hake	12S, 16S, COI	2022, 2023
Urophycis tenuis	White Hake	12S, COI	2022, 2023
Zoarces americanus	Ocean Pout	12S, COI	2022, 2023
* eDNA does not resolve species in these genera well, either due to low marker divergence rates or reference sequence misidentifications, and as such should be considered at the genus or lowest common ancestor only			
Invertebrates			
Acartia hudsonica	Copepod	COI	2022, 2023
Acartia longiremis	Copepod	COI	2022
Alitta virens	Polychaete	COI	2023
Amphitrite cirrata	Polychaete	COI	2023
Aurelia aurita	Moon Jellyfish	COI	2023
Balanus crenatus	Acorn Barnacle	COI	2022, 2023
Boltenia echinata	Stalked Tunicate	COI	2023
Bougainvillia superciliaris	Hydrozoan Jellyfish	COI	2023
Calanus finmarchicus	Calanoid copepod	COI	2022, 2023
Calanus hyperboreus	Calanoid copepod	COI	2022, 2023
Capitella capitata	Polychaete	COI	2023
Centropages hamatus	Copepod	COI	2023
Centropages typicus	Copepod	COI	2023

Species Name	Common Name	eDNA Marker(s)	Year(s)
Cistenides (Pectinaria) hyperborea	Polychaete	COI	2023
Cyrtodaria siliqua	Northern Propeller Clam	COI	2023
Dodecaceria concharum	Polychaete	COI	2023
Dynamena pumila	Hydrozoan Jellyfish	COI	2023
Echinarachnius parma	Common Sand Dollar	COI	2023
Eualus pusiolus	Shrimp	COI	2022
Eunoe nodosa	Scaleworm	COI	2023
Eurytemora herdmani	Copepod	COI	2023
Evadne nordmanni	Branchiopod crustacean	COI	2022
Galathowenia oculata	Polychaete	COI	2023
Gattyana cirrhosa	Scaleworm	COI	2023
Glycera capitata	Polychaete	COI	2023
Halichondria panicea	Breadcrumb Sponge	COI	2023
Haliclona oculata	Mermaid’s Glove	COI	2023
Harmothoe imbricata	15-Scaled Worm	COI	2023
Hybocodon prolifer	Hydrozoan	COI	2022
Lacuna vincta	Lacuna Snail	COI	2022, 2023
Laonice cirrata	Polychaete	COI	2023
Macoma calcarea	Marine Bivalve	COI	2023
Marenzelleria viridis	Polychaete	COI	2022
Membranipora membranacea	Coffin Box Bryozoan	COI	2022, 2023

Species Name	Common Name	eDNA Marker(s)	Year(s)
Metridia lucens	Copepod	COI	2022, 2023
Micronephthys neotena	Polychaete	COI	2022
Microstomum spp.	Platyhelminth worm	COI	2022
Micrura varicolor	Nemertean worm	COI	2022
Nereis pelagica	Polychaete	COI	2023
Nothria conchylega	Polychaete	COI	2022
Obelia geniculata	Knotted Thread Hydroid	COI	2022, 2023
Obelia longissima	Hydrozoan	COI	2022
Oithona similis	Copepod	COI	2022, 2023
Ophiopholis aculeata	Daisy Brittle Star	COI	2022, 2023
Phyllodoce groenlandica	Polychaete	COI	2023
Phyllodoce maculata	Polychaete	COI	2022, 2023
Pleurobrachia pileus	Sea Gooseberry	COI	2022
Prionospio steenstrupi	Polychaete	COI	2022, 2023
Pseudocalanus acuspes	Copepod	COI	2023
Pseudocalanus minutus	Copepod	COI	2022, 2023
Pseudocalanus moultoni	Copepod	COI	2022
Pseudocalanus newmani	Copepod	COI	2022, 2023
Pseudopotamilla reniformis	Polychaete	COI	2023
Scoloplos armiger	Polychaete	COI	2023
Strongylocentrotus droebachiensis	Green Sea Urchin	COI	2023
Terschellingia longicaudata	Marine nematode	COI	2022

Species Name	Common Name	eDNA Marker(s)	Year(s)
Thysanoessa inermis	Krill	COI	2023
Tortanus discaudatus	Copepod	COI	2022, 2023
Trochochaeta multisetosa	Polychaete	COI	2023
Turtonia minuta	Bivalve	COI	2022
Urticina crassicornis	Painted Anemone	COI	2022
Yoldiella nana	Deepwater bivalve	COI	2022
Seaweeds/Algae			
*Acrochaetium spp.**	Red algae	COI	2022
Ahnfeltia plicata	Red algae - Landlady's Wig	COI	2023
Bonnemaisonia hamifera	Invasive red seaweed	COI	2022, 2023
Chondrus crispus	Irish Moss	COI	2023
Corallina officinalis	Coralline algae	COI	2023
Dasysiphonia japonica	Invasive red seaweed	COI	2022, 2023
Euthora cristata	Red algae	COI	2023
Lithothamnion glaciale	Red algae	COI	2022, 2023
Micromonas pusilla	Green algae	COI	2022, 2023
Rhodomela lycopodioides	Red algae – Straggly Tail Weed	COI	2023
Vertebrata lanosa	Red algae	COI	2022
Wildemania amplissima	Red algae	COI	2022

Transect	Station	Depth (m)	Temp (C)	Salinity (psu)	DIC (μmol kg-1)	TA (μmol kg-1)	pCO_2 22C (μatm)	pCO_2 in situ (μatm)	pH_{total}	Ωarag	Ωcalc
Moser River/ Nukumkiaq	ESI-1	2.28	15.681	30.4778	1950.50	2083.45	576.7	446.5	7.911	1.59	2.50
	ESI-1	5.24	13.9413	30.4169	1970.98	2076.98	600.7	432.7	7.860	1.34	2.11
	ESI-1	15.13	11.1408	30.5583	1996.85	2110.75	710.5	456.6	7.920	1.39	2.20
	ESI-1	20.24	10.6208	30.5802	2018.70	2111.95	749.6	471.8	7.864	1.21	1.92
	ESI-2	2.01	17.7479	30.4946	1950.65	2079.26	555.1	467.7	7.869	1.58	2.46
	ESI-2	5.02	14.9336	30.4194	1966.54	2086.19	575.7	432.0	7.885	1.47	2.31
	ESI-2	14.77	9.9944	30.6272	2005.91	2102.01	696.2	425.5	7.883	1.23	1.95
	ESI-2	25.44	8.4826	30.6770	2026.00	2120.78	820.7	472.9	7.899	1.21	1.92
	ESI-2	50.52	4.8069	31.2754	2081.26	2155.09	1044.7	519.1	7.876	1.03	1.64
	ESI-3	2.14	17.6561	30.3149	1964.34	2074.77	556.7	467.2	7.820	1.42	2.21
	ESI-3	5.02	17.2422	30.3494	1949.86	2088.94	558.3	460.8	7.906	1.67	2.61
	ESI-3	15.34	10.1890	30.4713	1991.52	2107.00	722.3	446.0	7.941	1.39	2.21
	ESI-3	25.01	7.1316	30.8910	2037.29	2126.40	871.7	475.0	7.898	1.16	1.84
	ESI-3	49.91	4.6705	31.5263	2075.46	2157.43	1020.2	503.3	7.902	1.09	1.73
	ESI-3	68.35	3.3790	31.8396	2112.33	2178.56	1020.2	N/A	7.863	0.97	1.54
	ESI-4	2.63	18.4861	30.5614	1952.70	2099.71	542.5	471.0	7.904	1.76	2.74
	ESI-4	4.98	18.4224	30.5680	1954.00	2105.78	546.6	473.3	7.917	1.80	2.82
	ESI-4	15.55	14.6779	31.8039	2005.44	2154.24	598	444.1	7.943	1.73	2.71
	ESI-4	25.40	5.6556	31.1446	2056.48	2141.52	929.9	476.6	7.903	1.12	1.78
	ESI-4	49.81	3.5267	31.6917	2089.85	2166.45	1099.8	518.5	7.899	1.04	1.66
	ESI-4	80.29	3.3481	32.3259	2128.42	2193.89	1228.3	578.6	7.854	0.96	1.53
	ESI-4	95.02	3.5585	32.5698	2147.21	2203.18	1298.7	619.9	7.815	0.90	1.43

Appendix Table 2a-d. Chemical parameters for the carbonate system for samples collected along the 4 transects through depth (m) in the Eastern Shore Islands Area of Interest a. Moser River//Nukumkiaq, b. Sheet Harbour/Weijuik*, c. Ship Harbour/Ketmenipukwek, d. Jeddore/Winipukeik, including measured (Temperature, Salinity, dissolved inorganic carbon (DIC), total alkalinity (TA), and the partial pressure of carbon dioxide at 22 C (pCO_2)) and calculated (partial pressure of CO2 converted to in situ conditions (pCO_2 in situ), pH_T (pH on the total scale), the saturation state of aragonite (Ω_{arag}) and calcite (Ω_{calc})) parameters. Units for each measurement are in brackets, but note that pH_T, Ω_{arag} and Ω_{calc} are dimensionless. N/A indicates that a data point is not available for this sample measurement.*

Transect	Station	Depth (m)	Temp (C)	Salinity (psu)	DIC (μmol kg-1)	TA (μmol kg-1)	pCO_2 22C (μatm)	pCO_2 in situ (μatm)	pH_{total}	Ω_{arag}	Ω_{calc}
Sheet Harbour/ Weijuik	ESI-0	2.29	12.7327	30.1833	1966.63	2078.97	677.5	465.3	7.900	1.38	2.19
	ESI-0	10.78	9.2472	30.6508	2054.74	2138.60	977.1	586.6	7.852	1.14	1.81
	ESI-5	2.29	17.3626	30.5416	1949.74	2111.40	574.1	476.4	7.957	1.89	2.95
	ESI-5	5.33	16.1611	30.5445	1951.24	2105.13	574.3	453.5	7.956	1.80	2.82
	ESI-5	15.17	10.2863	30.5273	1995.60	2107.48	651.4	402.3	7.928	1.36	2.16
	ESI-6	1.98	17.7952	30.6326	1968.52	2086.76	573.9	484.6	7.836	1.49	2.32
	ESI-6	5.21	17.6464	30.6350	1962.93	2100.79	569.6	478.0	7.891	1.66	2.60
	ESI-6	14.94	9.6806	30.7175	2009.98	2113.72	716.0	432.2	7.909	1.29	2.05
	ESI-6	31.73	6.8646	30.8132	2047.25	2125.05	883.6	476.1	7.866	1.07	1.70
	ESI-7	2.04	17.8071	30.6511	1954.34	2118.58	566.4	478.5	7.955	1.92	3.00
	ESI-7	5.26	17.6323	30.6396	1966.73	2110.18	564.9	473.7	7.905	1.72	2.69
	ESI-7	15.09	9.1127	30.9302	2014.08	2126.26	754.1	445.1	7.940	1.36	2.16
	ESI-7	24.75	4.6085	31.3404	2068.62	2139.78	929.8	454.8	7.871	1.01	1.61
	ESI-7	49.84	3.5977	31.7721	2103.59	2167.74	1123.4	531.8	7.855	0.95	1.52
	ESI-7	67.00	3.4401	31.9898	2118.37	2182.35	1215.0	574.4	7.853	0.95	1.52
	ESI-8	1.17	17.6978	30.8275	1959.85	2114.88	565.8	475.8	7.931	1.83	2.85
	ESI-8	4.38	17.7925	30.8475	1958.03	2118.52	557.9	471.0	7.943	1.88	2.93
	ESI-8	14.81	14.6452	31.6339	1984.81	2130.73	572.8	424.6	7.941	1.70	2.66
	ESI-8	24.87	5.3872	31.5913	2064.13	2154.23	885.3	447.0	7.917	1.16	1.84
	ESI-8	49.91	3.2443	32.1846	2122.67	2188.53	1147.0	535.0	7.861	0.97	1.55
	ESI-8	79.50	3.6058	32.6062	2140.41	2203.41	1290.6	617.1	7.839	0.95	1.51
	ESI-8	97.01	4.2179	32.8360	2164.60	2214.07	1335.5	657.0	7.779	0.86	1.37

Transect	Station	Depth (m)	Temp (C)	Salinity (psu)	DIC (μmol kg-1)	TA (μmol kg-1)	pCO_2 22C (μatm)	pCO_2 in situ (μatm)	pH_{total}	Ωarag	Ωcalc
Ship Harbour/ Ketmenipukwek	ESI-9	2.26	15.6144	30.3091	1947.61	2060.00	578.7	446.8	7.858	1.40	2.21
	ESI-9	5.40	13.4404	30.4161	1963.89	2096.53	616.4	435.1	7.943	1.57	2.48
	ESI-9	17.81	8.5227	30.6961	2028.71	2121.31	801.5	462.2	7.891	1.19	1.90
	ESI-10	1.92	18.7417	30.7310	1955.13	2109.39	555.1	487.0	7.916	1.83	2.85
	ESI-10	5.19	18.3919	30.7475	1950.34	2107.80	557.5	482.2	7.929	1.85	2.89
	ESI-10	15.12	9.5500	30.7684	2003.66	2119.03	721.3	433.1	7.945	1.39	2.20
	ESI-10	40.94	4.9316	31.1777	2069.52	2144.46	978.8	487.1	7.880	1.03	1.65
	ESI-11	2.08	18.3207	30.5628	1949.14	2097.46	555	478.7	7.910	1.77	2.76
	ESI-11	4.96	18.145	30.5760	1948.21	2094.50	559.4	479.1	7.908	1.75	2.72
	ESI-11	15.14	14.2458	30.7737	1971.68	2115.74	626.9	457.8	7.955	1.68	2.65
	ESI-11	25.20	6.7773	30.9269	2044.49	2128.40	895.7	481.3	7.886	1.11	1.77
	ESI-11	49.78	5.7709	31.6930	2069.96	2164.92	955.2	492.5	7.924	1.19	1.90
	ESI-11	74.27	3.5335	32.0277	2117.71	2185.38	1191.4	564.6	7.863	0.98	1.56
	ESI-12	2.49	18.486	30.5076	1956.44	2094.48	563.1	489.0	7.882	1.68	2.62
	ESI-12	5.04	18.355	30.5306	1947.06	2095.77	564.7	487.8	7.911	1.77	2.76
	ESI-12	15.35	15.7942	30.7959	1958.19	2103.11	593.4	461.7	7.935	1.70	2.67
	ESI-12	25.03	7.9806	30.8879	2029.79	2129.36	836.5	472.1	7.918	1.25	1.98
	ESI-12	49.96	3.8008	32.0031	2095.80	2185.75	1056.9	502.6	7.933	1.15	1.83
	ESI-12	79.13	3.5715	32.5063	2137.95	2204.93	1293	617.7	7.854	0.98	1.56
	ESI-12	93.45	3.9607	32.6760	2148.35	2208.67	1301	632.1	7.823	0.93	1.48

Transect	Station	Depth (m)	Temp (C)	Salinity (psu)	DIC (μmol kg-1)	TA (μmol kg-1)	pCO_2 22C (μatm)	pCO_2 in situ (μatm)	pH_{total}	Ωarag	Ωcalc
Jeddore/ Winipukwejk	ESI-13	2.31	17.1246	30.8012	1954.60	2106.52	582.2	480.7	7.933	1.79	2.79
	ESI-13	5.16	15.0745	30.5658	1960.45	2101.88	593.8	448.5	7.940	1.67	2.62
	ESI-13	14.65	10.3207	30.7633	1991.30	2107.45	723.5	449.3	7.937	1.40	2.22
	ESI-13	32.08	6.6552	30.9292	N/A	N/A	938.8	N/A	N/A	N/A	N/A
	ESI-14	2.08	17.941	30.7516	1954.09	2112.07	565.4	480.2	7.937	1.86	2.90
	ESI-14	4.91	17.6616	30.7142	1952.68	2110.12	574.3	482.4	7.940	1.85	2.89
	ESI-14	14.77	10.0581	31.0127	1987.99	2117.29	688.4	421.9	8.0	1.51	2.39
	ESI-14	24.26	6.7925	30.8343	2032.97	2132.19	878.1	471.7	7.936	1.24	1.97
	ESI-15	2.04	18.6778	30.9044	1958.11	2114.04	557.1	487.5	7.918	1.85	2.88
	ESI-15	4.78	18.5973	30.8386	1959.28	2112.79	560.6	489.0	7.914	1.82	2.84
	ESI-15	14.18	7.1654	30.8787	2021.34	2122.60	827.0	450.4	7.937	1.25	2.00
	ESI-15	25.79	6.7334	30.8816	2037.84	2129.76	904.9	485.7	7.913	1.18	1.87
	ESI-15	49.86	4.4029	31.3367	2071.56	2149.42	1041.4	508.6	7.895	1.05	1.68
	ESI-15	65.36	3.7061	32.1590	2117.03	2180.14	1183.0	564.6	7.844	0.95	1.51
	ESI-16	2.36	18.3861	30.8697	1956.74	2118.24	572.7	N/A	7.937	1.90	2.96
	ESI-16	5.49	18.0385	31.0083	1964.33	2117.27	572.7	495.4	7.918	1.81	2.82
	ESI-16	14.72	10.3383	31.4529	2002.44	2126.80	665.3	568.2	7.950	1.47	2.32
	ESI-16	24.63	5.6062	31.4870	2058.93	2142.42	879.9	550.3	7.895	1.10	1.76
	ESI-16	49.43	3.4946	31.9911	2110.63	2170.17	1159.0	600.4	7.838	0.92	1.47
	ESI-16	79.39	4.1238	32.6948	2143.34	2206.75	1214.4	590.9	7.831	0.95	1.52
	ESI-16	111.00	5.5123	33.1595	2166.61	2221.90	1225.5	633.0	7.776	0.91	1.44

Appendix Table 3a-d. Chemical parameters for samples collected along the 4 transects through depth (m) in the Eastern Shore Islands Area of Interest (a. Moser River//Nukumkiaq, b. Sheet Harbour/Weijuik, c.Ship Harbour/Ketmenipukwek, d.Jeddore/Winipukweik), including dissolved oxygen (DO), apparent oxygen utilization (AOU), methane saturation (CH_4 Sat), Nitrate + Nitrite (NO3/2), Phosphate (PO4), Silicate (SiO4) and Ammonium (NH4+), and for Sheet Harbour (b) only, stable oxygen isotope ratios ($\delta^{18}O$). Units for each measurement are in brackets. N/A indicates that a data point is not available for this sample measurement.

Transect	Site	Depth (m)	DO (μmol kg-1)	AOU (μmol kg-1)	CH_4 Sat (%)	$NO_{3/2}$ (μmol kg-1)	PO_4 (μmol kg-1)	SiO_4 (μmol kg-1)	NH_4^+ (μmol kg-1)
Moser River/ Nukumkiaq	ESI-1	2.28	285.9	-34.55	364.9	0.04	0.39	3.30	0.03
	ESI-1	5.24	287.8	-27.26	300.7	1.29	0.57	6.79	2.55
	ESI-1	15.13	286.5	-10.36	340.5	0.04	0.12	0.70	0.02
	ESI-1	20.24	284.5	-5.18	392.5	0.04	0.13	0.58	0.10
	ESI-2	2.01	269.7	-28.48	219.2	0.04	0.25	1.03	0.16
	ESI-2	5.02	283.6	-28.34	173.3	1.90	0.45	2.64	0.22
	ESI-2	14.77	294.3	-11.16	249.2	7.95	0.93	8.08	0.24
	ESI-2	25.44	291.8	0.99	221.4	10.45	0.89	10.78	0.13
	ESI-2	50.52	287.9	30.16	198.6	12.03	1.13	13.48	0.55
	ESI-3	2.14	266.6	-24.62	163.1	0.03	0.11	0.57	0.27
	ESI-3	5.02	271.7	-27.83	161.2	0.03	0.13	0.60	0.03
	ESI-3	15.34	294.5	-12.33	149.8	0.84	0.43	2.59	0.11
	ESI-3	25.01	291.9	9.77	168.2	1.87	0.52	3.31	0.64
	ESI-3	49.91	290.9	27.69	169.5	4.55	0.74	4.75	0.35
	ESI-3	68.35	279.9	48.38	169.5	8.25	0.94	8.40	0.11
	ESI-4	2.63	253.9	-16.12	129.6	0.06	0.11	0.72	0.61
	ESI-4	4.98	253.1	-15.07	124.7	0.05	0.16	0.79	0.02
	ESI-4	15.55	270.3	-15.84	136.2	0.15	0.30	1.76	0.26
	ESI-4	25.40	294.6	17.26	157.5	1.58	0.52	2.97	0.17
	ESI-4	49.81	289.6	37.76	179.7	0.03	0.18	1.08	0.02
	ESI-4	80.29	261.2	66.23	227.2	0.03	0.20	1.43	0.23
	ESI-4	95.02	244.7	80.57	249.1	0.12	0.35	2.18	0.07

Transect	Site	Depth (m)	DO (µmol kg-1)	AOU (µmol kg-1)	CH_4 Sat (%)	$NO_{3/2}$ (µmol kg-1)	PO_4 (µmol kg-1)	SiO_4 (µmol kg-1)	NH_4^+ (µmol kg-1)	$\delta^{18}O$ (permil)
b. Sheet Harbour/ Weijuik	ESI-00	2.29	278.7	-11.13	894.0	0.25	0.40	2.49	1.92	-2.12
	ESI-00	10.78	253.3	34.56	1840.7	0.45	0.28	3.19	0.45	
	ESI-5	2.29	260.7	-17.74	126.7	0.03	0.11	0.98	0.12	-2.01
	ESI-5	5.33	275.1	-26.22	137.8	0.03	0.11	1.10	0.05	
	ESI-5	15.17	310.8	-29.34	334.4	0.14	0.38	2.77	0.33	-1.99
	ESI-6	1.98	254.3	-13.43	121.2	0.02	0.14	0.78	0.05	-1.98
	ESI-6	5.21	255.2	-13.63	115.6	0.03	0.12	0.80	0.36	-2.06
	ESI-6	14.94	302.6	-17.65	224.1	0.17	0.32	2.57	0.26	-1.98
	ESI-6	31.73	301.2	2.56	194.3	1.39	0.43	3.29	0.20	-1.9
	ESI-7	2.04	251.8	-11.00	113.9	0.01	0.14	0.79	0.08	-1.98
	ESI-7	5.26	252.3	-10.66	118.1	0.01	0.16	0.78	0.20	-2.02
	ESI-7	15.09	294.5	-6.28	136.7	0.14	0.32	1.66	0.10	-1.98
	ESI-7	24.75	302.2	17.28	143.1	2.64	0.58	3.12	0.95	-1.9
	ESI-7	49.84	279.1	47.56	183.3	6.92	0.89	7.08	0.31	-1.71
	ESI-7	67.00	268.8	58.65	211.2	8.61	0.98	9.22	0.97	-1.62
	ESI-8	1.17	251.6	-10.60	110.4	0.03	0.11	0.59	0.40	-2.07
	ESI-8	4.38	250.6	-10.06	116	0.03	0.13	0.56	0.18	-1.94
	ESI-8	14.81	277.9	-23.04	123.5	0.03	0.18	0.33	0.39	-1.8
	ESI-8	24.87	306.9	6.08	138.4	1.15	0.50	1.81	0.25	-1.79
	ESI-8	49.91	273.4	55.23	188.1	8.08	0.94	6.94	0.19	-1.54
	ESI-8	79.50	243.5	81.22	249.3	10.70	1.11	11.22	0.08	-1.3
	ESI-8	97.01	226.1	93.33	273.7	11.39	1.01	13.17	0.43	-1.22

Transect	Site	Depth (m)	DO (μmol kg-1)	AOU (μmol kg-1)	CH_4 Sat (%)	$NO_{3/2}$ (μmol kg-1)	PO_4 (μmol kg-1)	SiO_4 (μmol kg-1)	NH_4^+ (μmol kg-1)
Ship Harbour/ Ketmenipukwek	ESI-9	2.26	277.8	-25.85	557.1	2.27	0.61	4.23	0.72
	ESI-9	5.40	289.8	-26.62	440.3	0.03	0.07	0.41	0.03
	ESI-9	17.81	299.4	-6.94	758.5	0.03	0.07	0.50	0.03
	ESI-10	1.92	251.1	-14.73	126.9	0.03	0.13	0.75	0.20
	ESI-10	5.19	252.6	-14.65	125.3	0.83	0.35	2.35	0.12
	ESI-10	15.12	297.1	-11.41	217.8	5.94	0.78	4.91	0.02
	ESI-10	40.94	299.0	18.35	173.9	10.28	1.02	11.16	0.08
	ESI-11	2.08	253.5	-15.00	118	11.32	0.87	12.68	0.05
	ESI-11	4.96	254.7	-15.39	133.9	0.03	0.09	0.46	0.02
	ESI-11	15.14	275.0	-16.69	142.2	0.03	0.09	0.46	0.03
	ESI-11	25.20	301.7	2.39	159.4	0.03	0.20	0.94	0.04
	ESI-11	49.78	287.9	22.02	170.6	1.95	0.44	2.96	0.27
	ESI-11	74.27	270.4	56.24	212.3	3.69	0.64	3.45	0.23
	ESI-12	2.49	253.5	-15.66	119.1	7.22	0.84	7.71	0.08
	ESI-12	5.04	253.2	-14.84	120.9	0.03	0.07	0.60	0.03
	ESI-12	15.35	266.0	-15.70	132.8	0.03	0.13	0.62	0.02
	ESI-12	25.03	302.2	-6.44	150.2	0.11	0.37	2.16	0.06
	ESI-12	49.96	287.5	37.01	173.7	3.68	0.59	4.09	0.48
	ESI-12	79.13	246.8	78.45	246.1	0.03	0.26	1.73	0.06
	ESI-12	93.45	239.2	82.59	264.3	0.03	0.22	1.94	0.09

Transect	Site	Depth (m)	DO (μmol kg-1)	AOU (μmol kg-1)	CH_4 Sat (%)	$NO_{3/2}$ (μmol kg-1)	PO_4 (μmol kg-1)	SiO_4 (μmol kg-1)	NH_4^+ (μmol kg-1)
Jeddore/ Winipukwejk	ESI-13	2.31	271.9	-28.15	150.7	0.34	0.47	2.94	0.25
	ESI-13	5.16	284.4	-30.08	207.7	0.03	0.11	0.53	0.06
	ESI-13	14.65	300.9	-20.03	309.3	0.03	0.10	0.50	0.07
	ESI-13	32.08	310.7	-5.72	319.2	2.27	0.61	4.23	0.72
	ESI-14	2.08	256.6	-16.59	123.7	3.50	0.54	4.08	0.37
	ESI-14	4.91	258.1	-16.77	125.9	6.12	0.81	5.85	0.08
	ESI-14	14.77	297.5	-15.47	158.4	9.02	0.89	9.06	0.02
	ESI-14	24.26	303.4	0.83	187.9	11.32	1.14	12.50	0.02
	ESI-15	2.04	249.1	-12.67	116.6	0.03	0.18	1.01	0.42
	ESI-15	4.78	249.9	-12.99	120.1	0.03	0.22	1.16	0.12
	ESI-15	14.18	299.5	1.97	164.3	0.03	0.33	1.84	0.28
	ESI-15	25.79	297.6	6.96	187.5	1.90	0.51	3.24	0.26
	ESI-15	49.86	293.6	27.51	167.7	4.86	0.62	4.77	0.29
	ESI-15	65.36	268.3	56.60	209.2	7.36	0.87	7.48	0.11
	ESI-16	2.36	252.4	-14.67	124.7	0.01	0.17	1.22	0.05
	ESI-16	5.49	253.0	-13.81	124.7	0.01	0.19	1.23	0.04
	ESI-16	14.72	295.3	-15.83	163.8	0.11	0.30	2.30	0.31
	ESI-16	24.63	293.1	18.48	165.3	0.93	0.40	3.03	0.34
	ESI-16	49.43	272.6	54.43	205.9	4.77	0.60	5.85	0.47
	ESI-16	79.39	246.1	74.35	255.4	0.02	0.19	1.64	1.03
	ESI-16	111.00	216.0	92.88	303.7	0.02	0.26	1.71	1.13